Increasing the Sensitivity of Phospholipid Analyses from Biological Extracts via Trimethylation Enhancement using Diazomethane (TrEnDi) and Tandem Mass Spectrometry

by

Carlos Ramon Canez Quijada

A thesis submitted to the Faculty of Graduate and Postdoctoral

Affairs in partial fulfillment of the requirements for the degree of

Master of Science

in

Chemistry

Carleton University

Ottawa, Ontario

Abstract:

Trimethylation Enhancement using Diazomethane (TrEnDi) is a novel rapid in-solution technique for quaternization of phospholipid amino groups and methylation of phosphate groups via reaction with diazomethane and tetrafluoroboric acid. TrEnDi significantly enhanced the sensitivity of mass spectrometry (MS) and tandem MS studies of phosphatidylethanolamine (PE), phosphatidylserine (PS), phosphatidylcholine (PC) and sphingomyelin (SM) standards. Use of ^{13}C-labelled diazomethane enabled creation of exclusive and independent precursor ion scans (PIS) for modified PE and modified PC species which would otherwise share the same PIS and produce undistinguishable isobaric species if two PC and PE species with identical groups on the sn-1 and sn-2 position were present. The efficacy of the technique was tested on a complex biological sample by derivatizing the lipid extract of HeLa cells. ^{13}C-TrEnDi provided a drastic sensitivity enhancement for PE and PS species enabling the identification and quantitation of several species that were below the limit of detection and quantitation prior to modification. Derivatization provided a modest sensitivity enhancement for PC species and allowed quantitation of several PC species that were below the limit of quantitation prior to modification. SM species exhibited neither sensitivity increase nor hindrance after modification.

Preface

This section contains full bibliographical details for the two articles included in this thesis. The articles' content has been adapted to fit in the thesis structure. Use of copyrighted material is acknowledged in this section.

In accordance to the Integrated Thesis policy of Carleton University, the supervisor (Jeffrey C. Smith) and the author of the thesis (Carlos R. Canez Quijada) confirm the student was fully involved in setting up and conducting the research, obtaining data and analyzing results, as well as preparing and writing the material presented in the co-authored articles integrated in the thesis.

Chapter 2

Title of the publication: Trimethylation enhancement Using Diazomethane (TrEnDi) II: Rapid In-Solution Concomitant Quaternization of Glycerophospholipid Amino Groups and Methylation of Phosphate Groups via Reaction with Diazomethane Significantly Enhances Sensitivity in Mass Spectrometry Analyses via a Fixed, Permanent Positive Charge.

Adapted with permission from Wasslen, K. V[ΩΨ]; Canez, C. R[ΩΨ].; Lee, H[Ψ].; Manthorpe*[ΨΣ], J. M.; Smith*[ΨΣ], J. C. *Anal. Chem.* **2014**, *86* (19), 9523–9532. Copyright 2015 American Chemical Society.

[Ω]K.V.W. and C.R.C. contributed equally to this work. (Authorship contribution specified in page 9531 [page 9 out of 10 of the publication] under the Author information section and Author Contribution sub-section).

[Ψ]Department of Chemistry and [Σ]Institute of Biochemsitry, Carleton University, Ottawa, Ontario K1S 5B6, Canada

*Corresponding authors

The publication can be located with the following **DOI:** 10.1021/ac501588y

Minor changes were perfromed to the formatting of the document so that it could fit in the format of this dissertation.

Carlos R. Canez Quijada performed all tandem MS experiments, derivatized the lipid standard mixture, and optimized/ acquired the unmodified standards spectra with protonating or deprotonating agents. Hyunmin Lee developed the in-solution modification procedure and performed the initial derivatization of individual standards. Karl V. Wasslen optimized the derivatization procedure, derivatized individual and mixtures of lipid standards and performed the nanoemitter direct infusion experiments. Carlos R. Canez Quijada, Karl V. Wasslen, Jeffrey M. Manthorpe and Jeffrey C. Smith processed the data and created the tables and figures. Writing was collaborative between all co-authors.

Chapter 4

Canez, C. R. [Ψ]; Shields, S. W. J. [Ψ]; Bugno, M.[Φ]; Willmore[ΦΣ], W. G.; Manthorpe, J. M. *[ΨΣ]; Smith, J. C. *[ΨΣ] Trimethylation enhancement using ^{13}C-diazomethane (13C-TrEnDi): Increased sensitivity and selectivity of phosphatidylethanolamine, phosphatidylcholine, and phosphatidylserine lipids derived from complex biological samples. Manuscript is currently in preparation to be submitted to Analytical Chemistry.

[Ψ]Department of Chemistry, [Φ]Department of Biology and [Σ]Institute of Biochemsitry, Carleton University, Ottawa, Ontario K1S 5B6, Canada

*Corresponding authors

Minor changes were perfromed to the formatting of the document so that it could fit in the format of this dissertation.

Carlos R. Canez Quijada designed and performed all experiments in the article with exception of the synthesis of ^{13}C-diazomethane, culturing and harvesting of HeLa cells. Samuel S. W. Shields synthesized all ^{13}C-diazomethane. Magdalena Bugno performed HeLa cell culturing and harvesting. Carlos R. Canez Quijada performed all data processing, production of tables, figures and writing. Jeffrey C. Smith and Jeffrey M. Manthorpe revised the manuscript.

Acknowledgments:

I would sincerely like to thank everyone that helped me overcome the challenges presented in the past two years, with a special mention to the delightful financial burden of being an international student. I would like to thank Dr. Jeffrey C. Smith for all the support provided during my undergrad and graduate degree. I honestly would not have been able to make to finish the degree without his help. Dr. Smith has my deepest gratitude. I would like to thank the government of Ontario for gracefully providing OGS funding for the first year of my degree. I thank Dr. Owen Rowland for providing the awesome reference letter that helped in obtaining the provincial funding. Sincere thanks to Norma Alicia Canez Quijada and Johnathan Ramnarinesingh for the extensive support provided during the past hectic years. I really appreciate the cheap rent provided regardless of my poor merits as tenant; they have my deepest gratitude.

I would like to sincerely thank Dr. Jeffrey M. Manthorpe for his excellent guidance through the dark magic of organic chemistry. I would like to thank Dr. Willmore for all the support provided with the growth of lipid analyte sources. Thanks to Mr. Daredevil Samuel W.J. Shields for the prompt and friendly provision of diazomethane after every request. Thanks to Karl Vladimir Wasslen for my inclusion into the land of TrEnDi. Special thanks to Hillary Parker Weinert for all the help provided this summer. I would like to thank her for all the support provided in the formatting and editing of this document.

Thanks to Andrew Mackendrick Macklin for his official role as “singing buddy”. There is no better co-worker or friend to have shared my graduate studies with. Thanks to Katrin Blank

for all the food provided as well as avoiding the temptation of strangling me or Mr. Mackendrick in the past year.

Muchas gracias madre por todo el apoyo otorgado durante toda la vida. Que pena que hayamos estado separados durante los últimos años. Me gustaría agradecer una vez más a mi hermana por todo su afecto y todo el apoyo que me ha brindado y especialmente el apoyo que le ha dado a mi madre en los últimos años.

Table of Contents:

Tables

Chapter 2

Chapter 3

Chapter 4

Figures

Chapter 1

Chapter 2

- **Figure 2.4.1:** a) Derivatization of PE to $[PE^{Tr}]^+$ using diazomethane. b) Unmodified PE revealing protonated (m/z 718.52) ion and sodiated (m/z 740.50) adduct. c) Fragmentation of unmodified protonated PE at m/z 718.52 reveals MS signal divided among numerous fragmentation channels. d) Diazomethane adds four methyl groups to PE (m/z 774.58). e) MS/MS spectrum of $[PE^{Tr}]^+$ revealing a single fragmentation channel (m/z 198.10). f) Derivatization of PS to $[PS^{Tr}]^+$ using diazomethane. g) Unmodified PS revealing protonated, sodiated and doubly sodiated ions at m/z 788.52, m/z 810.49 and m/z 832.47, respectively. h) MS/MS of unmodified PS (m/z 788.52) reveals MS signal divided among numerous fragmentation channels. i) Diazomethane adds five methyl groups to PS (m/z 858.59). j) MS/MS spectrum of $[PS^{Tr}]^+$ revealing two dominant fragmentation channels (m/z 144.10 and m/z 256.09).

- **Figure 2.4.2:** The ionization efficiency of TrEnDi-modified lipids is enhanced resulting in improved sensitivity. a) Equimolar amounts of TrEnDi-modified and unmodified PE reveals an approximately two-fold increase in sensitivity following derivatization. b) Equimolar amounts of TrEnDi-modified and unmodified PS shows >30-fold increase in sensitivity following derivatization. c) Equimolar amounts of TrEnDi-modified and unmodified PC shows a modest gain in sensitivity following derivatization. d) Equimolar amounts of TrEnDi-modified and unmodified SM show an approximately 2.5-fold increase in sensitivity following derivatization.

- **Figure 2.4.3:** MS spectrum of an equimolar mixture of unmodified and TrEnDi-modified PC, PE, PS and SM indicating that simultaneous derivatization of all four species is possible. The spectrum also reveals sensitivity gains for each species following derivatization when electrosprayed from an ethanol solution containing sodium cations, as summarized in Table 2.4.3.

- **Figure 2.4.4:** Positive and negative MS/MS spectra of non-modified lipids accompanied by the proposed structures and dissociative derivation of each fragment. Lipids were dissolved in 10 mM ammonium hydroxide in ethanol for negative ion spectra and 10 mM ammonium acetate in ethanol for positive ion spectra. a) Negative PIS (m/z 196) of PE observed at m/z 716.9, b) positive NL scan (141 Da) of PE observed at m/z 718.8, c) negative NL scan (87 Da) of PS observed at m/z 786.9, d) positive NL scan (185 Da) of PS observed at m/z 788.9, e) relatively strong signal intensities for the positive PIS (m/z 184) for PC and SM observed at m/z 732.8 and m/z 703.8, respectively.

- **Figure 2.4.5:** MS/MS spectra of TrEnDi-modified lipids accompanied by the proposed structures and dissociative derivation of each fragment. a) Relatively stronger signal intensities for the precursor ion scan (m/z 198) for $[SM^{Tr}]^+$ (m/z 717.8), $[PC^{Tr}]^+$ (m/z 746.8) and $[PE^{Tr}]^+$ (m/z 774.8), b) relatively stronger signal intensity in the precursor ion scan (m/z 256) with CE of 40 eV for $[PS^{Tr}]^+$ (m/z 858.8), c) relatively stronger signal intensity for the precursor ion scan (m/z 144) with CE of 60 eV for $[PS^{Tr}]^+$ (m/z 858.8).

- **Figure 2.6.1:** Methylation of a phosphoethanolamine lipid head group with diazomethane.

- **Figure 2.6.2:** a) PC treated with diazomethane ($[PC^{Tr}]^+$) reveals addition of one methyl group (m/z 746.58). b) Collision-induced fragmentation of $[PC^{Tr}]^+$ revealed a single fragmentation channel (m/z 198.09) homologous to that known and observed for unmodified PC.

- **Figure 2.6.3:** a) SM treated with diazomethane ($[SM^{Tr}]^+$) reveals addition of one methyl group (m/z 717.62). b) Collision-induced fragmentation of $[SM^{Tr}]^+$ revealed a single fragmentation channel (m/z 198.10) homologous to that known and observed for unmodified SM.

- **Figure 2.6.4:** Tandem mass spectra of 10 pmol of PS and PE in various buffers. Lipid, scan type, instrument polarity and buffer type and concentration are indicated in each panel. Panels c) and d) indicate that 10 mM ammonium acetate provides the greatest signal strength in positive ion mode for both PE and PS.

Chapter 3

- **Figure 3.4.1:** Comparison between positive and negative non-tandem MS scans and tandem MS scans of a mixture of two lipid standards in 10mM NH_4OAc. The PE (8:0/8:0) and PS (8:0/8:0) standards were used. The NL of 141Da scan is specific to protonated PE species while the NL of 185 Da scan is specific to protonated PS species.

Chapter 4

- **Figure 4.4.1:** ^{13}C-TrEnDi modification differentiates modified PE species from modified PC species by providing a PC^{Tr}-specific +PIS of m/z 199.1 (A) and a PE^{Tr}-specific +PIS of m/z 202 (B). PC (16:0/18:1) and PE (16:0/18:1), which would have been isobaric (m/z 774.8, +PIS m/z 198.1) using unlabeled TrEnDi, yield m/z of 775.9 (A) and 778.9 (B), respectively, after ^{13}C-TrEnDi modification.

- **Figure 4.4.2:** Mass spectrum of unmodified PE from HeLa cell lipid extract acquired via +NL scan of 141.1 Da (A). Mass spectrum of ^{13}C-TrEnDi-modified PE from HeLa cells lipid extract acquired via +PIS of m/z 202 (B). The y-axis was set to the same scale for both spectra and only peaks above a 2% maximum intensity threshold are labelled. Both spectra were acquired via reversed phase LC-MS/MS and represent a 40 minute average of all spectra obtained during the time that lipid species eluted. The LC-MS parameters were optimized to provide the best signal possible for unmodified species to provide a fair assessment when comparing them against their modified counterparts.

- **Figure 4.4.3:** Comparison of standardized peak area averages between unmodified triplicates (red bars) and ^{13}C-TrEnDi chemical triplicates (green bars) for (A) PE, (B) PC and (C) SM extracted from HeLa cells. The twenty highest standardized peak area averages for PE species are presented (A) out of 63 PE species identified revealing a statistically significant intensity increase following modification. The twenty highest standardized peak area averages for PC species are presented (B) out of 63 PC species identified. A less prominent yet statistically significant increase was observed for the standardized area of PC species. All PE and PC species experienced statistically significant enhancements to their standardized peak area average values. The standardized area values of SM species (C) did not change following TrEnDi modification.

- **Figure 4.4.4:** The unmodified HeLa cell PS lipidome was dissolved in EtOH with 10 mM ammonium acetate or 10 mM ammonium hydroxide and analyzed via their respective +NL of 185.1 Da (A) or –NL of 87.0 Da scans (B). No PS species were identified with either scan. The ^{13}C-TrEnDi-modified HeLa cell PS lipidome was analyzed via +PIS of m/z 148.1 in EtOH (C) and +PIS of m/z 261.1 in EtOH (D). Both modified scans had an outstanding sensitivity increase allowing the identification of several modified PS species. The unmodified HeLa cell extract was concentrated 4 times and analyzed via +NL 185.1 Da in a solution of 10 mM ammonium acetate in EtOH (E). The three highest unmodified species in pane E correspond with the three highest species in pane C and D (after considering the 75 Da increase post-modification) corroborating their identity as unmodified and modified PS species. The y-axis was set to the same value for all spectra.

- **Figure 4.6.1:** Comparison of standardized peak area averages between unmodified triplicates (red bars) and ^{13}C-TrEnDi chemical triplicates (green bars) for PE extracted from HeLa cells. The

peaks represent 22 peaks with medium standardized peak area values out of 63 PE species found. All PE species experienced statistically significant enhancements to their standardized peak area average values.

- **Figure 4.6.2:** Comparison of standardized peak area averages between unmodified triplicates (red bars) and ^{13}C-TrEnDi chemical triplicates (green bars) for PE extracted from HeLa cells. These peaks represent 21 peaks with lowest standardized peak area values out of 63 PE species found. All PE species experienced statistically significant enhancements to their standardized peak area average values.

- **Figure 4.6.3:** Comparison of standardized peak area averages between unmodified triplicates (red bars) and ^{13}C-TrEnDi chemical triplicates (green bars) for PC extracted from HeLa cells. These peaks represent 22 peaks with medium standardized peak area values out of 63 PC species found. All PC species experienced statistically significant enhancements to their standardized peak area average values.

- **Figure 4.6.4:** Comparison of standardized peak area averages between unmodified triplicates (red bars) and ^{13}C TrEnDi chemical triplicates (green bars) for PC extracted from HeLa cells. These peaks represent 21 peaks with lowest standardized peak area values out of 63 PC species found. All PC species experienced statistically significant enhancements to their standardized peak area average values with exception of two PC species marked by the red # symbols.

- **Figure 4.6.5:** Mass spectrum of unmodified PS extracted from HeLa cells separated by reversed phase HPLC-ESI-MS/MS with an eluent containing 10 mM ammonium acetate and analyzed via +NL of 185.1 Da. The spectra presented is a two minute window average (24.2 to 26.2 min) corresponding to the time frame where all PS species present in the sample elute. The concentration of sample injected was twice the amount of sample injected via direct infusion. The quadrupole resolution for Q1 was set to low (in comparison to unit for direct spray studies) in order to achieve higher sensitivity for the PS species. The y-axis was set to the highest peak found in the unmodified spectra unlike the direct spray studies where all y-axis were set to 4.4×10^5 corresponding to the highest peak intensity found within all scans. The intensity threshold was deliberately lowered to 1×10^3 to showcase all the PS species with small intensities.

Scheme

Chapter 4

Abbreviations

AC – Alternating Current

APCI – Atmospheric pressure chemical ionization

BLoD – Below the Limit of Detection

CD_2N_2 – Deuterium-labelled diazomethane

CDP-DG – CDP-glycerols

CE – collision energy

CEM – Channel electron multiplier detector

CI – Chemical Ionization

CID – Collision-induced dissociation

CL – cardiolipins or glycerophosphoglycerophosphoglycerols

CLSI – Clinical and Laboratory Standards Institute (CLSI)

Co-enzyme Q – Ubiquinone

DC – Direct Current

Diazald – N-methyl-N-nitroso-p-toluenesulfonamide

EI – Electron Ionization

EMS – Enhanced Mass Spectrum

ESI – Electrospray ionization

GC – Gas Chromatography

[glycan]GP – glycosylglycerophospholipid

[glycan]PI – glycerophosphoinositolglycans

HBF_4 – Tetrafluoroboric acid

HeLa – Human Cervical Carcinoma cell line named after Henrietta Lacks, the patient with cervical cancer from which the cells were originally derived from.

HPLC – High Performance Liquid Chromatography

ILCNC – International Lipid Classification and Nomenclature Committee

IS – Ion Spray

LC – Liquid Chromatography

LCB – Long-chain base

LIT – Linear Ion Trap Analyzer

LoB – Limit of Blank

LoD – Limit of Detection

LoQ – Limit of Quantification

m/z – Mass-to-charge ratio

MALDI – Matrix-assisted laser desorption ionization

Menaquinone – Vitamin K

MPC – Micro-channel plate

MS – Mass Spectrometry

MS/MS – Tandem Mass Spectrometry

NL – Neutral Loss

NMPTS – *N*-methyl-*p*-toluenesulfonamide

NMR – Nuclear Magnetic Resonance

PA – Phosphatidic acid or glycerophosphate

PAF – Platelet-activating factors

PC – Phosphatidylcholine or glycerophosphocholine

PE – Phosphatidylethanolamine or glycerophosphoethanolamine

PG – Phosphatidylglycerol or glycerophosphoglycerol

PGP – Phosphatidylglycerol phosphates or glycerophosphoglycerophosphate

PI – Phosphatidylinositol or glycerophosphoinositol

PIP – Phosphatidylinositol phosphate or glycerophosphoinositol monophosphate

PIP2 – Phosphatidylinositol bis-phosphate or glycerophosphoinositols bis-phosphate

PIP3 – Phosphatidylinositol tris-phosphate or glycerophosphoinositols tris-phosphate

PIS – Precursor Ion Scan

PnC – Glycerophosphonocholine

PnE – Glycerophosphonoethanolamines

PPA – Glyceropyrophosphate

PS – Phosphatidylserine or glycerophosphoserine

q0 – Quadrupole Zero

SEM – Secondary Electron Multiplier

SM – Sphingomyelin

Th – Thompson

TLC – Thin Layer Chromatography

TOF – Time of Flight

TrEnDi – Trimethylation Enhancement using Diazomethane

XIC – Extracted Ion Chromatographs

Chapter 1: Introduction

1.1 Lipid Classification

Different lipid nomenclatures have been used in the scientific community in previous years. The need to have a universal classification system that would be compatible with bioinformatics platforms lead to Fahy and co-workers to develop a comprehensive lipid classification system with eight major lipid classes.[1] This classification system has been under the leadership of the International Lipid Classification and Nomenclature Committee (ILCNC) and encompasses lipid structures from mammals, plants, bacteria and fungi.[2] The eight lipid categories are fatty acyls, glycerolipids, glycerophospholipids, sphingolipids, sterol lipids, prenol lipids, saccharolipids and polyketides. Each lipid category has different classes, subclasses, subgroups and subsets of lipid molecules.[1] A representative lipid molecule from each subclass is presented in Figure 1. Six of the eight lipid categories will be introduced in this section. Sphingolipids and glycerophospholipids will be discussed in the following section.

Fatty acyls

Fatty acyls consist of a carboxylic acid with a long unbranched, hydrophobic aliphatic tail that can be saturated or unsaturated. Fatty acyls are diverse and contain distinct classes based on the degree of branching, chain length, number and position of double bonds, the *cis* or *trans* isomer conformation and presence of functional groups. Fatty acids occur predominantly in their esterified form. The majority of mammalian fatty acyls contain even chains, while plants and bacteria contain both odd and even chained fatty acyls. Oxygen, halogen, nitrogen, and sulfur heteroatoms can also be linked to the carbon chains. Fatty alcohols have terminal hydroxyl groups, fatty aldehydes have terminal oxo groups, fatty amides have amide groups.

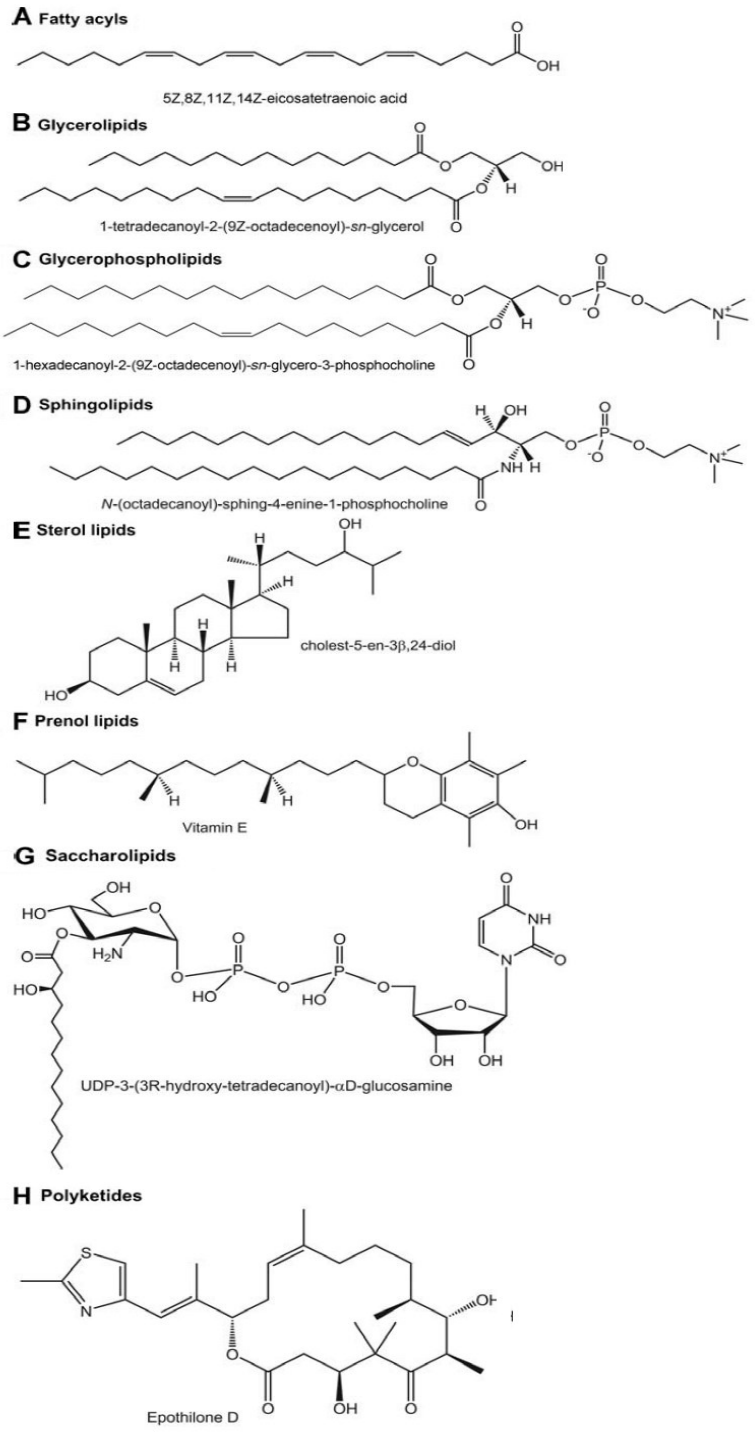

Figure 1.1.1: Representative lipids for the 8 subclasses of lipids (adapted from Bou Khalil et al., 2010[3]).

Each subclass provides distinct biological properties.[4–6] Fatty acyls are composed of the following 14 classes: fatty acids and conjugates, octadecanoids, eicosanoids, docosanoids, fatty alcohols, fatty aldehydes, fatty esters, fatty amides, fatty nitriles, fatty ethers, hydrocarbons, oxygenated hydrocarbons, fatty acyl glycosides, and other fatty acyls.[1,3] Each class is composed itself of many subclasses such as the fatty acids and conjugates, which is itself composed of 17 subclasses.

Glycerolipids

This category envelops all glycerol-containing lipids with exception of glycerophospholipids, which form their own category. Acylgycerols such as monoacylglycerols, diacylglycerols and triacylglycerols are the best known glycerolipids.[7] Glycerolipids and glycerophospholipids use a *sn* notation which stands for the stereospecific numbering. The numbering follows the numbering system used in Fischer's projections, with *sn*-1 being the carbon at the top and *sn*-3 the carbon at the bottom. The *sn*-2 position describes the central carbon with the hydroxyl group almost exclusively on the left.[8] Even though glycerolipids can occur in their L or D-enantiomeric form, most biological systems synthesize exclusively the L isomer. There are other subclasses of glycerolipids such as glyceroglycans, which contain sugar residues attached to the glycerol backbone via a glycosidic linkage and include glycosylmonoradylglycerols and glycosyldiradylglycerols and macrocyclic ether lipids.[9]

Sterol lipids

Sterol lipids are divided into the following six classes according to biological function: sterols, steroids, secosteroids, bile acids and derivatives, steroid conjugates and other sterols. Sterol lipids are usually characterized by adjacent cyclic organic rings. Cholesterol lipids and

their derivatives are the most studied lipids class in mammalian systems. They are key components of membrane lipids along with glycerophospholipids and sphingomyelin.s[10] Sterols are key hormones and signaling molecules in biological systems.[11] C18 steroids include the estrogen family while C19 steroids include androgens such as testosterone and androsterone. The C21 subclass includes progestogens, glucocorticoids and mineralocorticoids. Various forms of vitamin D are included into the secosteroid class.[12] Bile acids are predominantly found in the bile of mammals and are usually synthesized in the liver. Bile acids can be conjugated with glycine or taurine to form bile salts. The other subclasses are comprised of conjugates of the previous classes.[13]

Prenol Lipids

Prenol lipids are synthesized from the five carbon building units isopentenyl diphosphate and dimethylallyl diphosphate. The five classes of prenol lipids are: isoprenoids, quinones and hydroquinones, polyprenols, hopanoids and other prenols. Prenol lipids are essential for cell survival in all organisms. Carotenoids are prenol lipids that function as antioxidants and precursors of vitamin A.[14] Quinones and hydroquinones which are composed of an isoprenoid tail attached to a quinonoid core vitamin E, vitamin K2 (menaquinone) and ubiquinone (coenzyme Q).[15] Polyprenols play important roles in the transport of oligosaccharides across membranes, extracytoplasmic glycosylation reactions, and protein N-glycosylation in eukaryotes.

Saccharolipids

In saccharolipids fatty acids are linked to a sugar backbone instead of a glycerol backbone like in glycerolipids. Saccharolipids occur as glycans or phosphorylated derivatives in

the following six classes: acylaminosugars, acylaminosugar glycans, acyltrehaloses, acyltrehalose glycans, other acyl sugars, and other saccarolipids. Acylated glucosamine precursors of lipopolysaccharides in Gram-negative bacteria have been thoroughly studied. Acyl amino sugars in rhizobia, fatty acylated derivatives of glucose like acylated trehalose units in mycobacterial lipids, and acylated forms of glucose and sucrose in plants have also been reported.[16–18]

Polyketides

Polyketides classes are very diverse since polyketide synthases produce a great diversity of structures. Polyketides are for the most part secondary metabolites produced by organisms to impart a survival advantage.[19] Anti-microbial, anti-parasitic, anti-cancer agents, and potent toxins are commonly polyketides or polyketide derivatives.[20] Polyketides are synthesized from propionyl-CoA and methylmalonyl-CoA by polyketide synthases in an analogous process to fatty acid biosynthesis.[21,22] Class I polyketide synthases produce constrained macrocyclic lactones ranging in size from 14 to 40 atoms. Class II and III polyketide synthases produce complex aromatic ring systems. Polyketide backbones can then be further modified by glycosylation, methylation, hydroxylation, oxidation, or linked non-ribosomaly synthesized peptides from hybrid scaffolds. The fourteen classes of polyketides are: linear polyketides, halogenated acetogenins, ammonaceae acetogenins, macrolides, and lactones, ansamycins and related polyketides, polyenes, linear tetracyclines, angucyclines, polyether antibiotics, aflatoxins and related substances, cytochalasins, flavonoids, aromatic polyketides, non-ribosomal peptide/ polyketide hybrids, and other polyketides.[1,3]

1.2 Glycerophospholipids and sphingolipids

Glycerophospholipids

Glycerophospholipids are the main component of cellular membranes and function as binding sites for cellular and extracellular proteins. Glycerophospholipids and their metabolites have been identified to function as second messengers in processes such as proliferation and apoptotic cell injury.[23,24] Glycerophospholipids follow the same stereochemical nomenclature as glycerophospholipids as they are derivatives of *sn*-glycero-3phosphoric acid. Glycerophospholipids contain at least one *O*-acyl, *O*-alkyl or *O* alkyl-1'-enyl residue attached to the glycerol moiety in the *sn*-1 and *sn*-2 position and are referred as radyl groups. Lyso glycerophospholipids describe molecules lacking one of the radyl groups. Double bond geometry of the radyl group is described with the E/Z designation.[8] The *sn*-3 position is occupied by a polar headgroup composed by a nitrogenous base, a glycerol, or an inositol unit. The composition of polar head group in the *sn*-3 position of eukaryotes and eubacteria, or *sn*-1 position in archaea determines the glycerophospholipid class they belong to. The twenty-one classes of glycerophospholipids defined by the Lipid Map consortium with their two letter nomenclature are: phosphatidylcholines or glycerophosphocholines (PC), phosphatidylethanolamines or glycerophosphoethanolamines (PE), phosphatidylserines or glycerophosphoserines (PS), phosphatidylglycerols or glycerophosphoglycerol (PG), phosphatidylglycerol phosphates or glycerophosphoglycerophosphates (PGP), phosphatidylinositols or glycerophosphoinositol (PI), phosphatidylinositol phosphates or glycerophosphoinositols monophosphates (PIP), phosphatidylinositol bis-phosphates or glycerophosphoinositols bis-phosphates (PIP2), phosphatidylinositol tris-phosphates or glycerophosphoinositols tris-phosphates (PIP3), phosphatidic acid or glycerophosphates (PA),

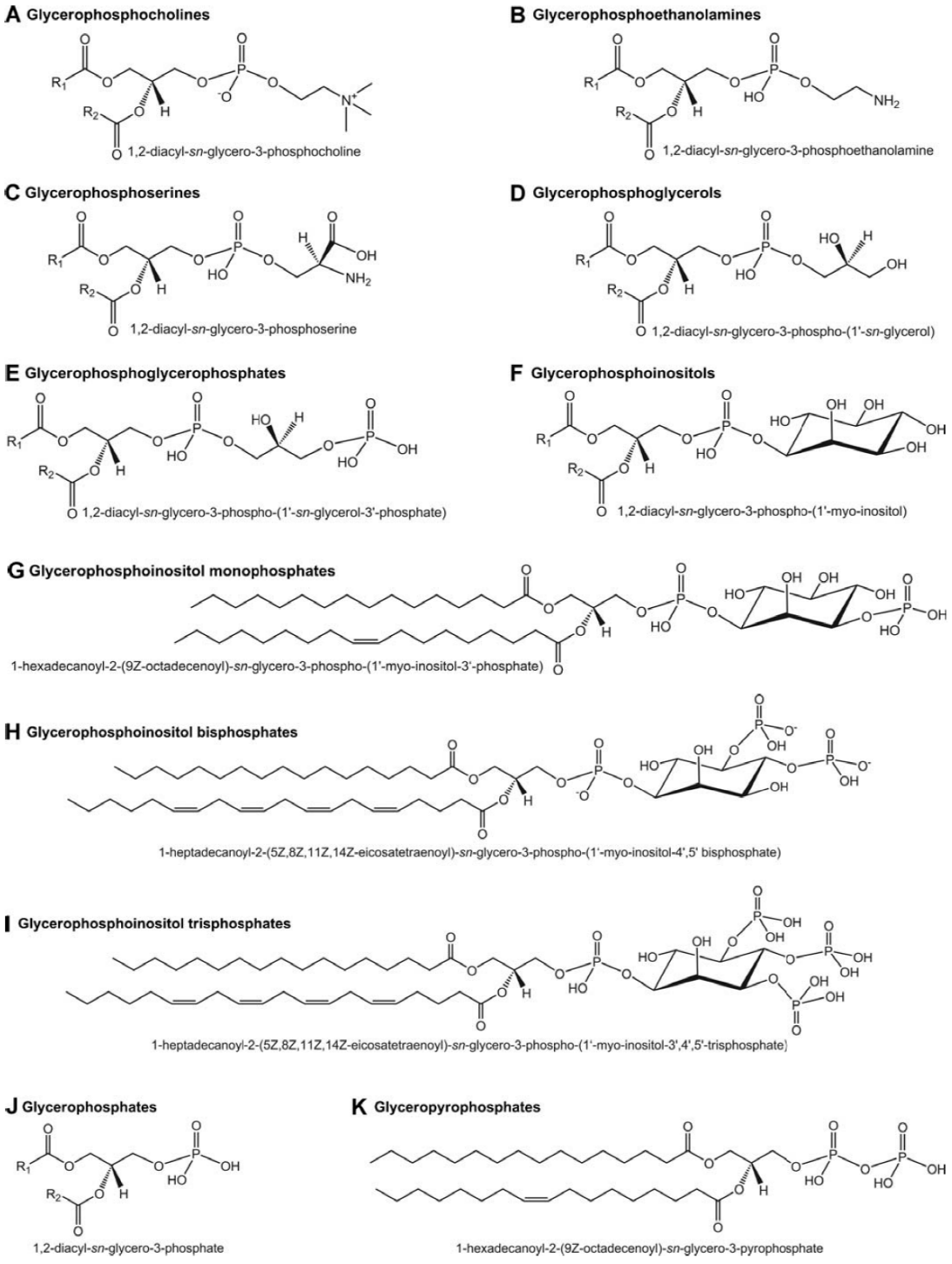

Figure 1.2.1: Representative structures for 11 of the 21 subclasses of glycerophospholipids adapted from Bou Khalil et al., 2010.[3]

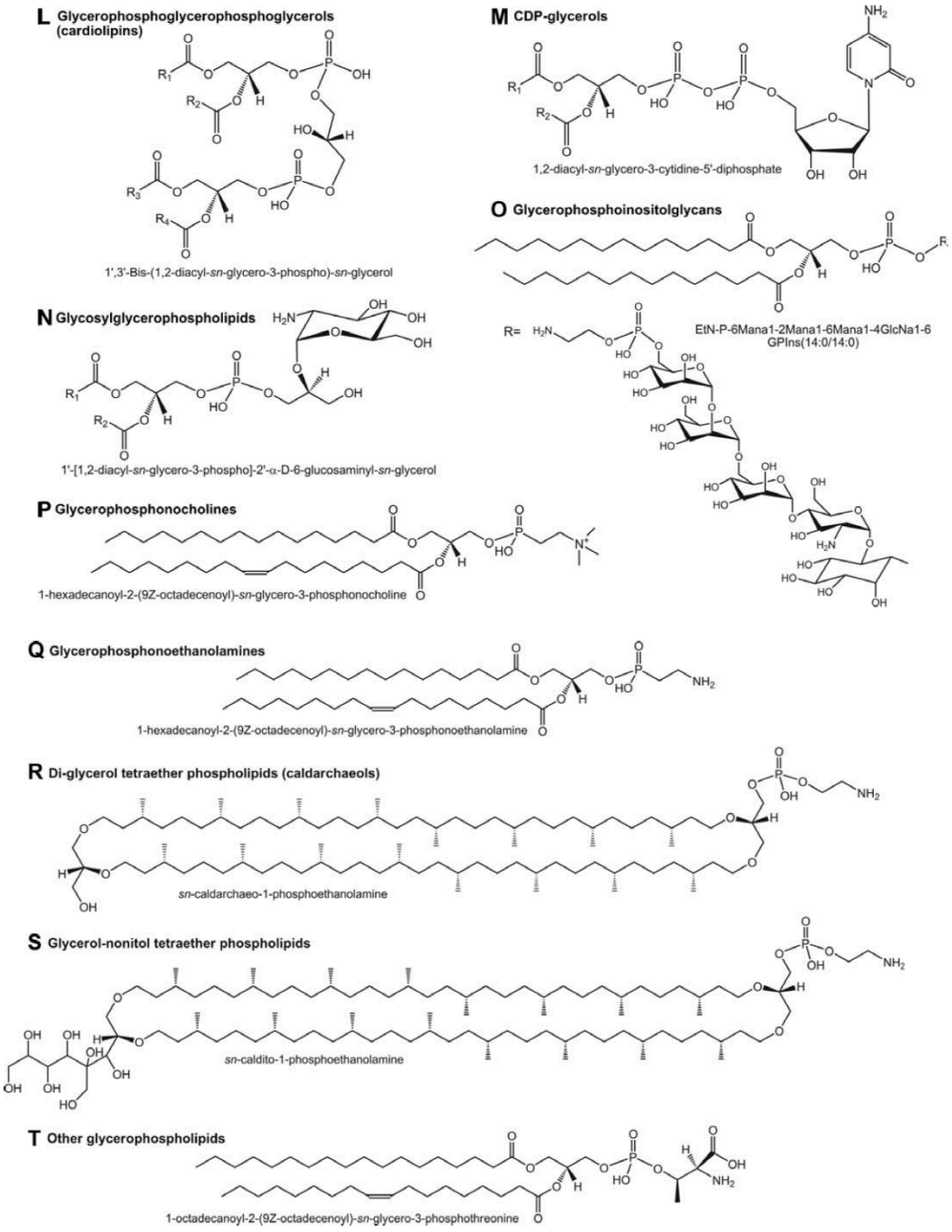

Figure 1.2.2: Representative structures for 9 of the 21 subclasses of glycerophospholipids adapted from Bou Khalil et al., 2010.[3] The oxidized glycerophospholipids subclass is not presented.

glyceropyrophosphates (PPA), cardiolipins or glycerophosphoglycerophosphoglycerols (CL), CDP-glycerols (CDP-DG), glycosylglycerophospholipids ([glycan]GP), glycerophosphoinositolglycans ([glycan]PI), glycerophosphonocholine (PnC), glycerophosphonoethanolamines (PnE), caldarchaeols or di-glycerol tetraether phospholipids, glycerol-nonitol tetraether phospholipids, oxidized glycerophospholipids and other glycerophospholipids. Examples for each class are presented in Figure 1.2.1 and 1.2.2. Subclasses within these groups are defined by the glycerol backbone substituents.[3] When the acyl substituents are replaced by ether or vinyl ether moieties they are categorized under plasmanyl and plasmenyl glycerophospholipids, respectively. Ether lipids are common in inflammatory cell membranes, while plasmalogen species are common in heart and brain tissue.[25,26] PC, PE, PS, PI, PG, PA, and CL are the most abundant and common mammalian lipid classes. Phosphorylated derivatives of PI have a variety of cellular roles in many eukaryotic cells.[3]

Sphingolipids

Sphingolipids are derived from the aliphatic amino-alcohol sphingosine or sphing-4-enine, which is synthesized *de novo* from serine and palmitoyl-CoA. Sphingolipids have important roles in signal transduction and cell recognition. Neural tissues usually contain a higher portion of sphingolipids.[27] The ten classes of sphingolipids are: sphingoid bases, ceramides, phosphosphingolipids, phosphonosphingolipids, neutral glycosphingolipids, acidic glycosphingolipids, basic glycosphingolipids, amphoteric glycosphingolipids, arsenosphingolipids, and other sphingolipids. Sphingoid base analogs which are also grouped under sphingolipids are inhibitors or antagonists of sphingolipids. Ceramides contain a sphingosine moiety that is amide-linked to a fatty acyl group. Ceramides are usually saturated or

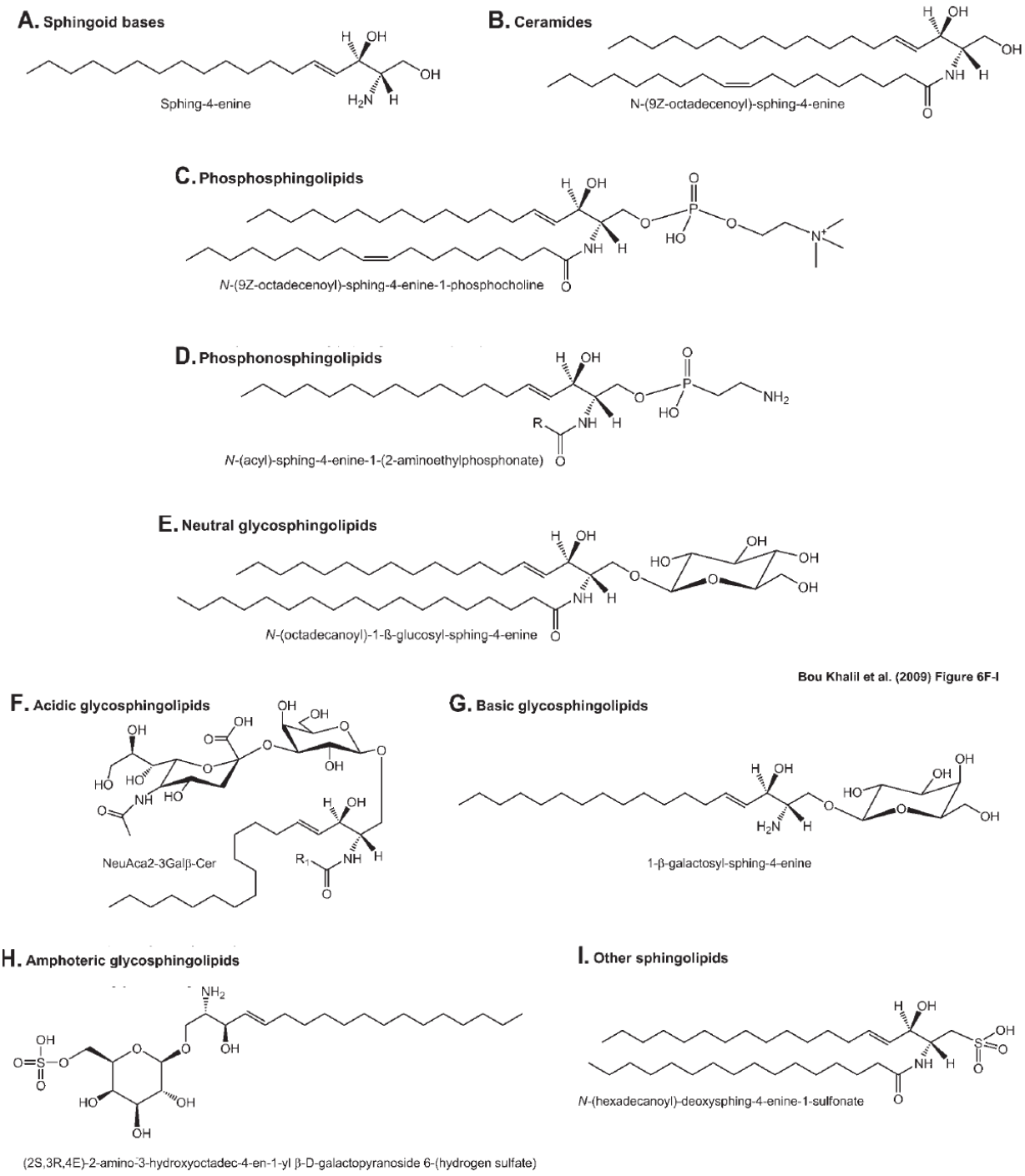

Figure 1.2.3: Representative structures for all 9 of the 10 subclasses of sphingolipids adapted from Bou Khalil et al., 2010.[3] The arsenosphingolipids subclass is not presented.

mono-unsaturated with chain lengths between 14 to 26 carbon atoms and rarely contain a hydroxyl group on carbon 2. Phosphosphingolipids are synthesized from ceramides in mammals by linking a choline, ethanolamine, serine or inositol headgroup to the ceramide backbone. Sphingomyelins are phosphosphingolipids with ceramide and choline moieties. Insects contain many ceramide phosphoethanolamines, while fungi contain phytoceramidephosphoinositols and mannose-containing headgroups.[28] Glycosphingolipids are subclassified based on their carbohydrate moieties composition leading to the neutral, acidic, basic and amphoteric glycosphingolipid classes. Acidic sphingolipids can contain charged sugar residues which are commonly referred as gangliosides or contain neutral sugars attached to phosphate or sulfate groups.[3]

1.3 Lipid studies before mass spectrometry

Previously, many methods have been employed to analyze and identify lipid species from synthetic and biological sources including thin layer chromatography (TLC), colorimetric assays, liquid chromatography (LC) and gas chromatography (GC). While recent methods have advanced to primarily use mass spectrometry, some older methods still have some merit in the field of lipidomics and have been incorporated into MS techniques. Several older techniques, and those that are predominantly featured in combination with MS in recent and current publications, are outlined below.

Thin layer chromatography (TLC) is a technique that can be used to separated, detect and monitor lipids, specifically phospholipids and glycosphingolipids.[29] TLC contains a stationary phase, usually composed of silica on a glass, aluminum or plastic plate.[3] A solute is spotted onto the bottom of the plate and then allowed to flow up the plate by capillary action of a liquid

mobile phase.[30] Lipids of different size and polarity will move through the plate at different rates, allowing for separation and detection of different lipid species. Once migration on the gel is complete, the lipids can be detected using iodine vapour or stain that are specific for certain lipid classes such as phosphorus containing lipids.[3] TLC is a simplistic method for performing an initial screen of lipid extracts, providing initial information on samples.[3] Despite the simplicity of this method, there are several complications associated with the process. Namely, the experiment is time consuming, lacks specificity, has low resolution power, and can have prominent silica gel contamination that limits the effectiveness of the technique.[3,29] Additionally, oxidative damage to lipids during the experiment is common because of the air exposure.[3] Overall, TLC leaves room for improvement in the specificity of identifying lipids and in less time consuming experiments.

Colorimetric methods, including spectrophotometry and spectrofluorometry, are used as a way to quantify the total lipid content in a particular sample.[31] Spectrophotometry uses the amount of light allowed to pass through the sample to determine the concentration of wanted molecules. Specific assays that react with lipids will change colour, thereby changing the amount of light passing through the sample, enabling the determination of lipid concentration. The sulfo-phospho-vanillin method is an example of lipid colorimetric assays. Spectrofluorometry uses a fluorescent dye, then emits light at a specific frequency when in contact with specific lipid molecules, also providing a way to determine the amount of lipid present in a sample. For example, the dye Nile red has been used for the analysis of lipids, despite the plethora of cytoplasm components that interfere with the assay. These methods are high-throughput, however, other cellular components often interfere with the assay and can give rise to misleading concentration values.[31] While useful for providing overall information about the total lipid

content in the cell, these methods are ineffective in determining various lipid species and isolating specific molecules.

Many other biochemical methods for identifying lipids exist, but they all suffer similar disadvantages as TLC and colorimetric assays, making them less than ideal techniques. Some of these methods include capillary electrophoresis, lipid blots, and calorimetric assays.[3] Capillary electrophoresis, which can be coupled to UV detection, can be used for characterizing saturated and unsaturated fatty acids, and the separation of triglycerides, sterols and phosphoinositol.[30] However, capillary electrophoresis suffers from limited sensitivity and solubility problems.[3] While lipid blots and calorimetric studies show increased lipid sensitivity, high throughput is difficult and the techniques are hard to perform.[30]

After the many difficulties experienced using various biochemical methods, the focus of lipidomics analysis was shifted towards analytical chemistry techniques. Nuclear magnetic resonance (NMR) can be used for the structural analysis of low complexity lipid samples as well as global phospholipid class quantification.[3] ^{31}P NMR is particularly effective in the quantitation of phospholipid species as the phosphorus nucleus experiences a different chemical environment with each phospholipid class.[32] A significant advantage of NMR spectroscopy is that it is a non-destructive technique, allowing further work with the lipid samples after analysis.[3] Also, the wide range of solvents that can be used for NMR solves many of the solubility problems common with biochemical techniques. While effective for many other organic molecules, problems still exist with this technique during lipid analysis, predominantly the low sensitivity of the signal.[3] Additionally, the phosphocholine and cholesterol subclasses dominate the spectra, making the quantitation of less abundant subclasses hard and the identification of an individual lipids extremely difficult.[3]

Gas chromatography (GC) is a separation technique used when separating several analyte molecules from one mixture by using the molecules' differing affinities for the stationary and mobile phase. GC is only compatible with volatile molecules capable of withstanding the high temperatures and therefore is unfit for the analysis of many biological macromolecules that would otherwise decompose during chromatographic separation. Some lipid categories such as glycerolipids and glycerophospholipids are not compatible with GC because the lipid molecules decompose into their glycerol and fatty acyl moieties. Other lipid classes such as fatty acyls and some sterols are compatible and effectively separated and identified via GC.[33] Depending on the stationary phase selection, most lipids can be separated based on their polarity.[3] The fatty acid profiles of lipid species incompatible with GC can be characterized.[34] The lipid molecules are first derivatized so their fatty acids are esterified using acid or base-catalyzed reactions.[34] After esterification, the fatty acids are run through the GC column. The fatty acid profiles obtained via GC provide a level of sensitivity and simplicity that cannot be achieved through typical biochemical methods.[34] However, the high temperatures used in GC that can also lead to unwanted isomerization.[3]

The sensitivity and simplicity of GC analysis can be replicated in high performance lipid chromatography (HPLC) without the need for sample volatility and high temperatures. HPLC is an effective method for separating glycerophospholipids, sterols, fatty acids and other lipid derivatives due to the versatility of normal-phase and reversed-phase columns and wide range of solvent options and gradients.[3] In normal-phase HPLC a polar stationary phase and non-polar solvents are used to separate lipids based on their head group polarity with neutral lipids eluting first and the most polar lipids eluting last. Reversed-phase HPLC uses a non-polar stationary phase with a polar solvent and separates lipids based on the hydrophobicity of their fatty acid

tails.[3] After the effective separation of lipids, HPLC can be coupled with many techniques to directly analyze lipid elution including UV, fluorescence, or flame ionization.[3] However, as discussed previously, these techniques have significant draw backs for positively identifying lipids.

The next advancement in lipidomics analysis came with mass spectrometry (MS). In combination with GC and HPLC, MS has been proven a sensitive, specific, and comprehensive method for analyzing lipid species. This new technology allows for precise lipid identification, including the differentiation between similar classes and sizes of phospholipids. HPLC-MS is prominently featured due its excellent separation of lipids, and then sensitive and specific analysis of the lipid molecules. Alternatively the direct infusion of lipid samples without prior chromatographic separation is referred as shotgun lipidomics.[35] Shotgun lipidomics usually requires the use of a high resolution MS, tandem MS analyses, or both. But whether phospholipids are analyzed via GC-MS, LC-MS or MS-based shotgun lipidomics, mass spectrometry is definitively the best analytical technique for phospholipid analysis.[36]

1.4 Mass spectrometry

Mass spectrometry (MS) has allowed revolutionary advancements in the field of lipidomics.[37] The unrivaled sensitivity of lipids provided via MS analyses dwarves the sensitivity provided by previous analytical techniques and allows a more thorough study of lipid species in biological samples. The modern design for mass spectrometers was developed by Ashton and Dempster and based on the original work performed by J.J. Thomson, who separated isotopes of neon gas by their mass-to-charge ratio (m/z).[38] The m/z ratio is also expressed as the eponymous unit, Thomson (Th) in his honour. The three fundamental components of a mass spectrometer

are: an ionization source, a mass analyzer and a detector. An ionization source is required to produce analytes with an overall positive or negative charge as neutral analytes won't be able to be analyzed. The ionization source also enables the analytes to reach the gas state if they were previously dissolved in liquid or part of a solid matrix. Electron ionization (EI) is commonly used to analyze highly volatile, non-polar compounds. Moderately polar and volatile analytes can be effectively ionized via atmospheric pressure chemical ionization (APCI). The most appropriate ionization mode for highly volatile and polar compounds is chemical ionization (CI).[39] These ionization techniques produce mostly fragments from the parent ion, with little to no parent ion molecules left and therefore are labelled as "hard" ionization techniques. Hard ionization techniques obliterate biological macromolecules and therefore require the use of matrix-assisted laser desorption ionization (MALDI) or electrospray ionization (ESI) which are "soft" ionization techniques. This allowed for the introduction of mass spectrometry studies and significant enhancement of the fields of proteomics, genomics, lipidomics and metabolomics.[40]

MALDI involves mixing the analyte with a suitable matrix material that is applied on a metal plate. A pulsed laser irradiates the sample enabling ablation and desorption of the sample and matrix material. Ionization is achieved by protonation or deprotonation in the hot plume of the ablated gases.[41]

The samples are introduced at flow rates of microliters per minute and oxidized by a highly-charged capillary when using ESI. The voltage difference between the charged capillary and the charged MS curtain plate allows for liquid droplets to be emitted from the capillary tip as a Taylor cone. Rapid droplet desolvation ensues until the droplet's Rayleigh limit is reached. The repulsion forces of cations or anions in close proximity overcome the droplet surface tension and dissociate into desolvated cations in the gas phase. The ions reach the charged curtain plate

where most of the ions get reduced except for the small percentage that enters through the orifice into the instrument. A general schematic of ESI is presented in Figure 1.4.1, which was adapted and modified from the review produced by Ho et al.[42] Nano-electrospray ionization nano-ESI uses the same principles used in ESI but with flow rates of nanoliters per minute. This allows for extremely low sample consumption as well as affecting the mechanism of ion formation.[42] Ion spray (IS) is a modification of ESI where a turbulent gas flow assists the nebulization of the liquid effluent.[43]

In this dissertation ESI and IS were used to introduce the lipid analytes into the MS. ESI was performed when using nano-electrospray emitters, while IS was performed with a syringe or HPLC eluent.

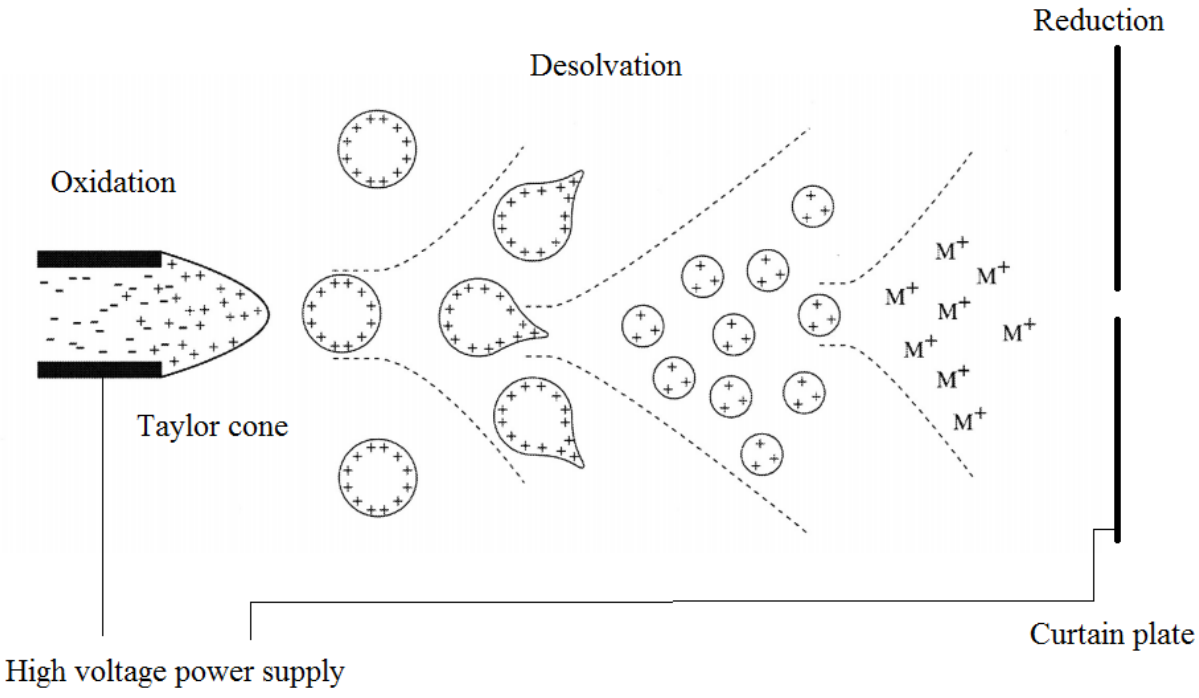

Figure 1.4.1: Schematic of electrospray ionization (ESI).[44]

Inert curtain gas is gently flowed inside the orifice of the mass spectrometer curtain plate which helps to further desolvate the ion stream. The ion stream supersonically expanding into a jet plume under vacuum conditions is refocused through the use of charged focusing rings and quadrupole 0 (q0). Sequential compartments inside the MS have a stronger vacuum which eliminates neutral molecules which could potentially interrupt the ion stream. After the ion beam is focused it continues its pathway into the mass analyzer. The most common mass analyzer component in most instruments is one or a set of quadrupoles.[44] Quadrupoles have four hyperbolic rods with oppositely positioned rods that are electrically connected and therefore carry the same charge polarity. A schematic of a quadrupole is presented in Figure 1.4.2. The ion beam's spiraling path along the quadrupole is controlled by producing a rapidly alternating electric field by applying an alternating current (AC) radio frequency to each pair of rods with cycling polarities. A direct current (DC) potential superimposed on the poles allows the selective transmission of resonant ions with a specific m/z. Increasing the electric field leads to an increase in the amplitude of the ions' motion in the quadrupole's x-y plane which results in the ion trajectory to become unstable and collide with the quadrupole making it unable to reach the detector. When the DC field is weaker than the RF field, the trajectories of heavy ions are destabilized, eliminating transmission while allowing transmission of low m/z ions. When the DC dominates the RF, the heavier ion trajectories are focused to the center allowing transmission while destabilizing low m/z ions trajectories and hence eliminating their transmission. The use of a DC potential allows to use quadrupoles as mass filters while their use in RF-only mode allows the transmission of all ions effectively producing a full mass scan.[45]

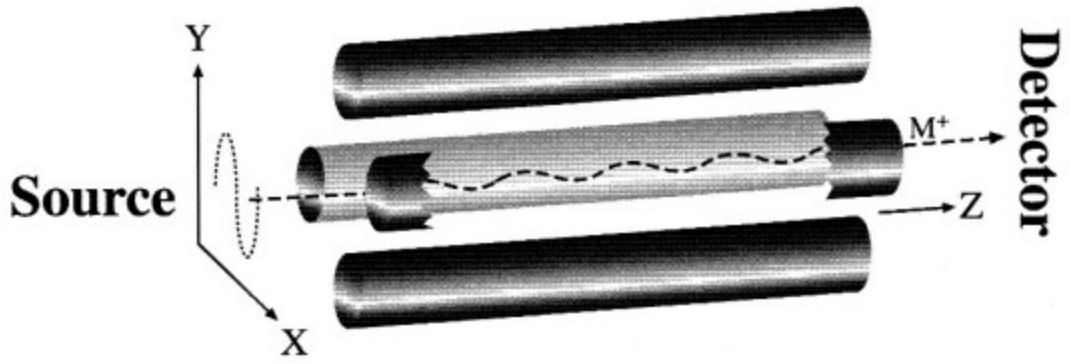

Figure 1.4.2: Schematic of the operation of a quadrupole mass analyzer.[44]

Placing three quadrupoles in line allows different versatile scans to be performed and is referred as tandem MS or MS/MS. The most common tandem MS scans are product ion scans, precursor ion scans, neutral loss scans and multiple reaction monitoring. Figure 1.4.3 presents the function of each quadrupole during each scan. All tandem MS/MS scans use the second quadrupole as the collision cell and fragment the incoming ions via collision-induced dissociation (CID). The second quadrupole is located in a chamber filled with a neutral inert gas. Collision energies of incoming ions with the inert gas are adjusted by controlling potential difference between q0 and q2 which in turn controls the speed and kinetic energy of the incoming ions. If the proper collision energy (CE) is used, the kinetic energy is transformed into internal vibrational energy after collision events which can result into bond fragmentation. The ion molecule selected for fragmentation is referred as the parent ion while the fragments are referred as daughter ions. A product ion scan uses Q1 as a mass filter selecting a single m/z ratio, fragments the parent ion of interest in q2 and sequentially scans for the m/z of daughter ions via ramping of the DC potential. This scan allows for the identification of all the charged fragments created by the parent ion, providing structural information. A precursor ion scan allows all ions

to sequentially reach q2 where they will be fragmented while Q3 is set to allow a single m/z fragment ion to reach the detector. This scan allows for the identification of all the molecules that yield a characteristic charged fragment. A neutral loss scan sequentially scans with Q1 while Q3 sequentially scans the fragments at the same rate as Q1 but with a set m/z difference. This scan allows for the identification of the loss of neutral fragments that cannot be directly analyzed by the detector because they possess no charge. Multiple reaction monitoring, also referred as selected reaction monitoring, selects a specific m/z for Q1, fragments it on q2, and monitors a single m/z in Q3. MRM is faster than the other three scans, allowing one to perform more monitoring cycles and therefore enhancing sensitivity. MRM does require the prior m/z knowledge of the parent ion and characteristic fragment.[46]

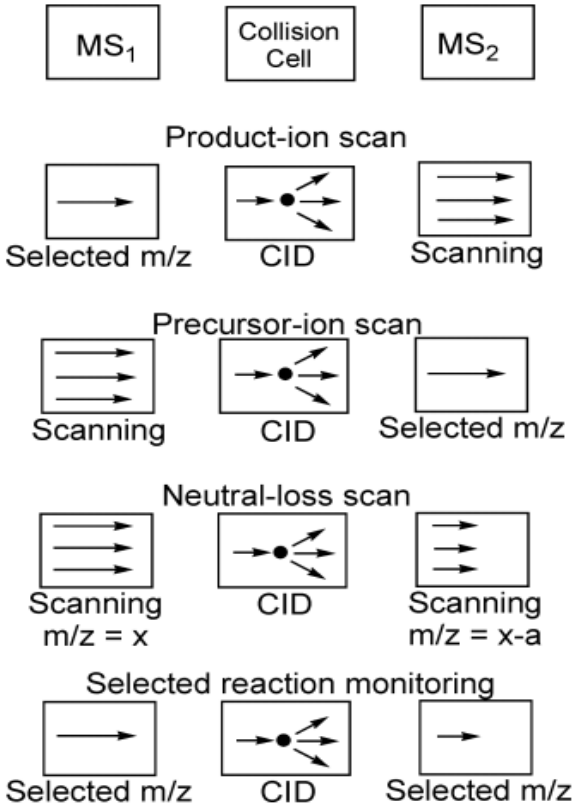

Figure 1.4.3: Common MS/MS scans modes.[46]

All MS experiments conducted in this dissertation were obtained with either a 4000 Qtrap® MS or a QStar® XL MS. A 4000 Qtrap® is a hybrid triple quadrupole-linear ion trap MS where Q1 is a regular quadrupole and the collision cell q2 is filled with N_2. The third quadrupole is a linear ion trap analyzer (LIT) composed of a quadrupole with two end electrodes connected to an AC generator at the ends of the quadrupole rod array. Ions are trapped axially by static DC potentials and trapped radially by the RF quadrupole field. Ions leave the LIT by radial mass-selective ion ejection which occurs when the RF voltage is ramped in the presence of an intense auxiliary AC voltage. Ions emerge from the LIT as the auxiliary AC resonance-ejection voltage is applied radially.[47] Fringing fields occur at both ends of the quadrupole because there is a diminution of the quadrupole field and coupling of radial and axial fields which leads to changes in the secular frequency and therefore ejection at unexpected stability coordinates.[48] Mass-selective axial ejection of ions from the LIT starts after a resonance excitation process gives a degree of radial excitation to the trapped ions that in the exit fringing-field results in axial ion kinetic energy that overcomes the exit DC barrier (of the exit lens), and allows the ions to reach the detector.[47,49] A modified schematic of a LIT is presented in Figure 1.4.4. Linear ion traps have greater ion capacity, higher trapping efficiencies, less mass discrimination and reduced effects of space charge in comparison to conventional three-dimensional ion traps.[49]

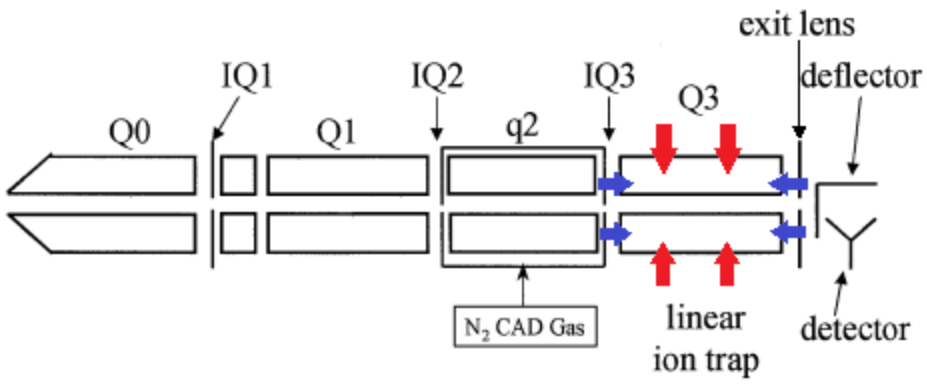

Figure 1.4.4: Modified schematic of the essential elements of the 4000 QTRAP® system. The red arrows represent the radial trapping while the blue arrows represent the axial trapping when Q3 is used as a LIT. IQ 1,2 & 3 demonstrate the three differential pumping apertures.[47]

The QStar® XL MS is a hybrid quadrupole-time of flight (TOF) MS. The instrument contains a Q1, a collision cell with q2 followed by an orthogonal TOF (Figure 1.4.5). A TOF is a mass analyzer that provides enhanced resolution, ion transmission and analysis speed in comparison to quadrupoles.[45] A TOF lacks the capability of acting as a mass filter, thus the only tandem MS scan that it is capable of performing is product ion scans. The ion accelerator accelerates ions orthogonally into the drift region via a pulsed magnetic field. Smaller ions travel faster than bigger ions and reach the detector at earlier times. The temporal separation that the TOF provides allows for the enhanced m/z resolution of the detected ions. TOF resolution can be compromised if ions arrive at the pulser with slight time difference which can be corrected via collisional dampening. Collisional dampening is achieved via a neutral inert gas used to slow down the ion beam and focus it in a smaller time frame. A reflectron ion mirror consisting of electrode rings that produce increasingly stronger magnetic fields enhance the mass accuracy by

doubling the time of flight path while correcting for slight variances in TOF arrival time for ions with identical m/z.[50]

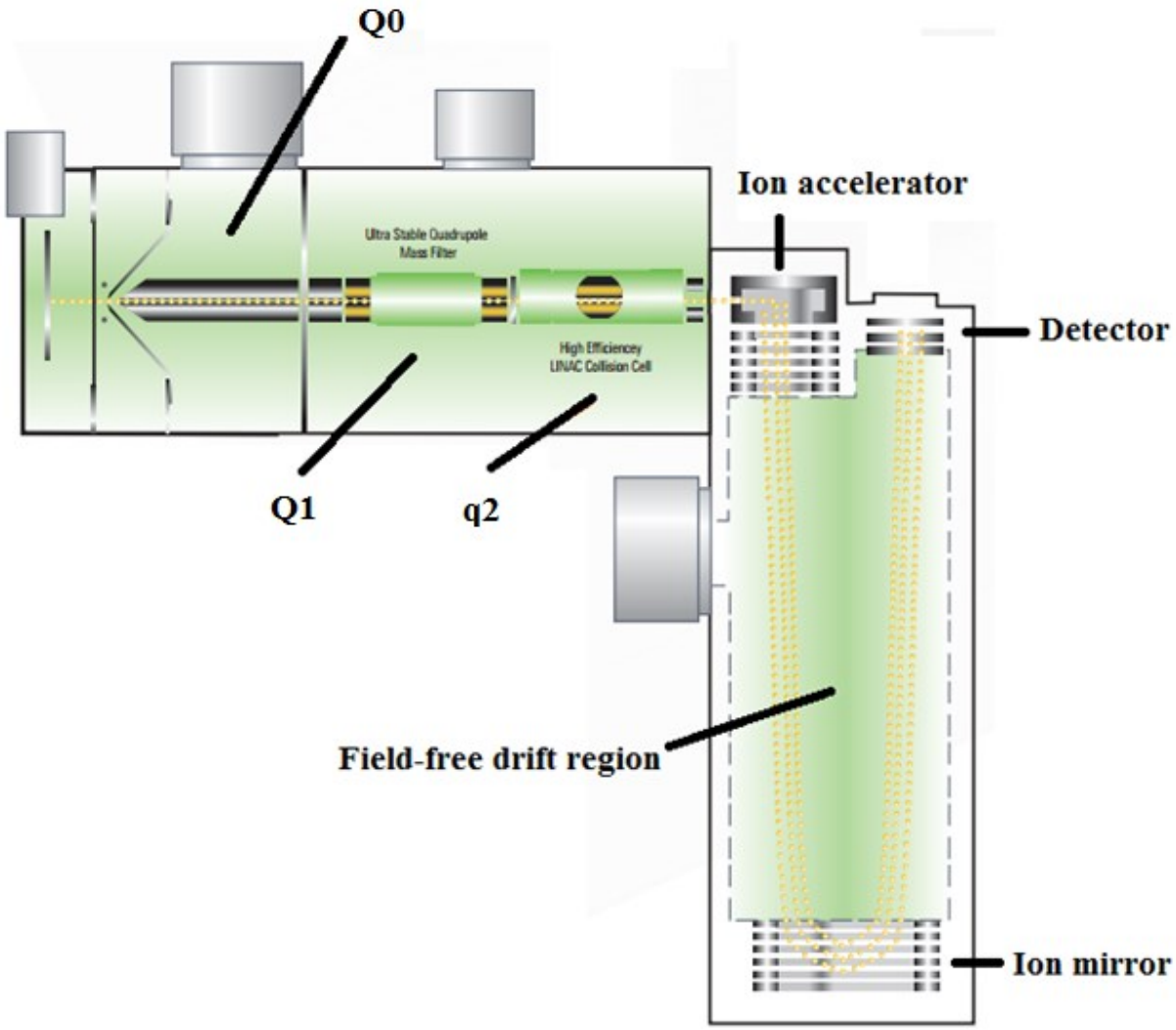

Figure 1.4.5: Adapted schematic diagram of a QStar® XL Hybrid LC/MS/MS system.[51]

After the ions are selected or scanned by the mass they reach the detector where the ion neutralization is converted into a quantifiable electric signal. The hybrid triple quadrupole-LIT uses a channel electron multiplier detector (CEM). A CEM is a type of secondary electron multiplier (SEM). Secondary electron emission is a fundamental process in which a single

electron can induce emission of one to three electrons when bombarded on secondary emissive material. An electric potential allows for emitted electrons to accelerate to the next metal plate resulting in more secondary emissions resulting in a process that can be repeated several times. A continuous dynode structure requires the material of the electrodes to have high resistance to merge voltage-division and functions of secondary emission resulting in a CEM.[14] The continuous SEM with discrete diodes and a CEM are presented in Figure 1.4.6. Ion impingement at the electrode of the MS detector results in secondary electron emission. The electron cascade is collected at an anode and converted into measurable electrical current providing ion intensities proportional to ion impingement.[52] The hybrid quadrupole-TOF MS uses a chevron micro-channel plate (MPC). TOF instruments require MPC detectors because of the spatial differences of incoming ions. Two microchannel plates with angled channels rotated 180 degrees from each other produce a chevron shape which results in ion feedback reduction. Ion impingement on the first plate results in electron emission. The emitted electrons travel through the channel resulting in further electron releases with each additional collision. The electron cascade reaches the second plate due to an applied electric field, resulting in electron emission being further amplified. The electron cascade is collected at an anode and measured like in the CEM detector.[53]

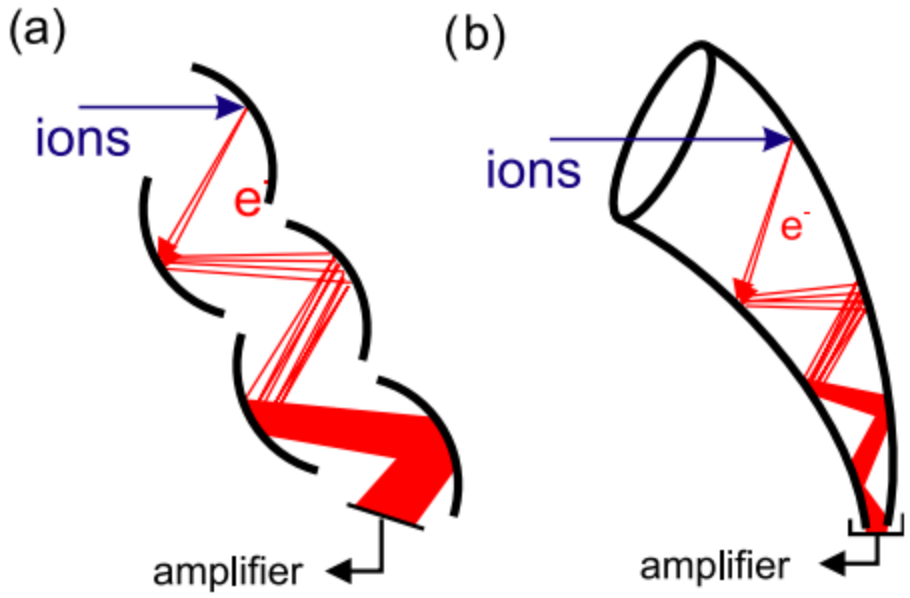

Figure 1.4.6: SEM with discrete dynodes (a) and CEM with one continuous dynode (b).[54]

1.5 Phospholipids studied and their MS analyses

Phospholipids encompass all lipid species with a phosphate group. All phospholipids are part of either the glycerophospholipids lipid category or the sphingomyelin class of sphingolipids. This dissertation focuses on four different classes of phospholipids, three glycerophospholipids classes (PC, PE & PS) and one sphingomyelin class (SM).[36] The general backbones for these four classes are presented in Figure 1.5.1.

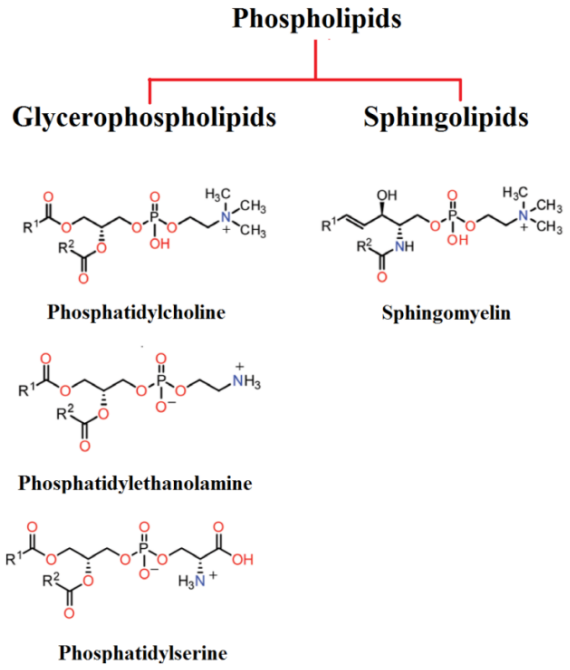

Figure 1.5.1: Phospholipids studied in this dissertation.

Phosphatidylcholine and sphingomyelin

PC species are the most abundant species of neutral phospholipids in eukaryotic cells and they composed approximately fifty percent of the lipid content in mammalian cells. The polar head group is composed of a choline molecule containing a quaternary ammonium species with three methyl substituents and a phosphate group linking the glycerol backbone and the choline

molecule. The first ESI-MS PC species studied were platelet-activating factors (PAF). They are PC with a short-chain acetate at the *sn*-2 position and an ether moiety on the *sn*-1 position. PAFs have been thoroughly studied because of their potent biological activity as activator and mediator of many leukocyte functions including platelet aggregation, degranulation, inflammation and anaphylaxis. They have also been involved with vascular permeability, oxidative burst, chemotaxis of leukocytes, and augmentation of arachidonic acid metabolism in phagocytes. PAFs have also been shown to induce apoptosis.[55,56] Sphingomyelins are main components of lipid rafts which are assemblies of phospholipids and cholesterol in the plasma membrane of cells forming domains with many protein components necessary for cell signaling.[57] Nerve cells, red blood cells and ocular lenses contain a significantly higher concentration of SM and SM is particularly common in the myelin sheath that surrounds some nerve cell axons.[58] More examples for the biological relevance of PC and SM can be found in section 4.2 (the introduction of Chapter 4).

ESI and MALDI are the most sensitive ionization methods to study PC and SM. ESI has proven to being 2 to 3 orders of magnitude better than fast-atom bombardment ionization[59], which was the best technique to study PC species before the advent of ESI and MALDI. Because of the permanently fixed charge on the choline head group, PC and SM species readily form an $[M+H]^+$ ion by ESI as the phosphate can be protonated during the electrospray process. The use of a weak acid as a protonating agent further promotes the phosphate protonation process and hence increases sensitivity. In biological extracts the presence of sodium leads to the favourable formation of $[M+Na]^+$ species. Both protonated and sodiated species can be analyzed via positive ion electrospray.[36] Even with the addition of a protonating agent, the PC signal will be divided between formation of protonated and sodiated adducts, resulting in lower sensitivity. If other

alkali metals, such as lithium and potassium, or cations such as ammonium are present the PC signal will be further divided and hindered. Negative ion species can be formed by the abstraction of a N-methyl group from the quaternary ammonium species during ESI.[60] Alternatively adducts with anions such as acetate and chloride result in the formation of $[M+OAc]^-$ and $[M+Cl]^-$ that can be analyzed via negative ion mode.[61] It is imperative to understand that PC and SM preferentially ionize via positive ion electrospray, resulting in the negative ion signal of PC and SM species being much lower than their positive counterpart. CID decomposition of positive protonated PC and SM ions yields a typical phosphocholine ion of m/z 184, characteristic of all phosphocholine containing species. This diagnostic ion leads to the characteristic PIS of m/z 184 for PC and SM species.[62]

Attention must be paid to the offset potential used for the CID of PC species. PC standards signal was found to be quite dependent on the molecular weight and radyl substituents of the analytes.[62] Collisional activation of PC lithium adducts results in the loss of the fatty acyl groups, enabling their identification.[63] Collisional activation of the potassium adduct of PC along with trifluoroacetic acid corresponds to the fatty-acyl groups, with the loss of the *sn*-1 fatty acyl substituent being more common.[64] The formation of acetate PC adducts via negative ion ESI and the subsequent decomposition of that ion into $[PC-15]^-$ after the loss of methyl acetate allows for the identification of fatty acyl groups.[61] It is important to remember that the fatty acyl signal produced either by positive ion mode alkali metal charge induced dissociation, or by negative ion adduct fragmentation is orders of magnitude smaller than the parent ion protonated signal. The fatty acyl composition of low abundance lipids cannot be identified since a significant amount of analyte must be present.

Atmospheric pressure chemical ionization (APCI) MS studies on protonated SM species have provided SM fragments produced by the higher energy ionization that can be further fragmented via CID to reveal loss of trimethylamine, loss of trimethylamine plus water, and loss of ceramide-specific ions.[65] It is important to note that high amounts of parent protonated SM species are required to carry the pseudo MS/MS/MS experiments. Studies on sodiated and lithiated SM species revealed specific information of the SM's ceramide and long-chain base (LCB) or N-acyl group produced via alkali metal charged induced dissociation.[66] The peaks produced for the ceramide and N-acyl group are small compared to the other peaks produced by alternate fragmentation pathways. A more detailed discussion of the advantage of phospholipid tandem MS scans for identification and quantitation is presented in the phospholipid tandem MS scan section below.

Phosphatidylethanolamine

PE is usually the second most abundant species in mammalian cells. Along with PC, PE species are the only two phospholipid classes with plasmalogen species.[36] PE plays a significant role in membrane fusion and in disassembly of the contractile ring during cytokinesis during cell division.[67] PE is highly enriched in the inner leaflet of the cellular plasma membrane. The extent of bilayer asymmetry is an important feature of cellular activation. The PE content can lead to differences in the membrane curvature. The PE content of nervous tissue contains a higher amount of PE species. PE produces a more viscous lipid membrane in comparison to PC.[68] More examples for the biological relevance of PE can be found in section 4.2 (the introduction of Chapter 4).

PE species readily protonate and deprotonate via positive and negative ESI to form the $[M+H]^+$ or $[M-H]^-$ ions . The addition of a weak acid or a weak base further enhances the protonation or deprotonation process. CID of the protonated PE yields the abundant and characteristic neutral loss of 141 Th[61] which corresponds to the loss of the polar headgroup. The CID of the deprotonated PE mainly yields carboxylate anions enabling the structural determination of the fatty acyl constituents.[69] A PE complexed with Ni^{++} allowed for the sn-1 and sn-2 substituents to be identified.[70] The CID study of lithiated PE demonstrated the predominant loss of the ethanolamine headgroup as aziridine, with the phosphate remaining attached to the glycerol backbone. The resulting $[M+Li]^+$ ion underwent a secondary loss of the fatty acyl groups as a neutral carboxylic acid or a neutral ketene. The *sn*-1 losses were more abundant than the *sn*-2 losses. When the dilithiated ion was studied $[M-H+2Li]^+$ only the *sn*-2 carboxylate anion was found.[71] The lithiated studies can provide insight into the positions of the radyl groups. If it weren't for this redeeming contribution, the lithiated PE studies would be inferior and more laborious than the negative ion mode identification of fatty acyl groups. Attaching various metals to PE species followed by CID yielded similar results to PC alkali metal studies.

Phosphatidylserine

In the plasma membrane, PS, like PE, is almost exclusively localized on the inner leaflet. During apoptosis the plasma membrane is altered so that PS molecules are translocated to the outer leaflet of the cellular plasma membrane by the enzyme flippase. The appearance of PS at the outer leaflet is in large part responsible for the recognition of the apoptotic cell by macrophages and subsequent phagocytosis, as well as cell adhesion and platelet aggregation.[72] PS is able to produce positive and negative ions by protonation and deprotonation via positive or

negative ESI. The addition of a mild acid or base further enhances the formation of a positive or negative ion. The negative ion has been reported to dominate over the positive ion.[73] This happens because the positive ion signal is heavily divided between protonated, sodiated and disodiated species. PS has a very high affinity for sodium. CID studies on protonated PS yield abundant ions corresponding to the neutral loss of 185 corresponding to the loss of the polar headgroup. CID studies on the deprotonated equivalent yields the predominant neutral loss of 87 corresponding the loss of serine and a more abundant loss of the *sn*-2 fatty acyl. The $[M-88-R_2COOH]^-$ ion is hypothesized to arise from the neutral loss of the *sn*-2 fatty acyl and formation of a cyclic phosphate anion. More importantly, carboxylate anions also result from the CID of deprotonated PS species allowing to identify the esterified fatty-acyl substituents.[74]

Phospholipid non-tandem MS scans

Non-tandem MS analysis of PC, SM, PS, PE or any other phospholipid is very effective when there is no sample complexity, which occurs rarely. Most lipid biological extracts are severely complex and different phospholipids with their different adduct formation lead to isobaric overlapping between different species preventing their identification or quantitation. Lipid m/z overlap with low resolution instruments is severe in complex samples. For example, with low resolution instruments each even m/z value could be attributed to a mixture of possible PC, PE, or PS protonated species, possible PC, PE and PS sodiated species or possible PA, PG and PI ammoniated species. Even when using high resolution MS instruments capable of providing extremely accurate m/z ratios, there is isobaric overlap between different species. $[PC+H]^+$ species with even chained radyl groups overlap with $[PE+H]^+$ species with one odd radyl group, as well as overlap with $[PA+NH_4]^+$ species with even chained radyl groups.

$[PS+H]^+$ species overlap with $[PG+NH_4]^+$ species.[75] The over-complication of spectra via shotgun lipidomics is further explained in Chapter3.

To avoid the formation of different adducts, the use of HPLC is imperative to remove all unwanted cations. Reversed phase separation enables the separation of phospholipid species based on the hydrophobicity of their radyl constituents. A high resolution instrument must be used with reversed phase separation since a plethora of radyl chain lengths, double bond number and distribution, and existence of E and Z configurations can result in the co-elution of different phospholipid species with the same m/z indistinguishable to low resolution instruments. Proton competition and an inherent decrease in signal will be proportional to the complexity of the sample. The use of normal phase HPLC separation enables the separation of different phospholipid classes, but severe proton competition due to all phospholipid species of a specific class eluting at the same time leads to decreased sensitivity. Normal phase lacks the ability that reversed phase has to differentiate between some isobaric species with different carbon distributions between their two radyl constituents. For example, two PC species with isobaric masses such as PC(10:0/10:0) and PC(16:0/4:0) will have different elution times via reversed phase and will therefore be easily differentiated, but will elute at the same time with normal phase.

A two dimensional separation of lipids composed by normal phase followed by reversed phase provides the best separation and sensitivity, at the expense of a long, labour intensive procedure. The solvents used between normal phase and reversed phase separation are incompatible with each other so fractions must be collected, the solvent removed and then introduced to the second dimension of separation. Some groups have developed online two dimensional procedures that reduce the labour and time required[76], but use specialized equipment

that is difficult to acquire. An easier alternative to circumvent the issues previously outlined is via the use of tandem MS analyses.

Phospholipid tandem MS scans

Tandem MS analyses that use a specific precursor ion or neutral loss fragment characteristic of the CID of a specific phospholipid headgroup allow the ability to obtain spectra specific to all the different species within that phospholipid class. The spectra obtained via tandem MS analyses allows for easy identification and quantitation of phospholipid species as there are no other species present besides the phospholipid class of interest. The noise levels for these scans are also much lower than non-tandem MS scans, greatly simplifying the identification of low abundant species. The use of HPLC separation with tandem MS scans is recommended since adduct formation and proton competition still result in decreased sensitivity. Reversed-phase is also useful for the temporal separation of some isobaric species. A PIS of m/z 184 in positive ion mode is specific for $[PC+M]^+$ and $[SM+M]^+$ species. A positive ion mode NL scan of 185 Da and 141 Da are specific to $[PS+M]^+$ and $[PE+M]^+$ species, respectively. Alternatively a negative ion mode NL scan of 87 Da is specific for $[PS-H]^-$ species. A negative ion mode PIS of m/z 196 with poor sensitivity is specific for $[PE-H]^-$ species.

1.6 Preamble

LC-MS/MS analyses provide a robust analytical technique to study phospholipids much more sensitive and versatile than any other analytical method used previously. But there are still several limitations in this field of study. The shotgun lipidomics approach is powerful when used with a high resolution mass spectrometer, but lack of sample desalting leads to the signal of several phospholipids being divided between 2, 3 or more ionization states that decreases analyte

sensitivity and complicates the spectra. Addition of optimal concentrations of protonating or deprotonating agents are not enough to eliminate other ionization states such as the formation of sodiated adducts which species like PC, SM, PE and PS readily form. Proton competition occurs prominently in shotgun lipidomics studies and is a major contributor to analyte sensitivity hindrance. Implementation of chromatographic separation such as HPLC adds analysis time, but allows desalting of the sample which eliminates for the most part the creation of different ionization states. Proton competition is reduced in comparison to the shotgun approach, but still causes a significant sensitivity hindrance to the affected analytes. Lipid carry-over between different samples is an issue when using HPLC and can severely hinder quantitation.

The goal of the studies presented in this dissertation was to develop a technique that solves the issues of signal splitting and proton competition for PE, PS, PC and SM analytes, while providing a general sensitivity enhancement to the phospholipid classes studied. The following chapters will thoroughly describe the methodology, experiments and findings of trimethylation enhancement using diazomethane (TrEnDi). TrEnDi enabled the eradication proton competition and signal splitting while providing drastic sensitivity enhancements to PE and PS species, and modest sensitivity enhancement to PC and SM species. TrEnDi was demonstrated to be compatible with shotgun and LC-MS studies (with exception of PS species which can only be analyzed via a shotgun approach). TrEnDi demonstrated to enhance analyte signal in MS and tandem MS studies. TrEnDi proved to be compatible with complex biological samples as well as with simple standard mixtures. Chapter 2 describes the development and application of TrEnDi on phospholipid standards via shotgun lipidomics. Chapter 3 provides some insights into tandem MS analyses as well as LC-MS procedure optimization. Chapter 4

describes the use of ^{13}C-TrEnDi for the successful methylation and sensitivity enhancement of complex biological lipid extracts.

1.7 References

(1) Fahy, E.; Subramaniam, S.; Brown, H. A.; Glass, C. K.; Merrill, A. H.; Murphy, R. C.; Raetz, C. R. H.; Russell, D. W.; Seyama, Y.; Shaw, W.; Shimizu, T.; Spener, F.; van Meer, G.; VanNieuwenhze, M. S.; White, S. H.; Witztum, J. L.; Dennis, E. A. *J. Lipid Res.* **2005**, *46* (5), 839–861.

(2) Fahy, E.; Subramaniam, S.; Murphy, R. C.; Nishijima, M.; Raetz, C. R. H.; Shimizu, T.; Spener, F.; van Meer, G.; Wakelam, M. J. O.; Dennis, E. A. *J. Lipid Res.* **2009**, *50 Suppl*, S9–S14.

(3) Bou Khalil, M.; Hou, W.; Zhou, H.; Elisma, F.; Swayne, L. A.; Blanchard, A. P.; Yao, Z.; Bennet, S. A.; Figeys, D. *Mass Spectrom. Rev.* **2010**, *29*, 877–929.

(4) Small, D. M. *The Physical Chemistry of Lipids. Handbook of Lipid Research*; Plenum Press: New York, 1986.

(5) Vance, D. E.; Vance, J. E. *Biochemistry of Lipids, Lipoproteins and Membranes*; Elsevier Science: New York, 2002.

(6) Ohlrogge, J. B.; Jaworski, J. G. *Annu. Rev. Plant Physiol. Plant Mol. Biol.* **1997**, *48*, 109–136.

(7) Coleman, R. A.; Lee, D. P. *Prog. Lipid Res.* **2004**, *43* (2), 134–176.

(8) Hirschmann, H. *J. Biol. Chem.* **1960**, *235* (10), 2762–2767.

(9) Påhlsson, P.; Spitalnik, S. L.; Spitalnik, P. F.; Fantini, J.; Rakotonirainy, O.; Ghardashkhani, S.; Lindberg, J.; Konradsson, P.; Larson, G. *Arch. Biochem. Biophys.* **2001**, *396* (2), 187–198.

(10) Bach, D.; Wachtel, E. *Biochim. Biophys. Acta - Biomembr.* **2003**, *1610* (2), 187–197.

(11) Tsai, M.; O'Malley, B. W. *Annu. Rev. Biochem.* **1994**, *63*, 451–486.

(12) Jones, G.; Strugnell, S. A.; DeLuca, H. F. *Physiol. Rev.* **1998**, *78* (4), 1193–1231.

(13) Russell, D. W. *Annu. Rev. Biochem.* **2003**, *72*, 137–174.

(14) Demmig-Adams, B.; Adams, W. W. *Science* **2002**, *298* (5601), 2149–2153.

(15) Ricciarelli, R.; Zingg, J. M.; Azzi, A. *FASEB J.* **2001**, *15* (13), 2314–2325.

(16) Helenius, A.; Aebi, M. *Science* **2001**, *291* (5512), 2364–2369.

(17) Raetz, C. R. H.; Whitfield, C. *Annu. Rev. Biochem.* **2002**, *71*, 635–700.

(18) Ghangas, G. S.; Steffens, J. C. *Proc. Natl. Acad. Sci. USA.* **1993**, *90* (21), 9911–9915.

(19) Katz, L. *Chem. Rev.* **1997**, *97* (7), 2557–2576.

(20) Reeves, C. *Crit. Rev Biotechnol* **2003**, *23*, 95–147.

(21) Khosla, C.; Gokhale, R. S.; Jacobsen, J. R.; Cane, D. E. *Annu. Rev. Biochem.* **1999**, *68*, 219–253.

(22) Walsh, C. T. *Science* **2004**, *303* (5665), 1805–1810.

(23) Peretó, J.; López-García, P.; Moreira, D. *Trends Biochem. Sci.* **2004**, *29* (9), 469–477.

(24) Cronan, J. E. *Annu. Rev. Microbiol.* **2003**, *57* (17), 203–224.

(25) Mueller, H. W.; Purdon, A. D.; Smith, J. B.; Wykle, R. L. *Lipids* **1983**, *18* (11), 814–819.

(26) Scherrer, L. A.; Gross, R. W. *Mol. Cell. Biochem.* **1989**, *88* (1-2), 97–105.

(27) Piomelli, D.; Astarita, G.; Rapaka, R. *Nat. Rev. Neurosci.* **2007**, *8* (10), 743–754.

(28) Chester, M. A. *Eur. J. Biochem.* **1998**, *257* (2), 293–298.

(29) Taki, T.; Ishikawa, D. *Anal. Biochem.* **1997**, *251* (2), 135–143.

(30) Harris, D. *Quantitative Chemical Analysis*, 8th ed.; Freeman: New York, 2010; pp 543-544.

(31) Cheng, Y. S.; Zheng, Y.; VanderGheynst, J. S. *Lipids* **2011**, *46* (1), 95–103.

(32) Yu, Y.; Vidalino, L.; Anesi, A.; Macchi, P.; Guella, G. *Mol. Biosyst.* **2014**, *10* (4), 878–890.

(33) Fletouris, D. J.; Botsoglou, N. A.; Psomas, I. E.; Mantis, A. I. *J. Dairy Sci.* **1998**, *81* (11), 2833–2840.

(34) Gutnikov, G. *J. Chromatogr. B Biomed. Appl.* **1995**, *671* (1-2), 71–89.

(35) Yang, K.; Cheng, H.; Gross, R.; Han, X. *Anal. Chem.* **2009**, *81* (11), 4356–4368.

(36) Pulfer, M.; Murphy, R. C. *Mass Spectrom. Rev.* **2003**, *22* (5), 332–364.

(37) Wang, M.; Hayakawa, J.; Yang, K.; Han, X. *Anal. Chem.* **2014**, *86* (4), 2146–2155.

(38) Griffiths, I. W. *Rapid Commun. Mass Spectrom.* **1997**, *11* (1), 2–16.

(39) Boggess, B. Ionization Modes. *University of Notre Dame Mass Spectrometry and Proteomics Facility.* [Online] **2015**. http://massspec.nd.edu/instruments-and-analyses/ionization-modes/ (accessed July 12, 2015).

(40) Aebersold, R.; Mann, M. *Nature* **2003**, *422* (6928), 198–207.

(41) Karas, M.; Krüger, R. *Chem. Rev.* **2003**, *103* (2), 427–439.

(42) Karas, M.; Bahr, U.; Dulcks, T. *Fresenius J. Anal. Chem.* **2000**, *366* (6-7), 669–676.

(43) Ikonomou, M. G.; Blades, A. T.; Kebarle, P. *Anal. Chem.* **1991**, *63* (18), 1989–1998.

(44) Ho, C. S.; Lam, C. W. K.; Chan, M. H. M.; Cheung, R. C. K.; Law, L. K.; Lit, L. C. W.; Ng, K. F.; Suen, M. W. M.; Tai, H. L. *Clin. Biochem. Rev.* **2003**, *24* (1), 3–12.

(45) Douglas, D. J. *Mass Spectrom. Rev.* **2009**, *28* (3), 937–960.

(46) Griffiths, W. J.; Wang, Y. *Chem. Soc. Rev.* **2009**, *38* (7), 1882–1896.

(47) Londry, F. A.; Hager, J. W. *J. Am. Soc. Mass Spectrom.* **2003**, *14* (10), 1130–1147.

(48) Prestage, J. D.; Dick, G. J.; Maleki, L. *J. Appl. Phys.* **1989**, *66* (3), 1013–1017.

(49) Hager, J. W. *Rapid Commun. Mass Spectrom.* **2002**, *16* (6), 512–526.

(50) Guilhaus, M.; Selby, D.; Mlynski, V. *Mass Spectrom. Rev.* **2000**, *19* (2), 65–107.

(51) Adams, J.; Manley, B. W. *IEEE Trans. Nucl. Sci.* **1966**, *13* (3), 88–99.

(52) Seah, M. P.; Lim, C. S.; Tong, K. L. *J. Electron Spectros. Relat. Phenomena* **1989**, *48* (1), 209–218.

(53) Wiza, J. L. *Nucl. Instrum. Methods* **1979**, *162*, 587–601.

(54) Benedikt, J.; Hecimovic, A.; Ellerweg, D.; von Keudell, A. *J. Phys. D. Appl. Phys.* **2012**, *45* (40), 403001.

(55) Weintraub, S. T.; Pinckard, R. N.; Hail, M. *Rapid Commun. Mass Spectrom.* **1991**, *5* (7), 309–311.

(56) Hondo, Z.; Ishii, S.; Shimizu, T. *J. Biochem.* **2002**, *131*, 773–779.

(57) Pike, L. J. *J. Lipid Res.* **2003**, *44* (4), 655–667.

(58) Cremesti, A. E.; Goni, F. M.; Kolesnick, R. *FEBS Lett.* **2002**, *531* (1), 47–53.

(59) Han, X.; Gross, R. W. *Proc. Natl. Acad. Sci. USA*. **1994**, *91* (22), 10635–10639.

(60) Harrision, K.; Murphy, R. *J. Mass Spectrom.* **1995**, *30* (August), 1772–1773.

(61) Kerwin, J. L.; Tuininga, A. R.; Ericssont, L. H. *J. Lipid Res.* **1994**, *35*, 1102–1114.

(62) Hsu, F. F.; Turk, J. *J. Am. Soc. Mass Spectrom.* **2003**, *14* (4), 352–363.

(63) Hsu, F. F.; Bohrer, A.; Turk, J. *J. Am. Soc. Mass Spectrom.* **1998**, *9* (5), 516–526.

(64) Ho, Y. P.; Huang, P. C. *Rapid Commun. Mass Spectrom.* **2002**, *16* (16), 1582–1589.

(65) Karlsson, a a; Michélsen, P.; Odham, G. *J. Mass Spectrom.* **1998**, *33* (12), 1192–1198.

(66) Hsu, F. F.; Turk, J. *J. Am. Soc. Mass Spectrom.* **2000**, *11* (5), 437–449.

(67) Emoto, K.; Kobayashi, T.; Yamaji, A.; Aizawa, H.; Yahara, I.; Inoue, K.; Umeda, M. *Proc. Natl. Acad. Sci. U. S. A.* **1996**, *93* (23), 12867–12872.

(68) Bevers, E.; Comfurius, P.; Dekkers, D.; Harmsma, M.; Zwaal, R. *Biol Chem* **1998**, *379* (8-9), 973–986.

(69) Hvattum, E.; Hagelin, G.; Larsen, A. *Rapid Commun. Mass Spectrom.***1998**, *12* (19), 1405–1409.

(70) Ho, Y.-P.; Huang, P.-C.; Deng, K.-H. *Rapid Commun. Mass Spectrom.* **2003**, *17* (2), 114–121.

(71) Hsu, F. F.; Turk, J. *J. Mass Spectrom.* **2000**, *35* (5), 595–606.

(72) Fadok, V. A.; De Cathelineau, A.; Daleke, D. L.; Henson, P. M.; Bratton, D. L. *J. Biol. Chem.* **2001**, *276* (2), 1071–1077.

(73) Koivusalo, M.; Haimi, P.; Heikinheimo, L.; Kostiainen, R.; Somerharju, P. *J. Lipid Res.* **2001**, *42* (4), 663–672.

(74) Hsu, F. F.; Turk, J. *Am. Soc. Mass Spectrom.* **2000**, *11*, 892–899.

(75) Fhaner, C. J.; Liu, S.; Ji, H.; Simpson, R. J.; Reid, G. E. *Anal. Chem.* **2012**, *84* (21), 8917–8926.

(76) Nie, H.; Liu, R.; Yang, Y.; Bai, Y.; Guan, Y.; Qian, D.; Wang, T.; Liu, H. *J. Lipid Res.* **2010**, *51* (9), 2833–2844.

Chapter 2: Trimethylation Enhancement using Diazomethane (TrEnDi) II: Rapid in-solution concomitant quaternization of glycerophospholipid amino groups and methylation of phosphate groups via reaction with diazomethane significantly enhances sensitivity in mass spectrometry analyses via a fixed, permanent positive charge.

Adapted with permission from Wasslen, K. V; Canez, C. R.; Lee, H.; Manthorpe, J. M.; Smith, J. C. *Anal. Chem.* **2014**, *86* (19), 9523–9532.

2.1 Abstract

A novel mass spectrometry (MS)-based lipidomics strategy that exposes glycerophospholipids to an ethereal solution of diazomethane and acid, derivatizing them to contain a net fixed, permanent positive charge is described. The sensitivity of modified lipids to MS detection is enhanced via improved ionization characteristics as well as consolidation of ion dissociation to form one or two strong, characteristic polar head group fragments. Our strategy has been optimized to enable *a priori* prediction of ion fragmentation patterns for four subclasses of modified glycerophospholipid species. Our method enables analyte ionization regardless of proton affinity, thereby decreasing ion suppression and permitting predictable precursor ion-based quantitation with improved sensitivity in comparison to MS-based methods that are currently used on unmodified lipid precursors.

2.2 Introduction

Lipids play an important role in a number of physiological functions. Their participation ranges from signal transduction pathways,[1-2] proliferation,[3] and apoptosis,[4-5] to membrane trafficking in the cell.[6-7] Aberrant lipid behavior has also been associated with a number of

neurodegenerative diseases,[8-9] diabetes[10] and cancer;[11] accordingly, many separation and analytical techniques have been implemented over the years to study lipids, including mass spectrometry (MS). The development of modern ionization techniques[12-15] has enabled much of the advancement that has been witnessed in this field, permitting MS to investigate the lipid composition of biological membranes and fluids.[16]

Glycerophospholipids are characterized by two fatty acyl groups and a polar head group attached to a common glycerol scaffold; sub-classification of glycerophospholipids is based on polar head group structure. The glycerophospholipid composition of membranes has been demonstrated to be dynamic and specific to different types of organelles.[16] For example, it has been reported that the outer membrane layer of plasma membranes are relatively rich in phosphatidylcholine (PC) and sphingomyelin (SM, a sphingolipid that is commonly analyzed with glycerophospholipids) species while the inner membrane layer has higher concentrations of phosphatidylethanolamine (PE) and phosphatidylserine (PS) lipids.[17] Furthermore, organellar membranes are modeled to have a higher degree of unsaturation compared to plasma membranes to enhance membrane fluidity and thereby facilitate protein migration and fusion-related events.[16-17] Phospholipase A2 enzymes cleave glycerophospholipids within cellular membranes to form products that are bioactive and play a role in cellular homeostasis. For example, platelet activating factor (PAF, 1-O-alkyl-2-acetyl-*sn*-glycero-3-phosphocholine) has been demonstrated to elicit the aggregation and degranulation of platelets, as well as play a role in the activation of neutrophils, contraction of smooth muscle and stimulation of glycogenolysis.[18] The importance of characterizing the prevalence and dynamics of glycerophospholipids has led to a dramatic rise in lipidomics literature and attention in the scientific community.[19]

Although numerous publications have emerged on MS-based lipidomics, many challenges remain in this field. Glycerophospholipids are a heterogeneous group of biomolecules with very similar chemical properties, most notably their hydrophobicity. The benefits of using chromatography on complex lipid samples are debated;[20] a great deal of research presently uses "shotgun lipidomics" approaches, where complex samples are directly electrosprayed and spectral data is summed over time. Although effective, there are drawbacks to shotgun methods, including the congestion of spectra if lower resolution instruments are employed, signal being divided between protonated and cationized states (e.g. sodium) due to a lack of chromatographic desalting and the risk of ion suppression for lipid species with low proton affinities. These drawbacks have been recognized by other groups who have previously established methods that enhance lipid ionization, including modifying glycerophospholipid species to contain fixed positive charges using isotopically-labeled sulfonium ions[21] as well as the functionalization of diacylglycerol lipids to contain a fixed quaternary ammonium group[22] or an amine group thereby increasing proton affinity.[23]

Chemical derivatization may also be conducted using diazomethane, which has been recently demonstrated to be useful for converting primary amines into quaternary amines and thus invoke a permanent fixed positive charge on peptide analytes.[24] Diazomethane has been previously used to methyl esterify fatty acids for separation via gas chromatography (GC) and analysis using MS.[25-27] It has been used to convert dipalmitoyl phosphatidylethanolamine to dipalmitoyl phosphatidyl [*N*-methyl-^{3}H] choline;[28] however, it has not been shown to successfully methylate both the primary amines and phosphate moieties found in glycerophospholipids. Trimethylsilyldiazomethane has also been used to methylate phosphate

moieties and carboxylic acids in glycerophospholipids,[29-30] yet was not reported to derivatize other functional groups, including primary amines.

Herein we describe a novel, rapid and cost-effective approach to enhance the sensitivity of MS-based lipidomic analyses by harnessing the reactivity and chemoselectivity of diazomethane. Trimethylation enhancement using diazomethane, or TrEnDi, is a chemical derivatization strategy that results in the complete and concomitant methylation of phosphate moieties, carboxylic acids and primary amines, rendering phosphatidylethanolamine (PE), phosphatidylcholine (PC), sphingomyelin (SM) and phosphatidylserine (PS) phospholipids permanently positively charged. Sensitivity enhancements were observed for all subclasses of lipids, particularly in tandem mass spectrometry (MS/MS) experiments where ion fragmentation was consolidated to only one or two channels, in agreement with previous literature.[16,31] This strategy represents a facile method to dramatically enhance the sensitivity of lipidomics analyses that investigate the roles that lipids play in cellular biochemistry.

2.3 Experimental

Chemicals and materials. *N*-methyl-*p*-toluenesulfonamide (NMPTS), formic acid and tetrafluoroboric acid dimethyl ether complex were purchased from Sigma-Aldrich (St. Louis, MO, USA); absolute ethanol was obtained from Commercial Alcohols Inc. (Brampton, ON, Canada); potassium hydroxide, isopropanol and ether were purchased from Caledon Laboratories Ltd. (Georgetown, ON, Canada); sodium nitrite was obtained from BDH Chemicals Ltd. (Poole, England); glacial acetic acid, 28% ammonium hydroxide, and ammonium acetate were acquired from Anachemia Canada Inc. (Montreal, QC, Canada). PE(16:0/18:1(9Z)), PC(18:1(9Z)/14:0),

PS(18:0/18:2(9Z,12Z)) and SM(d18:1/16:0) were synthesized by and obtained from Avanti Polar Lipids Inc. (Alabaster, Alabama, USA).

Preparation of lipid solutions. PE (16:0/18:1(9Z)), PC (18:1(9Z)/14:0) and SM (d18:1/16:0) lipids were purchased as solutions in chloroform and were dried using nitrogen gas and redissolved in ethanol. PS (18:0/18:2(9Z,12Z)) was purchased as a powder and was dissolved in ethanol.

***N*-methyl-*N*-nitroso-*p*-toluenesulfonamide (Diazald) production.** *N*-methyl-*N*-nitroso-*p*-toluenesulfonamide was synthesized from NMPTS as previously described[32] and reported by our groups.[24]

Diazomethane production. *All reactions involving the preparation of diazomethane should be carried out in an efficient chemical fume hood and behind a safety blast shield because of the toxic and potentially explosive nature of diazomethane.* The production of diazomethane was performed using a Sigma-Aldrich Mini Diazald Diazomethane generator with fire-polished clear-seal joints, as has been described elsewhere,[33] and previously reported by our groups.[24]

In-solution chemical derivatization. 2 mL clear glass vials were flushed with nitrogen gas for approximately 2 minutes prior to adding 10 μL of ethanol followed by either 15 nmol or 75 pmol of lipid as a solution in ethanol to ensure derivatization worked on a range of lipid concentrations. 0.5 μL of a 14:1 solution of freshly prepared and vigorously mixed ether and tetrafluoroboric acid (HBF_4) dimethyl ether complex was added to the vials containing the lipid standards. Lipids were derivatized by adding enough of the ethereal diazomethane solution (approximately 250-300 μL) to the vials such that the colour remained yellow for approximately 5 seconds. The solution was carefully swirled for several seconds followed by immediate drying

under a stream of nitrogen gas. Once completely dried, the modified lipids were resuspended in 100 μL ethanol.

ESI-MS and MS/MS analyses. 3 μL of the resuspended solution was inserted into a Proxeon nanoelectrospray emitter (Thermo Scientific, Odense, Denmark) followed by direct analysis of the methylated lipids using an AB Sciex QStar XL mass spectrometer equipped with a nanoESI source (AB Sciex, Framingham, MA, USA) that was externally calibrated prior to each experiment. Spectra were obtained using a nanoESI voltage of 1000 V, declustering and focusing potentials of 30 V and 120 V, respectively and an MS/MS collision energy of 40 eV for PE, PC, and SM species and both 40 eV and 60 eV for PS lipids. After verifying that the sample was completely methylated, an equimolar amount of unmodified lipid was added to each solution containing modified lipid. 3 μL of the equimolar solution of modified and unmodified lipid was analyzed via direct infusion, as described above.

Following this, equimolar amounts of unmodified and modified PC, PS, PE and SM were directly infused into an AB Sciex 4000 QTRAP via a Turbo V ionspray source (AB Sciex, Framingham, MA, USA) using a Harvard 11 Plus syringe pump (Harvard Apparatus, Holliston, MA, USA) such that 1.0 pmol of each lipid was injected in total. Lipids were analyzed using precursor ion scanning (PIS) and neutral loss (NL) scanning modes as summarized in Table 2.3.1. Positive and negative ion mode spectra were acquired using ESI voltages of 5000 V and -4500 V, respectively and a declustering potential of 40 V. The optimized collision energies used for both unmodified and modified lipid species are listed in Table 2.3.1. In order to compare the relative protonation or deprotonation efficiencies of different buffers, 10 pmol of PE and PS were dissolved in ethanol solutions containing 10 mM ammonium hydroxide, 10 mM ammonium acetate and 10 mM acetic acid and analyzed as described above.

Table 2.3.1: Details of MS/MS experimental conditions before and after TrEnDi derivatization

Lipid species	MS/MS scan prior to TrEnDi derivatization		MS/MS scan following TrEnDi derivatization	
	Scan type	Collision energy (eV)	Scan type	Collision energy (eV)
PC	Positive PIS of m/z 184	40	Positive PIS of m/z 198	40
PE	Positive NL of m/z 141	25	Positive PIS of m/z 198	40
	Negative PIS of m/z 196	-50		
PS	Positive NL of m/z 185	23	Positive PIS of m/z 256	40
	Negative NL of m/z 87	-28	Positive PIS of m/z 144	60
SM	Positive PIS of m/z 184	40	Positive PIS of m/z 198	40

2.4 Results and Discussion

Our groups have recently published on the reactivity of diazomethane and demonstrated that a variety of functional groups can be simultaneously methylated by diazomethane, most notably primary amines to produce a quaternary ammonium ion.[24] An attractive feature of primary amine permethylation is that analytes may be rendered permanently positively charged, eliminating the need for protonation or cationization for gas phase ionization. In addition to creating fixed positive charges, TrEnDi also neutralizes negative charges via methylation of both phosphate groups and carboxylic acids. HBF_4 is the key to the success of lipidomics-based TrEnDi because it is highly acidic, enabling the protonation of the phosphate groups while also supplying a non-coordinating counterion (Figure 2.6.1). This ultimately prevents diazomethane from methylating the conjugate base of the acid, thereby directing all methylation to the lipids. Critically, this reaction concomitantly produces a fixed positive charge on the lipid via the formation of a quaternary ammonium ion and neutralizes the negative charge of the phosphate

group (and, in the case of PS, the carboxylate group) via the formation of the corresponding methyl ester (see Supporting Information for more details).

1-Palmitoyl-2-oleoyl-*sn*-glycero-3-phosphoethanolamine [PE(16:0/18:1(9Z))], was first used to investigate the effect of diazomethane on the phosphoethanolamine (PE) head group (Figure 2.4.1a). The unmodified PE signal was divided into two peaks: the protonated ion $[PE+H]^+$ at m/z 718.52 and $[PE+Na]^+$ at m/z 740.50 (Figure 2.4.1b). The MS/MS scan of $[PE+H]^+$ (m/z 718.52) (Figure 2.4.1c) reveals numerous fragmentation channels yielding many different product ions. In contrast, TrEnDi-modified PE ($[PE^{Tr}]^+$) (Figure 2.4.1d), produced a single ion with m/z 774.58, a total mass shift of +56 Da from the unmodified $[PE+H]^+$ indicating that the lipid had been methylated four times. MS/MS analysis of $[PE^{Tr}]^+$ yielded a spectrum containing a single, high intensity fragment, as observed in Figure 2.4.1e.

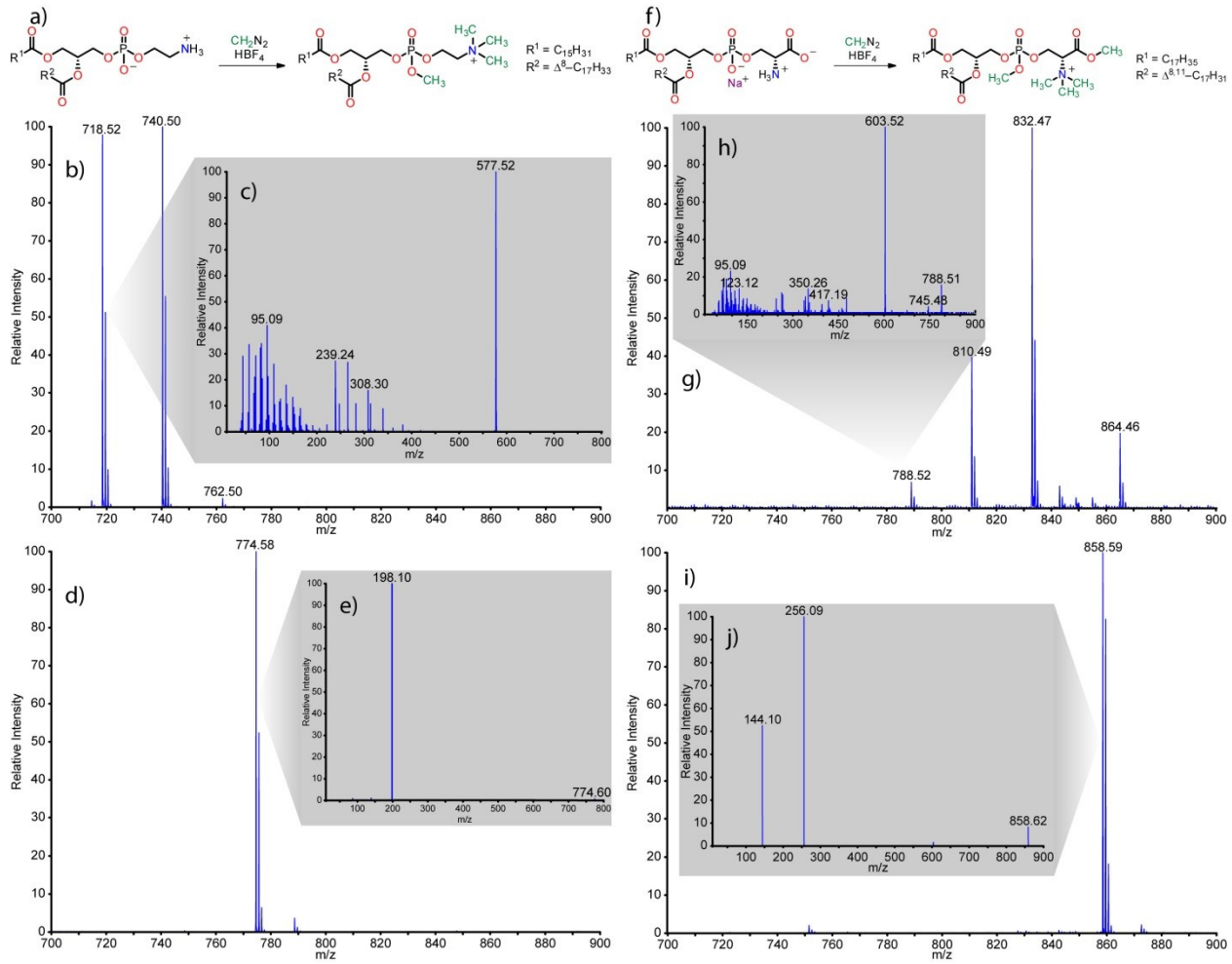

Figure 2.4.1: a) Derivatization of PE to $[PE^{Tr}]^+$ using diazomethane. b) Unmodified PE revealing protonated (m/z 718.52) ion and sodiated (m/z 740.50) adduct. c) Fragmentation of unmodified protonated PE at m/z 718.52 reveals MS signal divided among numerous fragmentation channels. d) Diazomethane adds four methyl groups to PE (m/z 774.58). e) MS/MS spectrum of $[PE^{Tr}]^+$ revealing a single fragmentation channel (m/z 198.10). f) Derivatization of PS to $[PS^{Tr}]^+$ using diazomethane. g) Unmodified PS revealing protonated, sodiated and doubly sodiated ions at m/z 788.52, m/z 810.49 and m/z 832.47, respectively. h) MS/MS of unmodified PS (m/z 788.52) reveals MS signal divided among numerous fragmentation channels. i) Diazomethane adds five methyl groups to PS (m/z 858.59). j)

MS/MS spectrum of $[PS^{Tr}]^+$ revealing two dominant fragmentation channels (m/z 144.10 and m/z 256.09).

MS/MS confirmed that four methyl groups[1Z] were added to the head group of $[PE^{Tr}]^+$, driving the fragmentation channels to a single product at m/z 198.09; this was likely due to the immobilization of charge on the newly formed quaternary ammonium ion. While it was predicted that the primary amine would trimethylate with diazomethane, our studies indicated that the phosphate oxygen was also methylated, resulting in a mass increase of 14 Da higher than an unmodified phosphocholine head group. Our observations reveal that TrEnDi derivatization collapses the signals of the protonated ion and the sodiated adduct of the unmodified lipid into a single peak (eliminating cationization) and consolidates ion fragmentation into a single characteristic channel for TrEnDi-modified PE lipids. The significance of these observations is that sensitivity is enhanced as PE is ionized in a single manner and may be analyzed by a highly sensitive PIS for m/z 198 rather than a NL scan for 141 Da, as is commonly employed.[16]

1-octadecanoyl-2-(9Z,12Z-octadecadienoyl)-*sn*-glycero-3-phospho-L-serine (sodium salt) [PS(18:0/18:2(9Z,12Z))] was evaluated to determine the chemistry of the ethereal diazomethane and HBF_4 solution to the phosphoserine head group (Figure 2.4.1f). Prior to modification, PS was observed to form multiple protonated and sodiated ions, due to competitive cationization with Na^+ (Figure 2.4.1g), while the MS/MS analysis of m/z 788.50 (Figure 2.4.1h) revealed a diversity of product ions dispersed among many fragmentation channels. The mass

[1Z] Throughout the document, the term methyl group is used with the acknowledgment that diazomethane is in fact contributing methylene group(s) to the lipid molecules thereby adding a mass of 14 Da. The chemistry replaces a hydrogen atom (1 Da) with a CH_3 group (methyl, 15 Da); however the net difference is the addition of a CH_2 group (methylene, 14 Da). The term methylation, or adding methyl groups, is consistent with the literature [Paik, Paik and Kim, Historical review: the field of protein methylation. In *Trends in Biochemical Sciences*, 2007; Vol. 32, pp 146-152.] and has been adopted in this manuscript.

spectrum of TrEnDi-modified PS ($[PS^{Tr}]^+$) revealed the base peak at m/z 858.59 (Figure 2.4.1i), indicating that PS is methylated five times and that the signal is no longer divided, as gas-phase cationization is eliminated on TrEnDi-modified lipids. MS/MS analysis confirmed that the methyl groups were all added to the polar head of PS: the primary amine was trimethylated and the phosphate and carboxylic acid groups were methylated (Figure 2.4.1j). Fragmentation of $[PS^{Tr}]^+$ revealed that ion dissociation was consolidated into two dominant channels, m/z 256.09 (lower collision energy) and m/z 144.10 (higher collision energy), highlighting new PIS modes for PS with enhanced sensitivity relative to methods that have been previously used (NL for 185 and 87 Da in the positive and negative ion modes, respectively).[16]

PC and SM are known to ionize well and fragment in a sensitive manner due to inherently possessing a quaternary ammonium-containing phosphocholine head group. It was therefore important to confirm that TrEnDi is compatible with PC and SM and observe if this chemistry affects the MS-based analytical sensitivity in any way. Prior to modification, MS/MS of PC and SM yielded the formation of the charged phosphocholine ion (data not shown), as expected and observed previously.[16, 31] Following TrEnDi, methylation of the phosphate group was observed, resulting in the removal of cationized species from the spectra and MS/MS analysis of $[PC^{Tr}]^+$ and $[SM^{Tr}]^+$ yielded one main fragment, m/z 198.10 (see Figures 2.6.2 and 2.6.3 in supporting information section of this chapter for details). The results of TrEnDi on each lipid are summarized in Table 2.4.1.

Table 2.4.1: Summary of results for TrEnDi-modified synthetic lipids

Lipid species	Unmodified			TrEnDi-modified			
	$[M+H]^+$ (Th)	$[M+Na]^+$ (Th)	$[M-H+2Na]^+$ (Th)	$[M^{Tr}]^+$ (Th)	Δm^a (Da)	% mod[b]	# Me[c]
PE(16:0/18:1(9Z))	718.52	740.52	N/A	774.59	56	100	4
PS(18:0/18:2(9Z,12Z))	788.50	810.59	832.57	858.67	70	100	5
PC(18:1(9Z)/14:0)	732.56	754.54	N/A	746.57	14	100	1
SM(d18:1/16:0)	703.60	725.58	N/A	717.60	14	100	1

[a]Difference in mass between the TrEnDi-modified lipid and the $[M+H]^+$ ion of the corresponding unmodified lipid.
[b]Percentage completion of the TrEnDi chemistry on the analyte sample
[c]Number of methyl groups added to each analyte molecule

As displayed in Table 2.4.1, all four lipid subclasses that were subjected to TrEnDi derivatization were successfully methylated to completion including phosphate, carboxy and primary amine groups. These results suggest that the efficacy of TrEnDi methylation is related to the pK_a values of the functional groups on the lipids: groups with pKa values of approximately 11 or less are rapidly modified to completion in the presence of ethereal diazomethane and HBF_4, in agreement with our previous findings on peptide analytes.[24]

MS sensitivity increases following TrEnDi. In order to investigate the effect of derivatization on sensitivity relating to inherent ionization efficiency and signal convergence to a single analyte peak in the presence of sodium cations (well-known interferents), equimolar amounts of unmodified lipid standards (containing sodium) and their TrEnDi-modified forms were dissolved in ethanol that was devoid of additional protonation agent and analyzed by MS, as summarized in Figure 2.4.2 and Table 2.4.2. In the case of PE (Figure 2.4.2a), there was an overall sensitivity increase of over two-fold following derivatization when $[PE^{Tr}]^+$ was compared to the sum of both the protonated and sodiated forms of unmodified PE. The largest increase in

sensitivity is visible in PS post-diazomethane treatment. Here we see that an equimolar amount of unmodified PS produces a very weak and divided signal in comparison to the one dominating ion of $[PS^{Tr}]^+$ (Figure 2.4.2b); a sensitivity gain of over 32-fold was observed for the sum of all unmodified PS species when compared to the intensity of the $[PS^{Tr}]^+$ ion. A sensitivity test was also performed on PC and SM (Figures 2.4.2c and 2.4.2d) to demonstrate that diazomethane treatment of PC and SM causes no adverse effects to the already strong signal of the unmodified PC and SM lipids. We observed a slight increase in sensitivity in $[PC^{Tr}]^+$ through the neutralization of the negatively charged oxygen on the phosphate group as well as signal convergence and an increase in sensitivity of over 2.5-fold for $[SM^{Tr}]^+$.

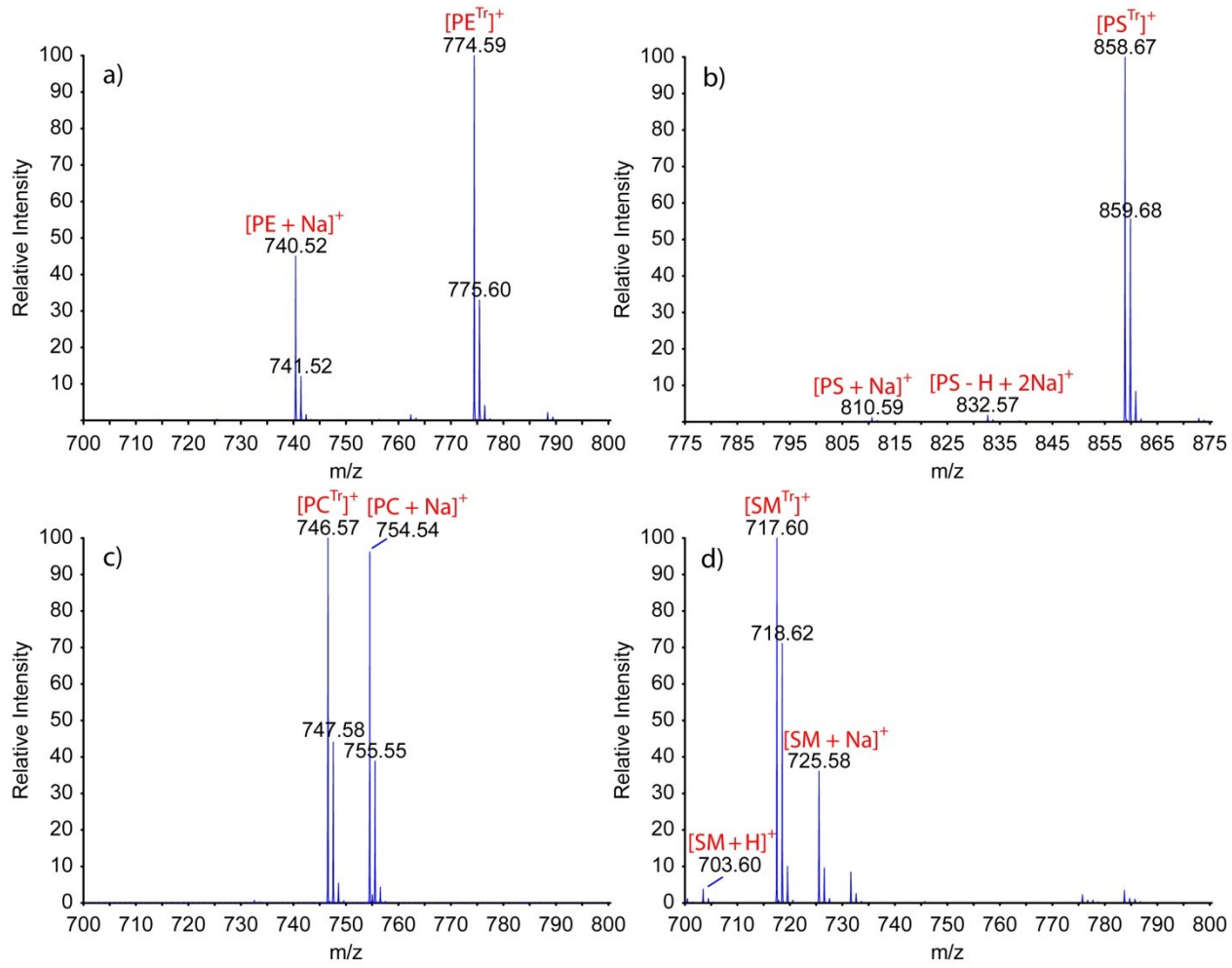

Figure 2.4.2: The ionization efficiency of TrEnDi-modified lipids is enhanced resulting in improved sensitivity. a) Equimolar amounts of TrEnDi-modified and unmodified PE reveals an approximately two-fold increase in sensitivity following derivatization. b) Equimolar amounts of TrEnDi-modified and unmodified PS shows >30-fold increase in sensitivity following derivatization. c) Equimolar amounts of TrEnDi-modified and unmodified PC shows a modest gain in sensitivity following derivatization. d) Equimolar amounts of TrEnDi-modified and unmodified SM show an approximately 2.5-fold increase in sensitivity following derivatization.

Table 2.4.2: Sensitivity increases of TrEnDi-modified lipids over unmodified lipids electrosprayed from an ethanol solution containing sodium cations.

Lipid	Unmodified			TrEnDi-modified		
	Species	m/z (Th)	Relative Intensity (%)	$[M^{Tr}]^+$ (Th)	Relative Intensity (%)	**Sensitivity increase**[a]
PE(16:0/18:1(9Z))	$[M+H]^+$	718.52	0.16	774.59	100	**625x**
	$[M+Na]^+$	740.52	45.0			**2.22x**
	Sum		**45.2**			**2.21x**
PS(18:0/18:2(9Z,12Z))	$[M+H]^+$	788.59	0.09	858.67	100	**1110x**
	$[M+Na]^+$	810.59	1.16			**86.2x**
	$[M-H+2Na]^+$	832.57	1.84			**54.3x**
	Sum		**3.09**			**32.4x**
PC(18:1(9Z)/14:0)	$[M+H]^+$	732.56	0.69	746.57	100	**145x**
	$[M+Na]^+$	754.54	96.2			**1.04x**
	Sum		**96.9**			**1.03x**
SM(d18:1/16:0)	$[M+H]^+$	703.60	3.79	717.60	100	**26.4x**
	$[M+Na]^+$	725.58	36.1			**2.77x**
	Sum		**39.9**			**2.51x**

[a]Fold increase calculated by dividing the relative intensity of the TrEnDi-modified lipid species to the relative intensity of the unmodified lipid species

Multiple lipids tested simultaneously. In order to test the efficacy of TrEnDi on multiple lipid subclasses simultaneously, a solution containing PE, PS, SM and PC standards were acidified with an ethereal solution of HBF_4 and modified with ethereal diazomethane. This solution was evaporated, the lipids were redissolved in pure ethanol and equimolar amounts of unmodified lipids standards were added. Again, the effect of TrEnDi on sensitivity relating to

inherent ionization efficiency and signal convergence to a single analyte peak in the presence of sodium cations was investigated. Our results demonstrated that the chemistry was equally effective on all lipids (Figure 2.4.3); PE, PS, SM and PC were all successfully methylated, yielding MS signals of m/z 774.59, 858.61, 717.58 and 746.55, respectively. MS/MS on all 4 lipids confirmed the formation of their respective modified head groups with their characteristic mass shifts (data not shown). This experiment demonstrated that the simultaneous methylation of different lipids is possible in a single experiment. Figure 2.4.3 further demonstrates the sensitivity enhancements that are gained when lipids are derivatized via TrEnDi, as summarized in Table 2.4.3. All species show an increased intensity following derivatization with the largest gain in sensitivity being observed for PS; unmodified PS peaks are split between protonated and cationized forms with intensities <4% relative intensity, whereas a significant enhancement in intensity is observed following TrEnDi derivatization.

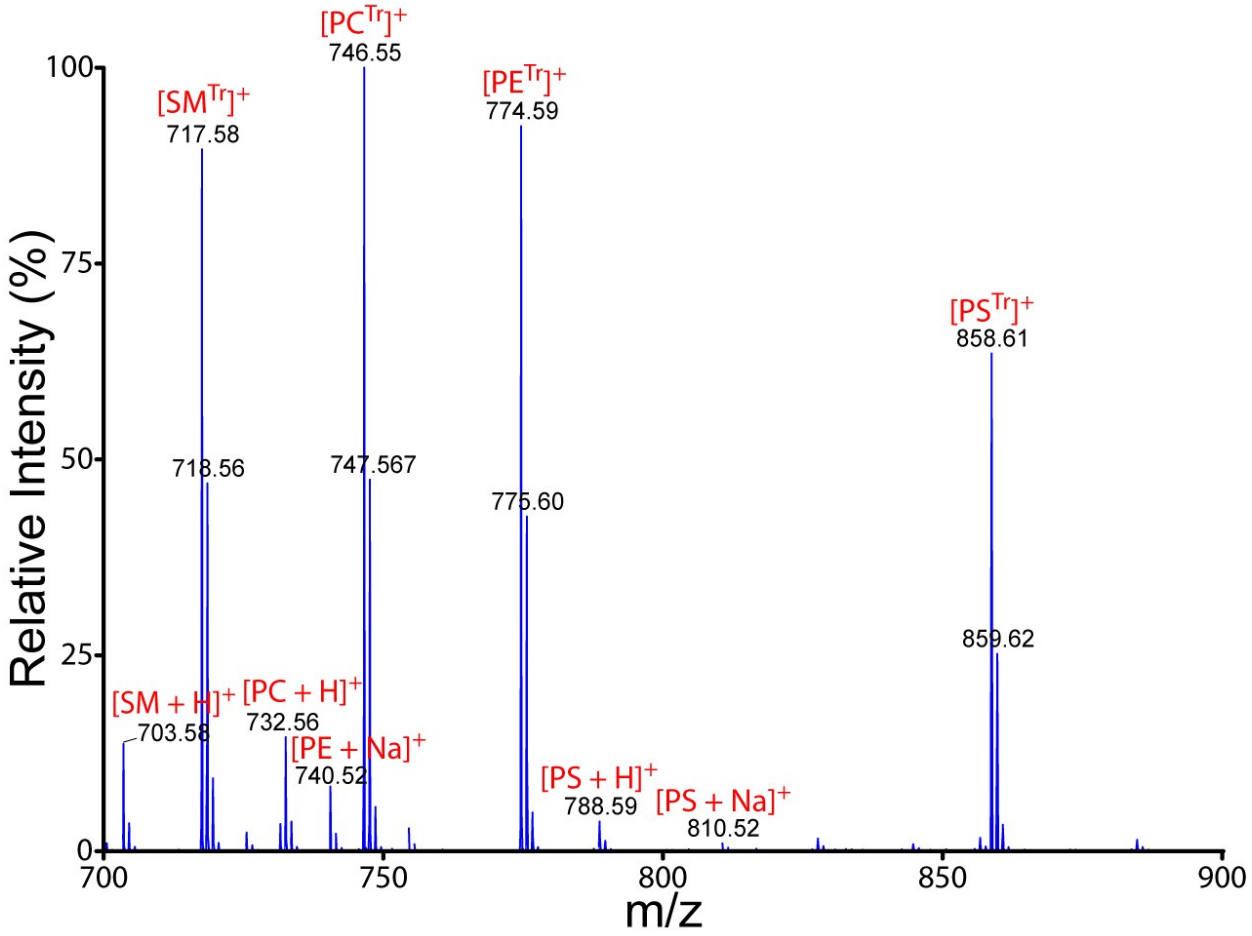

Figure 2.4.3: MS spectrum of an equimolar mixture of unmodified and TrEnDi-modified PC, PE, PS and SM indicating that simultaneous derivatization of all four species is possible. The spectrum also reveals sensitivity gains for each species following derivatization when electrosprayed from an ethanol solution containing sodium cations, as summarized in Table 2.4.3.

Table 2.4.3: Sensitivity increases of TrEnDi-modified lipids over unmodified lipids in combined sample when electrosprayed from an ethanol solution containing sodium cations.

Lipid	Unmodified			TrEnDi-Modified		
	Species	m/z (Th)	Relative intensity (%)	$[M^{Tr}]^+$ (Th)	Relative Intensity (%)	**Sensitivity increase**[a]
PE(16:0/18:1(9Z))	$[M+H]^+$	718.52	8.15[b]	774.57	92.55	**11.4x**
	$[M+Na]^+$	740.52	8.25			**11.2x**
	Sum		**16.40**			**5.64x**
PS(18:0/18:2(9Z,12Z))	$[M+H]^+$	788.59	3.79	858.61	63.54	**16.8x**
	$[M+Na]^+$	810.52	1.00			**63.5x**
	$[M-H+2Na]^+$	832.57	0.26			**244x**
	Sum		**5.05**			**12.6x**
PC(18:1(9Z)/14:0)	$[M+H]^+$	732.56	14.56	746.55	100	**6.87x**
	$[M+Na]^+$	754.54	2.92			**34.2x**
	Sum		**17.48**			**5.72x**
SM(d18:1/16:0)	$[M+H]^+$	703.58	13.67	717.58	89.59	**6.55x**
	$[M+Na]^+$	725.58	2.38			**37.6x**
	Sum		**16.05**			**5.58x**

[a]Fold increase calculated by dividing the relative intensity of the TrEnDi-modified lipid species to the relative intensity of the unmodified lipid species
[b]Calculated based on isobaric interference from $[SM^{Tr}]^+$ M+1 peak.

Sensitivity gains using MS/MS. When analyzing the glycerophospholipid complement of complex biological samples via MS, it is imperative to use MS/MS in order to determine the head group chemistry and delineate between isobaric species.[16,20] As outlined in Table 2.3.1, PC and SM lipids are typically analyzed via positive ion mode precursor ion scanning whereas PE

and PS lipids may be analyzed via neutral loss and precursor ion scanning in either positive or negative ion mode. In order to fully demonstrate that TrEnDi increases MS/MS ion intensity, sensitivity optimization experiments were conducted on unmodified PE and PS in both positive and negative ion modes. PE and PS were dissolved in three separate buffered ethanol solutions expected to enhance MS signal and were electrosprayed under identical concentrations and conditions (Figure 2.6.4, see the supporting information section of this chapter for more details). The experiments demonstrated that ammonium acetate produced the strongest ion intensities for both PE and PS in the positive ion mode and ammonium hydroxide in the negative ion mode; these buffers were selected to compare to TrEnDi-modified lipids. Sensitivity gains due to ionization efficiency have been demonstrated; however, further gains were expected from MS/MS scanning due to fragmentation channel consolidation. In order to evaluate MS/MS-based sensitivity gains, 1 pmol of unmodified lipids (Figure 2.4.4) and TrEnDi-modified lipids (Figure 2.4.5) were analyzed by neutral loss and precursor ion scans using a hybrid triple quadrupole/linear ion trap mass spectrometer. Table 2.4.4 summarizes the peak areas derived from each scanning mode for unmodified and TrEnDi-modified lipid species.

The PIS signal intensity of unmodified PE was relatively low and revealed minor contamination peaks (Figure 2.4.4a) while the NL signal intensity proved to be two orders of magnitude greater (Figure 2.4.4b). The PIS and NL signal intensities of unmodified PS yielded moderate peak intensities (Figures 2.4.4c and 2.4.4d). A PIS for unmodified PC and SM yielded peaks with relatively intense signals (Figure 2.4.4e). However, all four TrEnDi-modified lipid classes were detected via PIS with signal intensities significantly greater than those observed in the unmodified lipid analyses (Figures 2.4.5a, 2.45b and 2.4.5c). It was observed that roughly one quarter of SM is methylated a second time (presumably on the *sn*-1 hydroxyl group since it

has a lower pK_a than the *sn*-2 secondary amine[35-38] and the precursor ion mass does not change) dividing the signal into monomethylated SM (m/z 717) and dimethylated SM (m/z 731). Despite this, the monomethylated SM peak represented a two-fold increase in sensitivity compared to unmodified SM. Table 2.4.4 summarizes the sensitivity gains considering monomethylated SM alone (2.1 fold increase) as well as the addition of the peak area of dimethylated SM (2.86 fold increase). No other variable methylation states were observed for any of the four lipid classes. PS exhibited the greatest signal intensity increase – more than 15-fold – with a precursor scan at m/z 144 using a CE of 60 eV over the NL scanning modes used on non-modified PS.

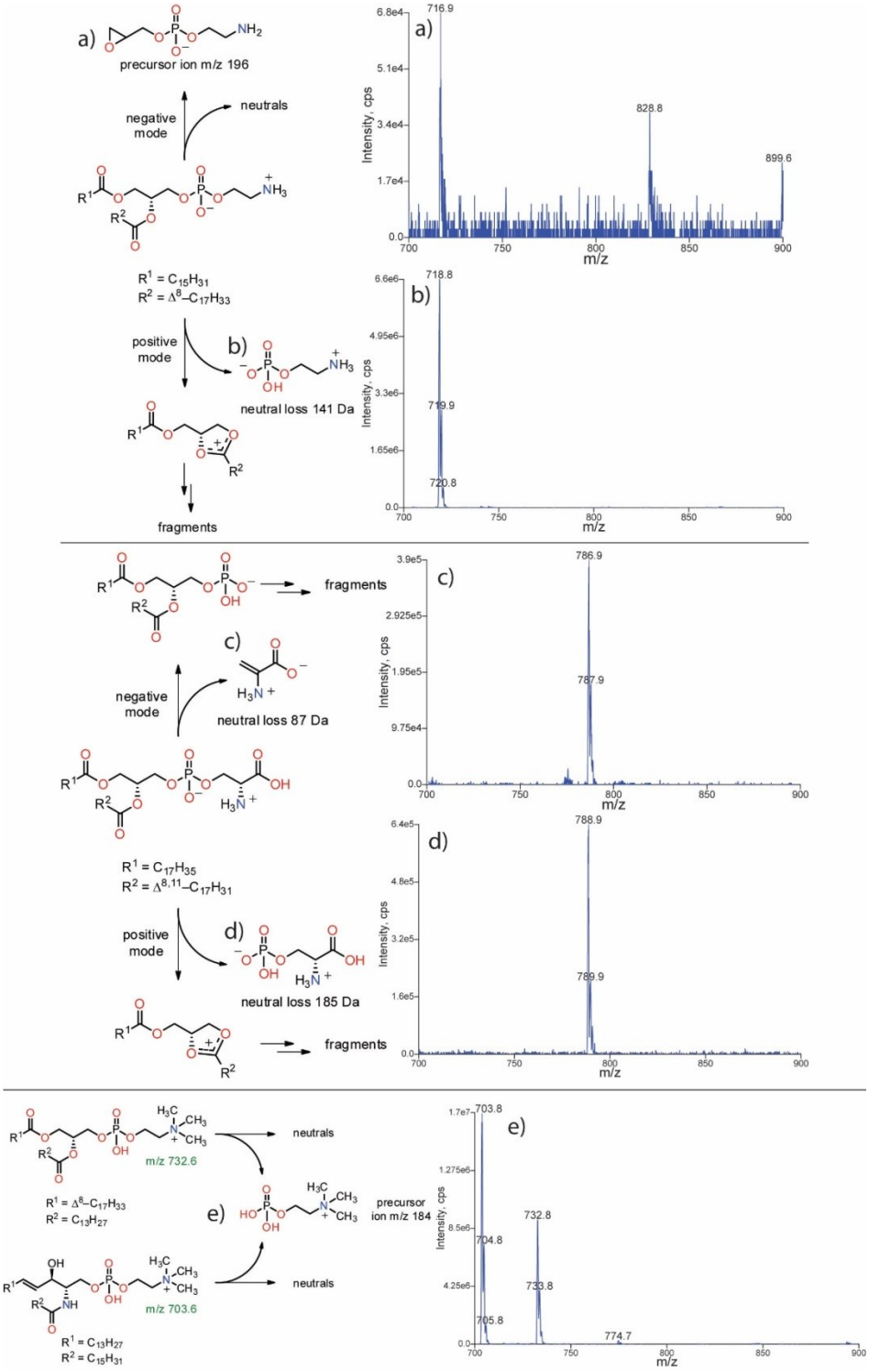

Figure 2.4.4: Positive and negative MS/MS spectra of non-modified lipids accompanied by the proposed structures and dissociative derivation of each fragment. Lipids were dissolved in 10 mM ammonium hydroxide in ethanol for negative ion spectra and 10 mM ammonium acetate in

ethanol for positive ion spectra. a) Negative PIS (m/z 196) of PE observed at m/z 716.9, b) positive NL scan (141 Da) of PE observed at m/z 718.8, c) negative NL scan (87 Da) of PS observed at m/z 786.9, d) positive NL scan (185 Da) of PS observed at m/z 788.9, e) relatively strong signal intensities for the positive PIS (m/z 184) for PC and SM observed at m/z 732.8 and m/z 703.8, respectively.

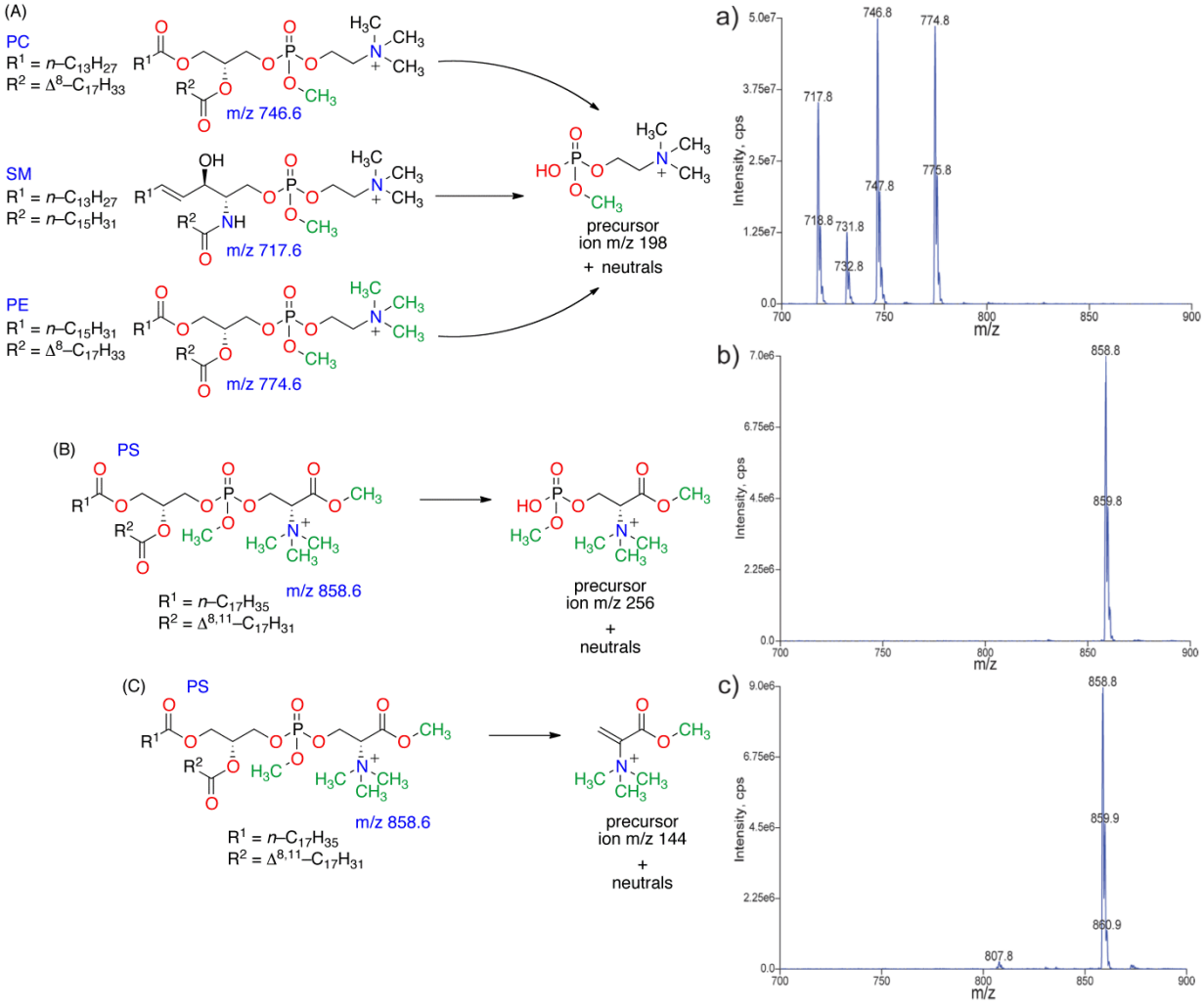

Figure 2.4.5: MS/MS spectra of TrEnDi-modified lipids accompanied by the proposed structures and dissociative derivation of each fragment. a) Relatively stronger signal intensities for the precursor ion scan (m/z 198) for $[SM^{Tr}]^+$ (m/z 717.8), $[PC^{Tr}]^+$ (m/z 746.8) and $[PE^{Tr}]^+$ (m/z 774.8), b) relatively stronger signal intensity in the precursor ion scan (m/z 256) with CE of 40 eV for $[PS^{Tr}]^+$ (m/z 858.8), c) relatively stronger signal intensity for the precursor ion scan (m/z 144) with CE of 60 eV for $[PS^{Tr}]^+$ (m/z 858.8).

Our results demonstrate that, even when comparing against lipids dissolved in optimized buffers, TrEnDi-modified lipids produce significantly stronger signal intensities when performing MS/MS analyses, with increases in signal intensity of greater than two-fold for SM, five-fold for PC, eight-fold for PE and 1.5 orders of magnitude for PS (Table 2.4.4).

Table 2.4.4: MS/MS sensitivity increases of TrEnDi-modified lipids over unmodified lipids.

Lipid	Unmodified			TrEnDi-modified			
	Scan	m/z (Th) Identity	Peak area	Scan	$[M^{Tr}]^+$ (Th)	Peak area	**Sensitivity Increase[a]**
PE(16:0/18:1(9Z))	+ NL (141 Da)	718.8 $[M+H]^+$	$4.05x10^7$	PIS (198 Th)	774.8	$3.23x10^8$	**7.96x**
	- PIS (196 Da)	716.9 $[M-H]^-$	$3.95x10^5$				**816.32x**
PS(18:0/18:2(9Z,12Z))	+NL (185 Da)	788.9 $[M+H]^+$	$4.08x10^6$	PIS (144 Th)	858.8	$6.22x10^7$	**15.23x**
				PIS (256 Th)		$4.58x10^7$	**11.21x**
	-NL (87 Da)	786.9 $[M-H]^-$	$2.66x10^6$	PIS (144 Th)		$6.22x10^7$	**23.37x**
				PIS (256 Th)		$4.58x10^7$	**17.21x**
PC(18:1(9Z)/14:0)	PIS (184 Th)	732.8 $[M+H]^+$	$6.09x10^7$	PIS (198 Th)	746.8	$3.47x10^8$	**5.70x**
SM(d18:1/16:0)	PIS (184 Th)	703.8 $[M+H]^+$	$1.14x10^8$	PIS (198 Th)	717.8	$2.38x10^8$	**2.10x**
				PIS (198 Th)	717.8 + 731.8	$3.25x10^8$	**2.86x**

[a]Fold increase calculated by dividing the fragment ion area of the TrEnDi-modified lipid species to the area of the unmodified lipid species

2.5 Conclusion

The trimethylation enhancement using diazomethane (TrEnDi) technique has been successfully developed on four different classes of phospholipids. Complete methylation has been demonstrated on functional groups with pK_a values lower than 11 resulting in the production of quaternary ammonium groups on PE and PS primary amines. Phosphate moieties and carboxylic acids were also shown to be methylated and neutralized using this chemistry.

TrEnDi modifies lipids such that they contain fixed, permanent positive charges, increasing the sensitivity of ESI MS analysis by driving the charge state of each lipid to a single value and opening the possibility of using aprotic solvents in MS analyses of lipids. The derivatization chemistry is predictable and TrEnDi-modified lipids demonstrate a propensity to release the charged head groups of the lipids upon collisional activation. Fully modified head group fragments were observed to be the most intense fragment for PC, PE, and SM lipids, while higher collision energies produced a second diagnostic fragment for PS with even greater signal intensity. The chemistry was effective on a mixture of lipid classes and demonstrated significant enhancements in sensitivity when compared on an equimolar basis to unmodified lipids. TrEnDi represents a rapid and facile lipid derivatization strategy that offers sensitivity enhancements for three of the most common classes of glycerophospholipids and one of the most common classes of sphingolipids and shows promise to be a valuable tool in the analysis of low abundance lipids in biological samples.

2.6 Supplementary Information

The method we have developed is successful at fully methylating lipids (such as PE, PC, SM and PS) when they are subjected to very small amounts of diazomethane in the presence of tetrafluoroboric acid (HBF_4). HBF_4 is the key to the success of in-solution lipid-based TrEnDi because it is extremely acidic, enabling the protonation of the phosphate groups in the lipids of interest, but also produces a non-coordinating, non-nucleophilic counterion. This ultimately prevents diazomethane from methylating the conjugate base of the acid, thereby directing all methylation to the lipids (Figure 2.6.1). Figure 2.6.1 illustrates the reaction of diazomethane with a primary amine; the acidic ammonium ion protons protonate diazomethane, creating an unstable diazonium cation, which carries out an S_N2 reaction, methylating the amine while releasing N_2 gas. Critically, this reaction produces a fixed positive charge on the lipid via the formation of a quaternary ammonium ion while also neutralizing the negative charge of the phosphate group via the formation of the phosphate methyl ester.

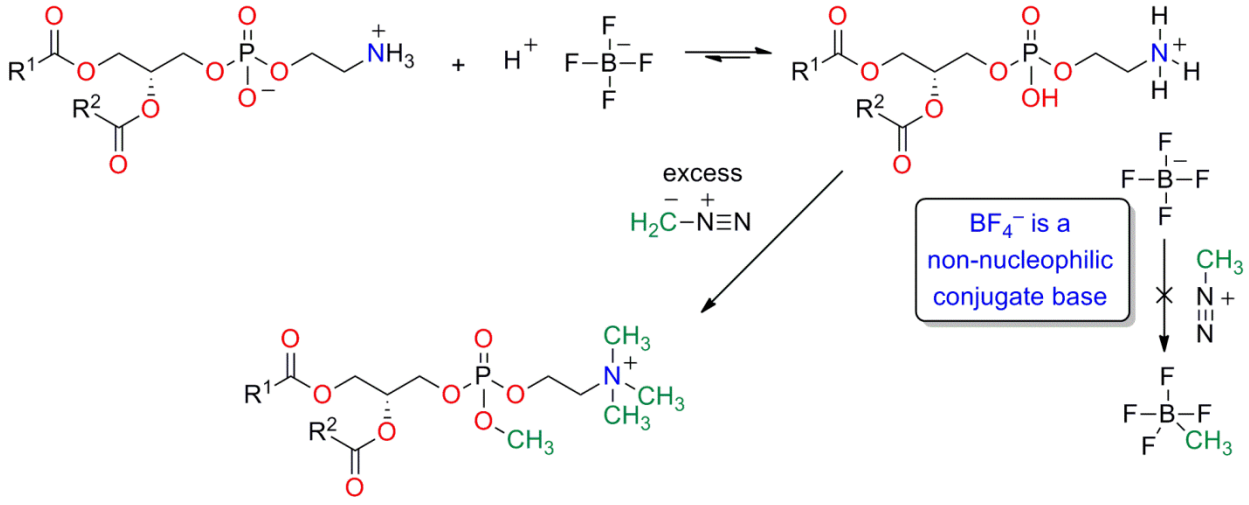

Figure 2.6.1: Methylation of a phosphoethanolamine lipid head group with diazomethane.

To determine the reactivity of diazomethane with more frequently studied lipids, PC and SM standards were purchased and subjected to our methylation strategy. While other studies have shown the characteristic fragments formed in MS/MS analysis of PC and SM lipids, here we observe the methylation of the phosphate group, adding a mass of 14 Da to the loss of the phosphocholine head group during MS/MS (Figure 2.6.2 and Figure 2.6.3). The results of the treatment of each lipid with diazomethane and HBF_4 in solution are summarized in Table 2.4.1 of the article.

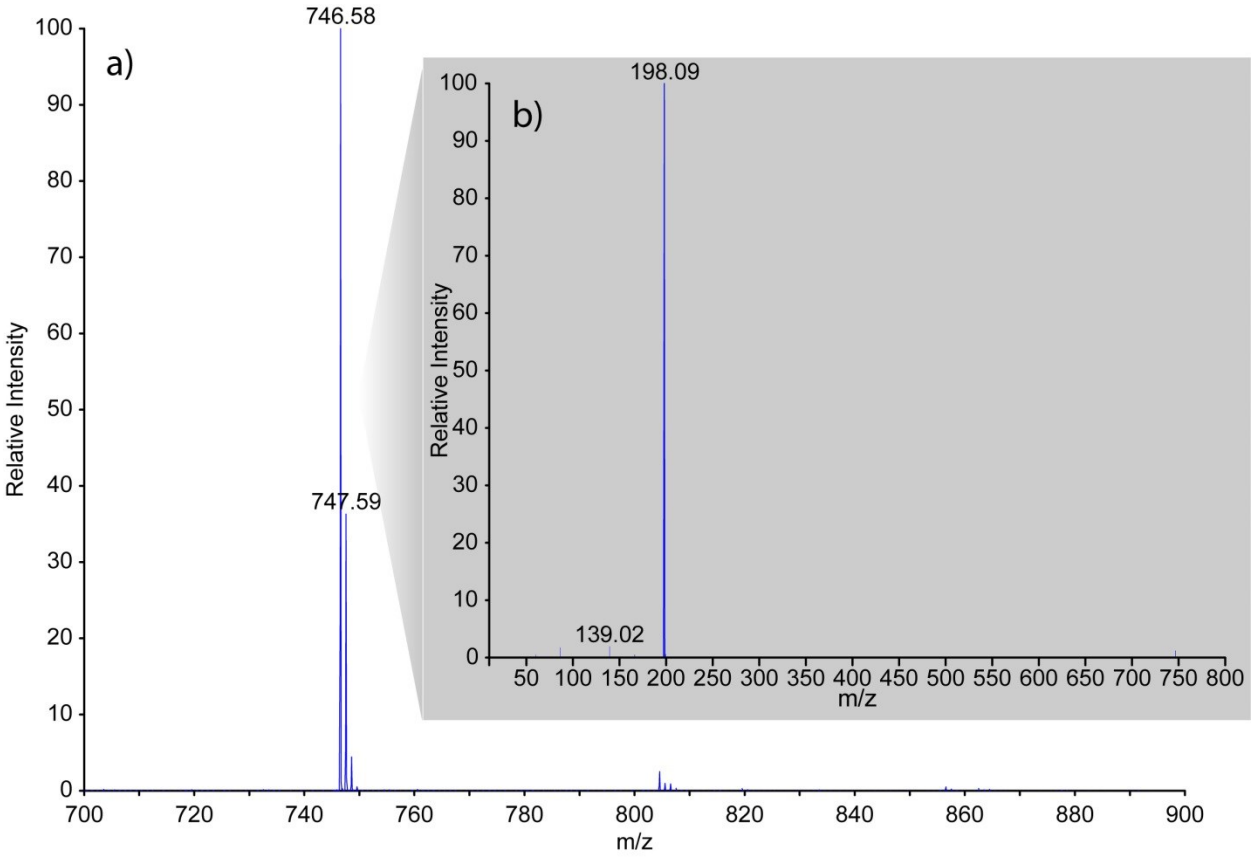

Figure 2.6.2: a) PC treated with diazomethane ($[PC^{Tr}]^+$) reveals addition of one methyl group (m/z 746.58). b) Collision-induced fragmentation of $[PC^{Tr}]^+$ revealed a single fragmentation channel (m/z 198.09) homologous to that known and observed for unmodified PC.

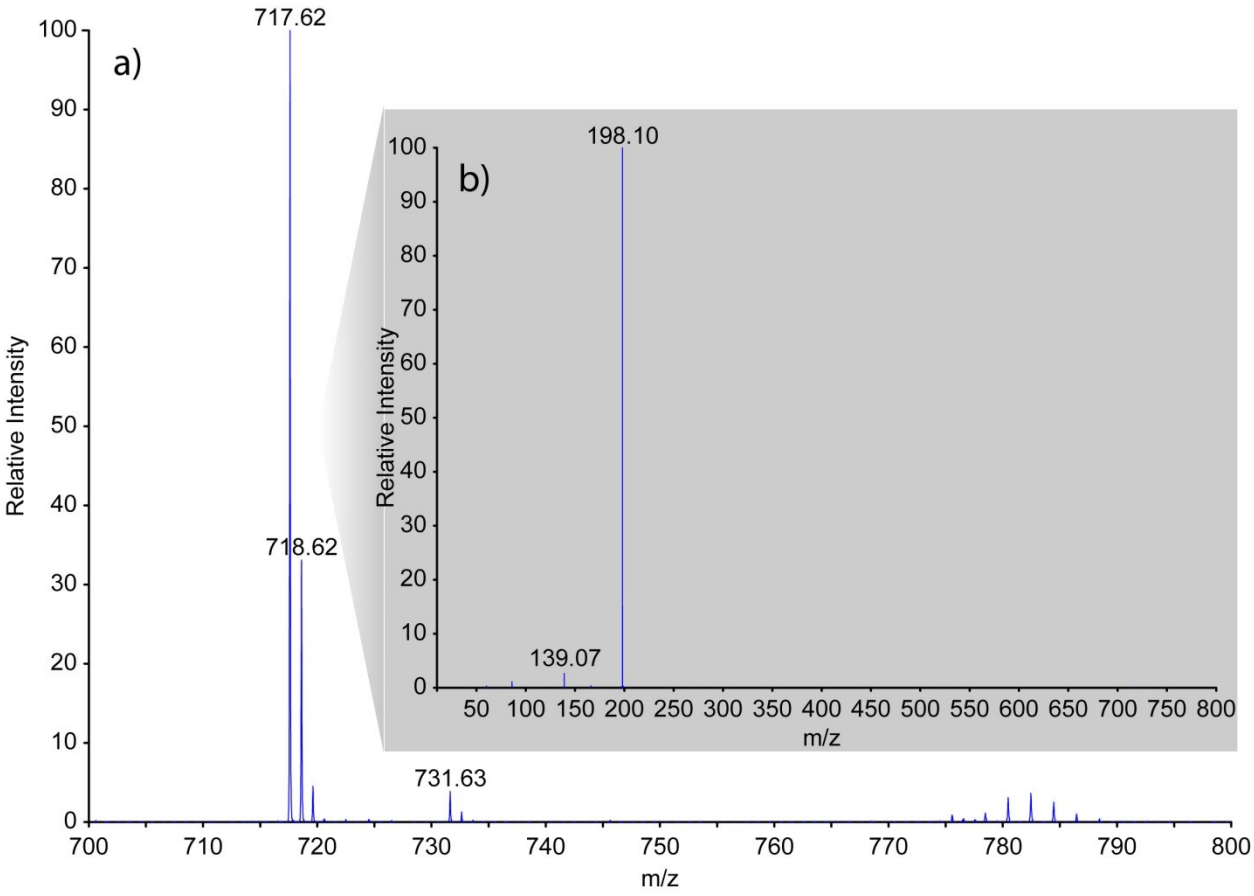

Figure 2.6.3: a) SM treated with diazomethane ($[SM^{Tr}]^+$) reveals addition of one methyl group (m/z 717.62). b) Collision-induced fragmentation of $[SM^{Tr}]^+$ revealed a single fragmentation channel (m/z 198.10) homologous to that known and observed for unmodified SM.

In order to demonstrate that TrEnDi-modified lipids show greater signal intensity than non-modified lipids and are useful in real analytical scenarios, it was important to ensure that non-modified lipids were being electrosprayed in a buffer and using a scanning mode that maximized intensity. It was known that PC and SM electrospray most efficiently in positive ion mode in an acidified buffer; however, PE and PS are known to ionize in positive and negative ion modes and may benefit from volatile reagents such as NH_4OH, CH_3CO_2H or NH_4OAc. We could not find a consistent trend in the literature regarding which solvents/reagents best promoted ion sensitivity best for each lipid type, nor could we find a consistent pattern that

indicated which MS/MS ion transition was in fact the most sensitive for each lipid type. As a result, these variables were tested to determine the optimal ESI conditions for PS and PE to which we could compare our TrEnDi signal intensity. The results of these experiments are indicated in Figure 2.6.4 and Table 2.6.1, where it is demonstrated that 10 mM NH_4OH provides the most intense ions in negative ion mode for PE and PS while 10 mM NH_4OAc provides the most intense ions for both PE and PS in positive ion mode. These buffers were therefore used to generate Figure 2.4.4 and Table 2.4.5 in the results and discussion section of this chapter.

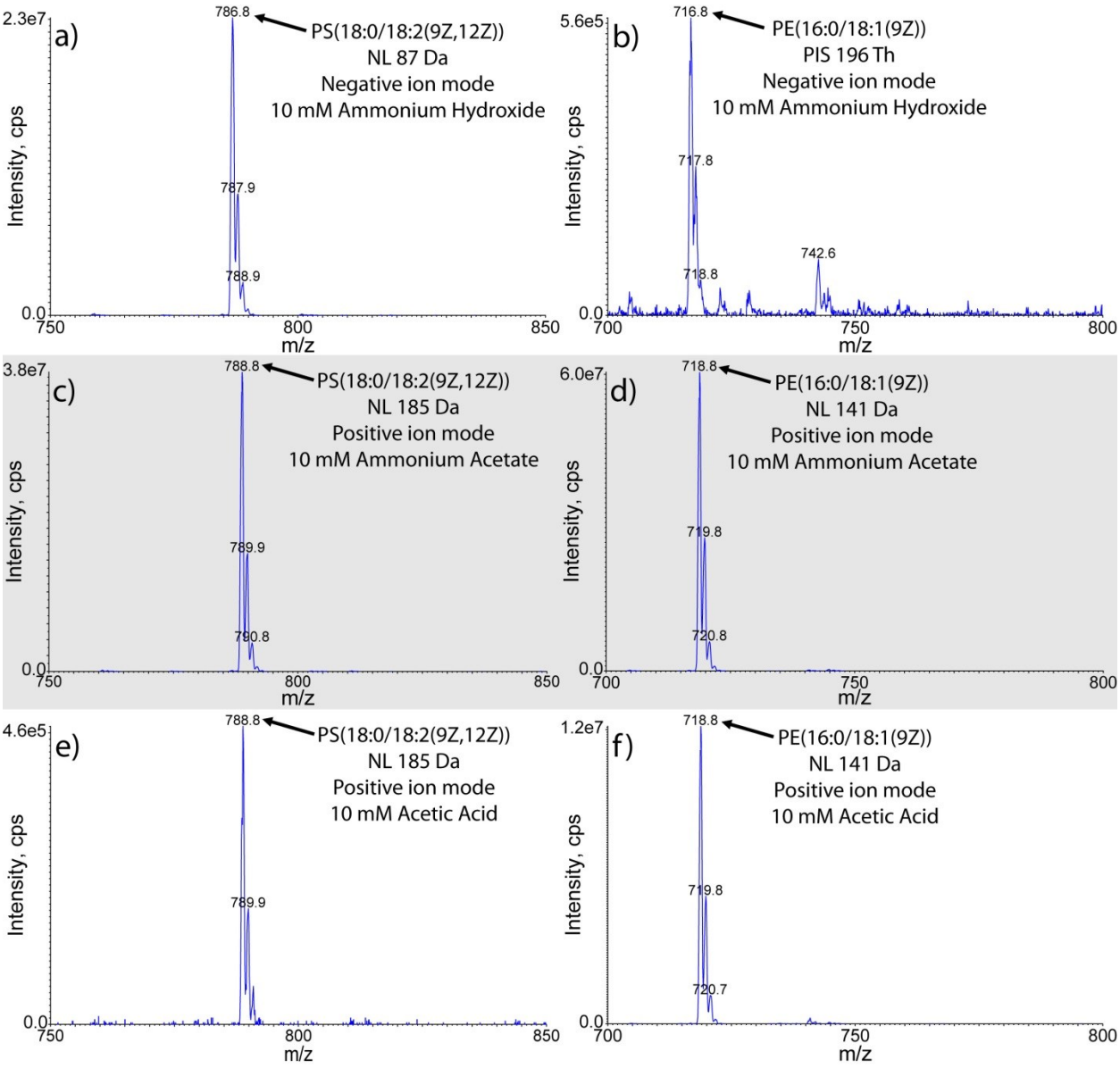

Figure 2.6.4: Tandem mass spectra of 10 pmol of PS and PE in various buffers. Lipid, scan type, instrument polarity and buffer type and concentration are indicated in each panel. Panels c) and d) indicate that 10 mM ammonium acetate provides the greatest signal strength in positive ion mode for both PE and PS.

Table 2.6.1: Areas generated from electrospraying 10 pmol of PE or PS in various buffers in both positive and negative ion modes.

Lipid		**10 mM NH_4OH**	**10 mM NH_4OAc**	**10 mM CH_3CO_2H**
	m/z (Th) Identity	Area (counts)	Area (counts)	Area (counts)
PE(16:0/18:1(9Z))	718.8 $[M+H]^+$	N/A	$3.75x10^8$ (100%)	$7.48x10^7$ (19.94%)
	716.8 $[M-H]^-$	$3.96x10^6$ (1.05%)	N/A	N/A
PS(18:0/18:2(9Z,12Z))	788.8 $[M+H]^+$	N/A	$2.38x10^8$ (100%)	$5.90x10^7$ (24.76%)
	786.8 $[M-H]^-$	$1.71x10^8$ (71.57%)	N/A	N/A

2.7 References

(1) Bosetti, F. *J. Neurochem.* **2007**, *102*, 577-586.

(2) Shimizu, T. *Annu. Rev. Pharmacol. Toxicol.* **2009**, *49*, 123-150.

(3) Meyer zu Heringdorf, D.; Jakobs, K. H. *Biochim. Biophys. Acta* **2007**, *1768*, 923-940.

(4) Kirschnek, S.; Paris, F.; Weller, M.; Grassme, H.; Ferlinz, K.; Riehle, A.; Fuks, Z.; Kolesnick, R.; Gulbins, E. *J. Biol. Chem.* **2000**, *275*, 27316-27323.

(5) Maestre, I.; Jordan, J.; Calvo, S.; Reig, J. A.; Cena, V.; Soria, B.; Prentki, M.; Roche, E. *Endocrinology* **2003,** *144*, 335-345.

(6) Lemmon, M. A. *Nat. Rev. Mol. Cell. Biol.* **2008**, *9*, 99-111.

(7) Vicinanza, M.; D'Angelo, G.; Di Campli, A.; De Matteis, M. A. *EMBO J* **2008**, *27*, 2457-2470.

(8) Kita, Y.; Ohto, T.; Uozumi, N.; Shimizu, T. *Biochim. Biophys. Acta* **2006**, *1761*, 1317-1322.

(9) Sanchez-Mejia, R. O.; Newman, J. W.; Toh, S.; Yu, G. Q.; Zhou, Y.; Halabisky, B.; Cisse, M.; Scearce-Levie, K.; Cheng, I. H.; Gan, L.; Palop, J. J.; Bonventre, J. V.; Mucke, L. *Nat. Neurosci.* **2008**, *11*, 1311-1318.

(10) Han, X.; Abendschein, D. R.; Kelley, J. G.; Gross, R. W. *Biochem. J.* **2000**, *352*, 79-89.

(11) Distler, U.; Hulsewig, M.; Souady, J.; Dreisewerd, K.; Haier, J.; Senninger, N.; Friedrich, A. W.; Karch, H.; Hillenkamp, F.; Berkenkamp, S.; Peter-Katalinic, J.; Muthing, J. *Anal. Chem.* **2008**, *80*, 1835-1846.

(12) Fenn, J. B.; Mann, M.; Meng, C. K.; Wong, S. F.; Whitehouse, C. M. *Science* **1989**, *246*, 64-71.

(13) Gale, D.; Smith, R. *Rapid Commun. Mass Spectrom.* **1993**, *7*, 1017-1021.

(14) Tanaka, K.; Waki, H.; Ido, Y.; Akita, S.; Yoshida, Y.; Yoshida, T.; Matsuo, T. *Rapid Commun. Mass Spectrom.* **1988**, *2*, 151-153.

(15) Wilm, M.; Mann, M. *Int. J. Mass Spectrom. Ion Processes* **1994**, *136*, 167-180.

(16) Bou Khalil, M.; Hou, W.; Zhou, H.; Elisma, F.; Swayne, L. A.; Blanchard, A. P.; Yao, Z.; Bennett, S. A.; Figeys, D. *Mass Spectrom. Rev.* **2010**, *29*, 877-929.

(17) Holthuis, J. C.; Levine, T. P. *Nat. Rev. Mol. Cell Biol.* **2005**, *6*, 209-220.

(18) Wykle, R. L.; O'Flaherty, J. T.; Thomas, M. J. *Methods Enzymol.* **1988,** *163*, 44-54.

(19) Brugger, B. *Annu. Rev. Biochem.* **2014**, *83*, 79-98

(20) Han, X.; Yang, K.; Gross, R. W. *Mass Spectrom. Rev.* **2012,** *31*, 134-178.

(21) Fhaner, C. J.; Liu, S.; Ji, H.; Simpson, R. J.; Reid, G. E. *Anal. Chem.* **2012**, *84*, 8917-8926.

(22) Li, Y. L.; Su, X.; Stahl, P. D.; Gross, M. L. *Anal. Chem.* **2007**, *79*, 1569-1574.

(23) Wang, M.; Hayakawa, J.; Yang, K.; Han, X. *Anal. Chem.* **2014**, *86*, 2146-2155.

(24) Wasslen, K. V.; Tan le, H.; Manthorpe, J. M.; Smith, J. C. *Anal. Chem.* **2014**, *86*, 3291-3299.

(25) Graff, G.; Anderson, L. A.; Jaques, L. W.; Scannell, R. T. *Chem. Phys. Lipids* **1990**, *53*, 27-36.

(26) Mueller, H. W. *J Chromatogr., B* **1996**, *679*, 208-209.

(27) Schlenk, H.; Gellerman, J. L. *Anal. Chem.* **1960**, *32*, 1412-1414.

(28) Smith, G. A.; Montecucco, C.; Bennett, J. P. *Lipids* **1978**, *13*, 92-94.

(29) Lee, J. W.; Nishiumi, S.; Yoshida, M.; Fukusaki, E.; Bamba, T. *J Chromatogr., A* **2013**, *1279*, 98-107.

(30) Kielkowska, A.; Niewczas, I.; Anderson, K. E.; Durrant, T. N.; Clark, J.; Stephens, L. R.; Hawkins, P. T. *Adv. Biol. Reg.* **2014**, *54*, 131-141.

(31) Hsu, F. F.; Turk, J. *J. Am. Soc. Mass Spectrom.* **2003**, *14*, 352-363.

(32) de Boer, T. J.; Backer, H. *J. Org. Synth.* **1956**, *36*, 16.

(33) *Aldrich Technical Bulletin AL-180 [Online]*; Sigma-Aldrich: St. Louis, MO, 2007.

(34) Paik, W. K.; Paik, D. C.; Kim, S. *Trends in Biochem. Sci.* **2007**, *32*, 146-152.

(35) Bras, N. F.; Perez, M. A. S.; Fernandes, P. A.; Silva, P. J.; Ramos, M. J. *J. Chem. Theory Comput.* **2011**, *7*, 3898-3908.

(36) Clayden, J., *Organic chemistry,* 2nd ed.; Oxford University Press: New York, 2001; p 1512.

(37) Mujika, J. I.; Ugalde, J. M.; Lopez, X. *Theor. Chem. Acc.* **2011**, *128*, 477-484.

(38) Wang, W. H.; Cheng, C. C. *Bull. Chem. Soc. Jpn.* **1994**, *67*, 1054-1057.

Chapter 3: Optimization experiments required prior to the study of TrEnDi on a complex lipid sample including a discussion of problems generated by TrEnDi and their prospective solutions.

3.1 Introduction

Chapter 2 discusses the sensitivity enhancement of PC, SM, PE and PS lipid standards after derivatization with diazomethane.[1] TrEnDi proved to significantly enchance the signal of all four standards tested, but was not tested on a complex biological lipid extract. Further examination of the results lead to the realization that the technique as presented in Chapter 2 had significant limitations when applied to complex lipid samples, because PC and PE species with identical radyl groups would become isobaric after derivatization. Two possible solutions to the problem of isobaric derivatized PC and derivatized PE species are discussed in this chapter. Chapter 4 explores one solution to the previously mentioned isobaric problem via the use of isotopically labelled diazomethane. Several optimization experiments needed to be performed prior to analysis of the efficacy of isotopically-labelled TrEnDi on the lipid extract of a complex biological sample. A shotgun lipidomics approach had been used in all previous experiments,[1] but due to the complexity of the biological lipid extract and the limitations caused by the instrumentation used, a LC-MS lipidomics approach was tested. This chapter presents and discusses key experiments performed to optimize the LC-MS lipidomic approach. Experiments were performed to evaluate why tandem MS ionization efficiency experiments, presented on Table 2.2.6 of the supplementary information section of the previous chapter, yielded a higher signal for the PS standard using positive-ESI contrary to previous literature stating the signal of deprotonated PS using negative-ESI as a superior alternative.[2] MS and tandem MS studies were

compared to assess which methodology is more efficient in the analysis of complex lipid samples with the instrumentation available. During optimization of an effective LC-MS lipidomic method, prominent lipid carryover was identified as a significant problem. To address this issue a system cleanup method was developed and optimized to provide the least amount of carryover, while being the most time effective. All these experiemnts are discussed in further detail in this chapter.

3.2 Experimental

Chemicals and materials. Absolute ethanol was purchased from Commercial Alcohols Inc. (Brampton, ON, Canada); methanol, chloroform, and isopropanol, were purchased from Caledon Laboratories Ltd. (Georgetown, ON, Canada); glacial acetic acid, 28% ammonium hydroxide and ammonium acetate were obtained from Anachemia Canada Inc. (Montreal, QC, Canada). Formamide was purchased from Promega Corp. (Fitchburg, WI, USA); Kasil® 1 was obtained from PQ Corporation (Malvern, PA, USA). PE(8:0/8:0) PS(8:0/8:0) and PC(5:0/5:0) were synthesized by and obtained from Avanti Polar Lipids Inc. (Alabaster, Alabama, USA).

Direct infusion of PE and PS standards. PE(8:0/8:0) and PS(8:0/8:0) and desalted PE(8:0/8:0) and PS(8:0/8:0) via a Bligh & Dyer extraction were mixed and dried in several containers. The samples were resuspended with a 100 μL of solvent resulting in both PE and PS standard concentrations of 8 μM. The two standards were resuspended in solutions of 10mM ammonium acetate in EtOH, 10 mM ammonium hydroxide in EtOH or 10 mM acetic acid in EtOH. The lipid extracts were directly infused into the ionspray source at a rate of 1.5 μL per minute using a Harvard 11 Plus syringe pump (Harvard Apparatus, Holliston, MA, USA). An ESI voltage of 5000 V and DP of 40 V were used for positive ion mode scans and a voltage of -4000 V and DP of -40 V for negative ion scans. A scan rate of 250 Da/s, unit resolution for Q1

and Q3 and an ion source gas value of 8 were used for all scans. Each mass spectrum was obtained by performing and averaging 30 scans. A positive ion mode enhanced mass spectrum (EMS) scan was performed from 400 to 600 Th; a negative ion mode EMS scan was performed from 400 to 600 Th. A +NL scan of 141 Da was performed from 400 to 600 Th (CID = 25 eV). A +NL of 185 Da was performed from 400 to 600 m/z (CID = 23 eV).

Cell culture and lipid extraction. Human cervical carcinoma (HeLa) cells were purchased from ATCC (CCL-2) (Manassas, VA, USA) and grown using 87% Eagle's Minimum Essential Medium, 10% FBS and 3% P/S/A (Life Technologies Inc., Burlington, ON, Canada). Cells were cultured in a humidified atmosphere at 37 °C and 5% CO_2 using triple-gas incubators (Thermo Forma, Rockford, Illinois). Phospholipids were extracted using a modified Bligh and Dyer procedure.[3] A volume of 40 µL of 10 µM PC(5:0/5:0) were added prior to the extraction as an internal standard. After extracting lipids in the chloroform phase, chloroform evaporation was followed by resuspension of the extracted lipidome in 600 µL of EtOH.

Reversed phase high pressure liquid chromatography. An aliquot of 10 µL of the lipid was mixed with 30 µL of deionized H_2O and added to the auto sampler of a Dionex Ultimate 3000 HPLC (Thermo Scientific, Odense, Denmark). Lipids were separated using an in-house C4 reversed-phase column and a ternary gradient program consisting of 30% MeOH, 70% H_2O & 10 mM $NH_4C_2H_3O_2$ (mobile phase A), 100% IPA &10 mM $NH_4C_2H_3O_2$ (mobile phase B) and 100% Hexane (mobile phase C). The in-house reversed-phase column was prepared by packing a fritted 14cm long piece of fused silica (200 µm ID) (Molex Inc., Lisle, IL, USA) with 5.5 cm of Reprosil-Pur C4 beads (Dr. Maisch GmbH HPLC, Ammerbuch-Entringen, Germany). The HPLC gradient started at 100% A, 0-36.3 min, B = 0-100%, 36.3-39.5 min, C = 0-90% at an average flowrate of 135 µL/min. A 1.25 mL system wash of 10% B & 90% C ensued one set of

runs, while a 4.5 mL system wash of 10% B & 90% C ensued the other set of runs. A blank run to measure the amount of lipid carry over followed the hexane washes. The blank used the same chromatographic gradient and solvents as the sample runs.

HPLC-ESI-MS/MS analyses. The HPLC eluent was introduced into an AB Sciex 4000 QTRAP via a Turbo V ionspray source (AB Sciex, Framingham, MA, USA). All LC-MS/MS studies were acquired in positive ion mode at an ESI voltage of 5000 V, a scan rate of 250 Da/s, a declustering potential (DP) of 80 V, and an ion source gas value (GS) of 20. All scans were performed in positive ion mode using low resolution for Q1and Q3. A PIS for m/z 184 from 400 to 1200 Th (CID = 45 eV) and an EMS scan from 400 to 1200 Th were used.

Data analysis. Analyst 1.5.1 software was used for the acquisition and analysis of the mass spectra. The area of the standard peaks present in the EMS and NL scans were used for the standard experiments. The highest peak area in the sample and its respective area in the blank were selected to calculate percent carry over.

3.3 Positive and negative PE and PS ionization.

After direct spray of all four PC, PE, PS and SM standards used in Chapter 2, it was evident that the standards provided by Avanti Polar lipids contained significant amounts of sodium. A Bligh and Dyer extraction on PC standards enabled the reduction of sodium contamination in the standard while providing a slight improvement on the signal of the standard. In order to reduce sodium contamination in the PE and PS standards, Bligh and Dyer extractions were performed. The sodiated equivalents of the standards were eliminated but surprisingly the protonated signal of PE was hindered while the protonated signal of the PS standard completely disappeared. The intact standards with sodium contamination on the other

hand, had significant protonated and sodiated peaks showing in the spectra. It was hypothesized that sodium is an integral part to the stability of PS. Biological extracts containing modest amount of PS do reveal PS in the spectra post Bligh and Dyer extraction. This suggests that other biological membrane lipids manage to stabilize PS integrity during these extractions, unlike extractions of pure PS standard. Further experimentation needs to be performed in order to prove there is no PS hindrance in biological extracts after Bligh and Dyer extraction. Further experimentation also needs to be performed on the PS standard to explain its signal disappearance post-extraction. With this knowledge, positive and negative ionization experiments were performed directly on the lipid standards' solutions with Na^+ contamination.

On the supplementary information section of Chapter 2, optimization experiments were performed on PE and PS standards to investigate the optimal protonating or deprotonating agent that would yield the highest signal. Acetic acid and ammonium acetate were tested as protonating agents while ammonium hydroxide was tested as a deprotonating agent. Ammonium acetate was observed to be the optimal protonating agent for both PE and PS standards in tandem MS analyses. Ammonium acetate provided a higher protonated analyte signal in comparison to protonation by acetic acid or deprotonation by ammonium hydroxide.[1] Our results were inconsistent with previous literature that reported a stronger signal for deprotonated PS via negative ionization in comparison to protonated PS via positive ionization.[2,4] But literature studies only reported a superior signal via negative ionization for MS studies, not tandem MS studies. The results presented in Table 2.6.1 were specific for tandem MS experiments.

The efficacy of the two protonating agents and one deprotonating agent previously used were now tested for MS experiments (via non-tandem MS analyses on PE and PS standards (Table 3.3.1). As a result of the abundant sodium contamination in the standards, the strongest

signals in the spectra were sodiated PE species. This demonstrates that a protonating agent is not able to eliminate sodium adduct formation, but rather generates a mixture of protonated and sodiated states. Without the protonating agent the signal of the standards is fully dominated by the sodium adduct. The deprotonation of PE effectively produces a higher signal than protonated PE, contrary to the results obtained by tandem MS.[1] This suggests that the CID neutral loss of 141 Da of protonated PE is a more common fragmentation pathway than the CID precursor ion generation of 196 m/z of deprotonated PE, which explains why positive ionization provides a better signal via tandem MS studies while negative ionization provides a better signal with MS studies. It was also found that acetic acid produces a higher sodiated signal but a lower protonated signal than ammonium acetate. This corroborates ammonium acetate as the best protonating agent since tandem MS studies (NL of 141 Da) only analyze the loss of the headgroup from protonated PE species, not sodiated PE species.

Table 3.3.1: Areas generated from positive and negative ESI of PE and PS standards using various buffers in non-tandem MS.

Lipid		**10 mM NH_4OH**	**10 mM NH_4OAc**	**10 mM CH_3CO_2H**
	m/z (Th) Identity	Area (counts)	Area (counts)	Area (counts)
PE(8:0/8:0)	490.5 $[M+Na]^+$	N/A	$2.56x10^8$	$5.87x10^8$
	468.5 $[M+H]^+$	N/A	$9.66x10^7$	$5.8x10^7$
	466.5 $[M-H]^-$	$1.08x10^8$	N/A	N/A
PS(8:0/8:0)	556.5 $[M-H+2Na]^+$	N/A	$7.16x10^7$	$5.82x10^7$
	534.5 $[M+Na]^+$	N/A	$2.37x10^8$	$8.42x10^7$
	512.5 $[M+H]^+$	N/A	$1.89x10^8$	$1.75x10^8$
	510.5 $[M-H]^-$	$6.35x10^8$	N/A	N/A

The MS results in Table 3.3.1 demonstrated, in agreement with literature results,[2,4] that deprotonation of PS yields a higher signal than protonation of PS. As with PE, these results suggests that the CID neutral loss of 185 Da of protonated PS is a more common fragmentation pathway than the CID neutral loss of 87 Da of deprotonated PS, which explains why positive ionization provides a better signal via tandem MS studies while negative ionization provides a better signal with MS studies. Acetic acid and ammonium acetate produced similar protonated PS area values, with the ammonium acetate area being marginally better.

3.4 Advantages of tandem MS analyses over MS analyses

As discussed in section 1.7 of Chapter 1, tandem MS experiments provide much simpler spectra than MS experiments. Tandem MS spectra enable more accurate quantitation of phospholipid species because the spectra produced are specific to a CID induced fragmentation event (PIS or NL) characteristic of a phospholipid class, effectively reducing isobaric signal contamination from other ionizable species that are present in the lipid extract. Figure 3.4.1 visually demonstrates the advantage of tandem MS analyses over MS analyses. Only two lipid standards were used to produce Figure 3.4.1 and yet the positive and negative MS spectra demonstrate a plethora of peaks. In comparison the NL scan of 141 Da and 185 Da specifically demonstrate their respective PE and PS standards' peaks. The MS spectrum is complex with two lipid standards. A biological extract sample would produce a more complicated spectrum. It is noteworthy that the positive ion mode spectrum is more complex than the negative ion mode spectrum, as a result of multiple ionization states. The identity of all other contaminant peaks in the positive and negative MS spectra is unknown. Figure 3.4.1 demonstrates that identification and quantitation of phospholipid species is more precise when using tandem MS scans.

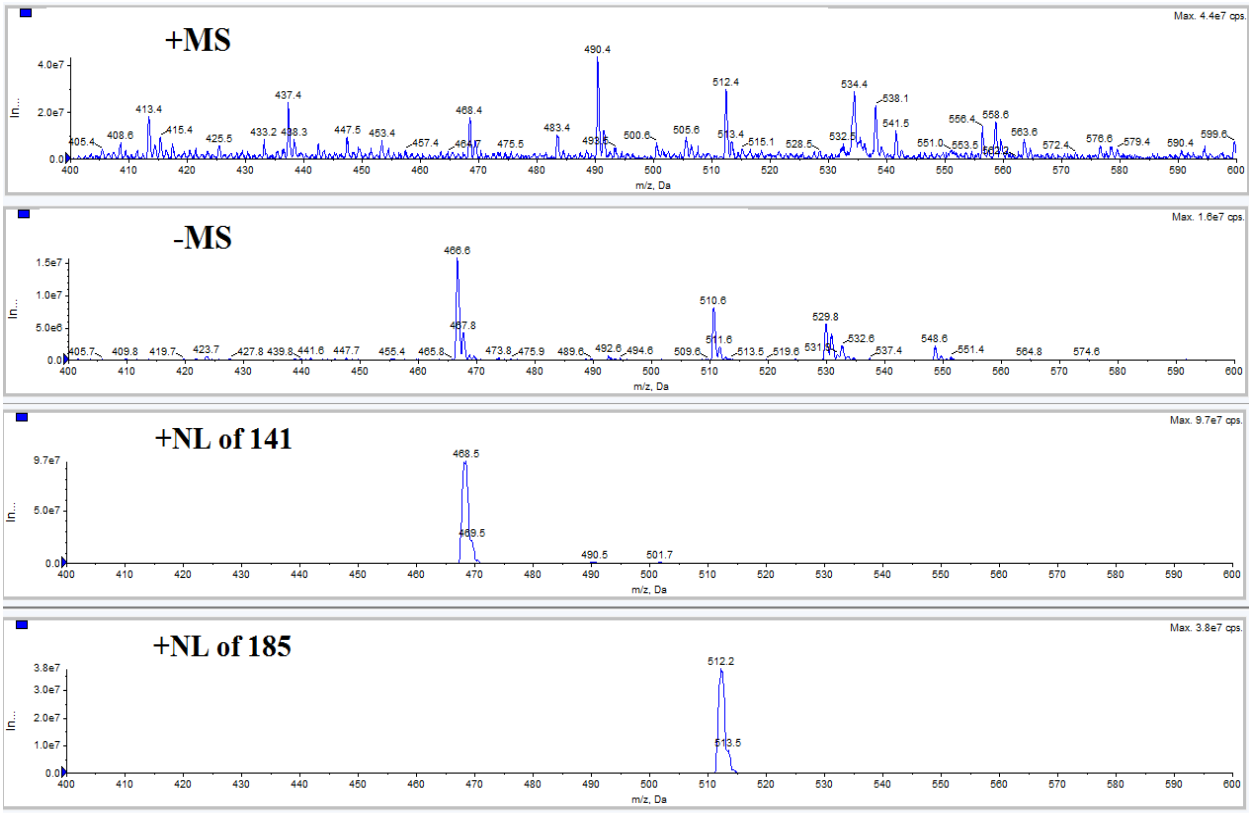

Figure 3.4.1: Comparison between positive and negative non-tandem MS scans and tandem MS scans of a mixture of two lipid standards in 10mM NH_4OAc. The PE (8:0/8:0) and PS (8:0/8:0) standards were used. The NL of 141Da scan is specific to protonated PE species while the NL of 185 Da scan is specific to protonated PS species.

3.5 PC and PE isobaric issues and LC-MS lipid carry-over.

As presented in Figure 2.4.5 of the results and discussion section of Chapter 2, derivatization of PC and PE species produces chemically identical headgroups for modified PC and modified PE species. Because TrEnDi-modified PC and TrEnDi-modified PE species have the same headgroup, they both produce ions with a m/z of 198 after CID, eliminating the capability of using PC or PE specific tandem MS scans. If an unmodified PC and PE species share the same radyl groups, they will become chemically identical post-modification. After TrEnDi modification the ability to differentiate between two previously different PC and PE

species (with the same radyl groups) is lost. The drastic sensitivity enhancement of PE species after modification is futile if it is accompanied by the inability to differentiate them from isobaric modified PC species.

To overcome the problem of isobaric PC and PE species two effective solutions were conceived. The first solution was to use isotopically labelled diazomethane (diazomethane-^{13}C) to produce TrEnDi-modified PE species with headgroups different from modified PC species, allowing to create specific tandem MS scans for both modified classes. This solution is thoroughly discussed in Chapter 4. An alternative solution is to separate the PC and PE content from the lipid extract prior to derivatization via normal phase HPLC separation. Separating the PC and PE content eliminates the need to use isotopically labelled diazomethane. Both fractions can be derivatized and analyzed independently of each other. The latter approach is more labour intensive and time consuming due to the chromatographic separation step added and the need to have separate MS analyses for each fraction.

In order to effectively and objectively evaluate the sensitivity enhancement provided by TrEnDi, both unmodified and modified lipids were evaluated via LC-MS/MS analysis. These experiments and the results are further explained in Chapter 4. LC-MS/MS analyses of unmodified phospholipids provide better sensitivity than direct infusion of unmodified phospholipids (shotgun approach) by desalting the sample (reducing signal splitting) and reducing proton competition; however the use of LC-MS is much lengthier than direct infusion. Lipid samples readily contaminate the HPLC lines, resulting in sample carry-over between samples. Sample carry-over can seriously compromise quantitation experiments and unfortunately is an issue often overlooked in LC-MS lipidomic studies. A protocol that minimizes lipid carry-over was developed. The cleaning protocol consists of a 90% hexane/10%

IPA 4.5 mL wash followed by a blank run after each sample analyzed. The hexane/isopropanol wash and blank ensures that less than 1% of the area from the most abundant peak of the previous sample remains in the system, while simultaneously removing any trace of lower abundance species. This cleaning protocol greatly reduced clogging incidents in the system. Despite successfully eliminating lipid carry-over, different volumes of hexane/isopropanol used to wash the system had not been tested. To test the efficacy of different washing volumes, the area of the most abundant lipid in a sample and the area of its carry-over after washing were measured. The 4.5 mL hexane/isopropanol wash proved effective, but not time or cost efficient. The total volume of the system is approximately 0.041 mL. A 4.5 mL wash would approximately wash the system 110 times. The effectiveness of a shorter 1.25 mL hexane/isopropanol wash was analyzed. That volume would be equivalent to washing the system approximately 30 times. The results are presented in Table 3.5.1. The 4.5 mL hexane wash had an average 0.54% carry-over with a relative standard deviation of ±58.6%. The 1.25 mL hexane wash had an average 0.83% carry-over with a relative standard deviation of ±65.6%. The average percent and relative standard deviation demonstrates that there is no statistical difference between both values. The 1.25 mL 90% hexane/10% isopropanol wash effectively reduced the cleaning volume and time down to 28% of the original washing volume and time, and provided less than 1% average lipid carry-over of the most abundant peak in the spectra. The 1.5 mL hexane/isopropanol wash was used in all subsequent studies.

Table 3.5.1: Percentages of lipid carry-over after different wash volumes were used.

4.5 mL hexane wash			
	1	2	3
Sample's largest peak area	$2.50x10^6$	$2.08x10^6$	$2.99x10^6$
Are of the largest peak in the blank run	$1.68x10^4$	$3.73x10^3$	$2.30x10^4$
Percentage of carry-over sample (%)	0.67	0.18	0.77
Percent carry-over average (%)	0.54	**Relative standard deviation**	± 58.6%
1.25 mL hexane wash			
	1	2	3
Sample's largest peak area	$3.67x10^6$	$3.98x10^6$	$3.31x10^6$
Are of the largest peak in the blank run	$1.52x10^4$	$6.60x10^4$	$2.74x10^4$
Percentage of carry-over sample (%)	0.41	1.66	0.83
Percent carry-over average (%)	0.83	**Relative standard deviation**	± 65.6%

3.6 Conclusion.

Direct MS studies and tandem MS studies of PE species were most effective via positive ESI. Direct MS studies of PS species were more sensitive via negative ESI, while the tandem MS studies of PS species were more sensitive via positive ESI. The use of deprotonating or protonating agents effectively increased the sensitivity of all scans performed. Due to the complexity of biological extracts in combination with the use of a low resolution MS, it was concluded a tandem MS approach would be most effective in the identification and quantitation of PC, PE, PS and SM species. A 1.5 mL hexane/isopropanol (9:1) wash proved to be equally effective to its 4.5 mL counterpart but more time efficient and was used for all subsequent studies. The results presented in this chapter indicated the use of HPLC chromatographic separation, positive ESI and tandem MS are the best approach to analyze complex biological lipid extracts with the instrumentation available. These results enabled to determine and optimize the fundamental conditions used in all experiments presented in Chapter 4.

3.7 References.

(1) Wasslen, K. V; Canez, C. R.; Lee, H. *Anal. Chem.* **2014**, *86*, 9523–9532.

(2) Koivusalo, M.; Haimi, P.; Heikinheimo, L.; Kostiainen, R.; Somerharju, P. *J. Lipid Res.* **2001**, *42* (4), 663–672.

(3) Bonin, F.; Ryan, S. D.; Migahed, L.; Mo, F.; Lallier, J.; Franks, D. J.; Arai, H.; Bennett, S. A. *J. Biol. Chem.* **2004**, *279* (50), 52425–52436.

(4) Pulfer, M.; Murphy, R. C. *Mass Spectrom. Rev.* **2003**, *22* (5), 332–364.

Chapter 4: Trimethylation enhancement using ^{13}C-diazomethane (^{13}C-TrEnDi): Increased sensitivity and selectivity of phosphatidylethanolamine, phosphatidylcholine, and phosphatidylserine lipids derived from complex biological samples.

4.1 Abstract

^{13}C-TrEnDi modification provided drastic sensitivity enhancement of phosphatidylethanolamine (PE) and phosphatidylserine (PS) species and a modest sensitivity enhancement of phosphatidylcholine (PC) species via precursor ion scans (PIS) on lipid extract of HeLa cells. Sphingomyelin (SM) species exhibited neither an increased or decreased sensitivity after modification. The use of isotopically-labeled diazomethane enabled the distinction of modified PE and modified PC species that would yield isobaric species with unlabeled diazomethane. ^{13}C-TrEnDi created a PE-exclusive PIS for m/z 202, two PS-exclusive PISs for m/z 148.1 and 261.1, and a PIS for m/z 199.1 for PC species (observed at odd m/z values) and SM species (observed at even m/z values). The standardized average area increase after TrEnDi modification was 10.72-fold for PE species, 2.36-fold for PC and 1.05-fold for SM species. The sensitivity increase of PS species was not quantified, as there were no unmodified PS species identified prior to derivatization. ^{13}C-TrEnDi allowed for the identification of 4 PE and 7 PS species as well as the identification and quantitation of another 4 PE and 4 PS species that were below the limit of detection (LoD) prior to modification. A total of 24 PE species and 6 PC species that could only be identified when unmodified surpassed their respective limit of quantitation (LoQ) area thresholds after modification.

4.2 Introduction

Of the eight general lipid classes,[1] glycerophospholipids constitute the majority of lipids in the cell and have been identified as key components in various diseases such as cancer.[2] Consequently, their study and identification as cellular biomarkers enables a greater understanding of disease and holds promise for new therapeutic avenues.[3] Glycerophospholipids contain a glycerol backbone, a polar head group on the *sn*-3 position, and two fatty acyl groups with variable lengths and degrees of unsaturation on the *sn*-1 and *sn*-2 positions;[2] the *sn*-3 group distinguishes between subclasses of glycerophospholipids.[2] Sphingomyelin (SM), a sphingolipid[4], is a phosphocholine ester of a ceramide[5] and hence is classified as a phospholipid.

Phosphatidylcholine (PC), phosphatidylethanolamine (PE) and phosphatidylserine (PS), three of the most common lipids in eukaryotic membranes,[6] have been found to play important roles in cellular health and disease.[3] For example, increases in intracellular levels of ether-linked PCs and PEs have been connected to metastatic colorectal cancer.[2] Reduced levels of PC in the brain have been shown to lead to degeneration of cell membranes, which is directly linked to the development of Alzheimer's disease, and allows PC to be used as a predictive disease biomarker.[7] The production of PC in the brain is achieved by the methylation of PE, thereby linking both PC and PE to Alzheimer's disease.[8] PE has also been identified as a eukaryotic membrane receptor for promoting antimicrobial activity through host defence peptides, a component of the immune system that works against a multitude of microbes as well as cancer cells.[9] Sickle cells show increased expression of PS, contributing to a shortened erythrocyte lifespan and vascular occlusion, effectively escalating the disease state.[10] Commonly found on the inner plasma membrane of cells, PS can also be used to identify tumor cells and hypoxic cardiomyocytes, which express PS on the surface of the cell, providing a method of

identification.[11] Atherosclerotic diseases, such as ischemic heart disease, have been linked to increased SM levels in the body, allowing SM to be used as a comprehensive biomarker.[5] These, and other similar discoveries have highlighted the importance phospholipid characterization and analysis, leading to a significant increase in lipidomics research and literature.[12] Most notably, mass spectrometry has been at the forefront of the revolutionary advancements in the field of lipidomics in recent years, and is continually allowing insight into the composition of cellular membranes and identification of previously unknown biomarkers.[3]

Despite the prevalence of lipid research in recent years, there are still significant difficulties in this field. Many cellular biomarkers are present in lower concentrations, requiring enhanced sensitivity or novel methods of identification. Some improvements have been made by modifying the various species using isotopically labeled sulfonium ions, a fixed quaternary ammonium group, or amine group to impart a fixed positive charge.[2,3,13]

The methylation of ester fatty acids using diazomethane has enhanced their analysis via gas chromatography (GC) and MS.[14-16] Dipalmitoylphosphatidylethanolamine has been successfully converted to dipalmitoylphosphatidyl [tris(*N*-methyl-^{3}H)] choline[17] using diazomethane and T_2O, but was ineffective when attempting to concurrently methylate the primary amine and phosphate moieties of glycerophospholipids. The methylation of phosphate moieties and carboxylic acids can be achieved using trimethylsilyldiazomethane, but primary amines and other functional groups remain unmodified.[18,19] We have previously developed novel, rapid, and cost-effective methods to enhance the sensitivity of phospholipid MS[20] and proteomic MS analyses.[21] Chemical derivatization of PE, PC, SM and PS via trimethylation enhancement using diazomethane led to the complete methylation of phosphate moieties, carboxylic acids, and primary amines, resulting in permanently positively charged analytes with a concomitant

sensitivity enhancement. Sensitivity of tandem MS experiments was particularly improved, as ion fragmentation of derivatized analytes was consolidated to only one or two channels.[20]

In this study, we employ ^{13}C-labelled diazomethane to address the issue of differentiation between isobaric PE and PC species created by derivatization with unlabeled diazomethane – a significant limitation of our initial studies. Furthermore, the effectiveness of ^{13}C-TrEnDi in analyzing complex lipid extracts is demonstrated through the analysis of the membrane composition of human cervical carcinoma (HeLa) cells.

4.3 Experimental

Chemicals and materials. Formic acid and tetrafluoroboric acid dimethyl ether complex were purchased from Sigma-Aldrich (St. Louis, MO, USA); absolute ethanol was purchased from Commercial Alcohols Inc. (Brampton, ON, Canada); potassium hydroxide, methanol, chloroform, isopropanol, and ether were purchased from Caledon Laboratories Ltd. (Georgetown, ON, Canada); sodium acetate was purchased from Bioshop Canada Inc. (Burlington, ON, Canada), sodium nitrite was obtained from BDH Chemicals Ltd. (Poole, England); glacial acetic acid, 28% ammonium hydroxide and ammonium acetate were obtained from Anachemia Canada Inc. (Montreal, QC, Canada). PE(16:0/18:1(9Z)), PC(16:0/18:1(9Z)), PE(8:0/8:0) PS(8:0/8:0) and PC(5:0/5:0) were synthesized by and obtained from Avanti Polar Lipids Inc. (Alabaster, Alabama, USA). *N-(Methyl-^{13}C)-N-nitroso-p-toluenesulfonamide was readily prepared from ^{13}C-methanol (Cambridge Isotope Laboratories, Cambridge, Massachusetts, USA), an inexpensive and widely available material ^{13}C label source, according to the procedure reported by Shields and Manthorpe.*[22]

***^{13}C*-Diazomethane production**. *All reactions involving the preparation of diazomethane were carried out in an efficient chemical fume hood and behind a safety blast shield.* The production of ^{13}C-diazomethane was performed analogously to unlabeled diazomethane using a Sigma-Aldrich Mini Diazald diazomethane generator with fire-polished clear-seal joints, as has been described elsewhere[23] and previously reported by our groups.[20-22]

Cell culture and lipid extraction. Human cervical carcinoma (HeLa) cells were purchased from ATCC (CCL-2) (Manassas, VA, USA) and grown using 87% Eagle's Minimum Essential Medium, 10% fetal bovine serum and 3% penicillin/streptomycin/antimycotic (Life Technologies Inc., Burlington, ON, Canada). Cells were cultured in a humidified atmosphere at 37 °C and 5% CO_2 using triple-gas incubators (Thermo Forma, Rockford, Illinois). Phospholipids were extracted using a modified Bligh and Dyer procedure.[24] After extracting lipids in the chloroform phase, chloroform evaporation was followed by resuspension of the extracted lipidome in 600 µL of EtOH.

In-solution chemical derivatization. The same lipid extract was used for all modified and unmodified experiments. The lipid extract was divided into 25 µL aliquots. In-solution chemical derivatization used 1.0 µL of a freshly prepared and vigorously homogenized 14:1 (v/v) solution of diethyl ether and tetrafluoroboric acid dimethyl ether complex (HBF_4•OMe_2) instead of 0.5 µL,[20] after optimization experiments were performed. The rest of the in-solution chemical derivatization was performed as previously described by our group.[20] Once completely dried, each aliquot of the modified lipidome extract was re-suspended in 50 µL of ethanol and 10 µL of 8 µM PC(5:0/5:0) was added as a lipid standard to allow relative quantitation. As a control, aliquots of non-derivatized lipidome extract were dried down and resuspended in 50 µL ethanol

and 10 µL of 8 µM PC (5:0/5:0) was added. Chemical derivatization was performed in triplicates.

Reversed phase high pressure liquid chromatography. Ten µL of the modified lipid sample containing the lipid standard was mixed with 30 µL of deionized H_2O and added to the autosampler of a Dionex Ultimate 3000 HPLC (Thermo Scientific, Odense, Denmark). Lipids were separated using a C_4 reversed phase column and a ternary gradient program consisting of 30% MeOH, 70% H_2O with 10 mM $NH_4C_2H_3O_2$ (mobile phase A), 100% IPA with 10 mM $NH_4C_2H_3O_2$ (mobile phase B) and 100% hexane (mobile phase C). The C_4 column was prepared by packing a fritted 14 cm long piece of fused silica (200 µm ID) (Molex Inc., Lisle, IL, USA) with 5.5 cm of Reprosil-Pur C_4 beads (Dr. Maisch GmbH HPLC, Ammerbuch-Entringen, Germany). The HPLC gradient began at 100% A, increased to 100% B over 36.3 min, followed by 10% B/90% C by 39.5 min at an average flowrate of 135 µL/min. The run was then completed with a 2 mL system wash of 10% B/90% C. Each analytical run was followed by a full blank run to further clean the system and ensure no lipid carryover occurred.

ESI-MS/MS analyses. The HPLC eluent was introduced into an AB Sciex 4000 QTRAP via a Turbo V ionspray source (AB Sciex, Framingham, MA, USA). All LC-MS/MS studies were acquired in positive ion mode at an ESI voltage of 5000 V, a scan rate of 250 Da per second, a declustering potential (DP) of 80 V, and an ion source gas value (GS) of 20. For the modified and unmodified samples, five scans were performed per chromatographic run using low resolution for Q1 and unit resolution for Q3 (unless stated otherwise). The unmodified scans included three PISs for m/z 184.1 from 400 to 450 Th (CE of 35 eV, lipid standard), 600 to 1300 Th (CE of 40 eV, PC species) and 600 to 900 Th (CE of 40eV with Q1 and Q3 being set to unit resolution, PC and SM species), a NL scan for 141.1 Da from 600 to 1000 Th (CE of 25 eV, PE

species), and a NL scan for 185.1 Da from 600 to 1000 Th (CE of 23 eV, PS species). The modified scans included a PIS for m/z 184.1 from 400 to 450 Th (CE of 35 eV, lipid standard), two PISs for m/z 199.1 from 615 to 1315 Th (CE of 40 eV, PC^{Tr} species) and 615 to 915 Th (CE of 40 eV with Q1 and Q3 being set to unit resolution, PC^{Tr} and SM^{Tr} species), a PIS for m/z 202.1 from 660 to 1060 Th (CE of 40 eV, PE^{Tr} species) and a PIS for m/z 148.1 from 675 to 1075 Th (CE of 60 eV, PS^{Tr} species). The chemical triplicate derivatized aliquots were individually analyzed. Unmodified aliquots were also analyzed in triplicate.

For the direct infusion analyses on PS, unmodified lipid extracts were resuspended in 75 µL of EtOH with 10 mM $NH_4C_2H_3O_2$ or 75 µL of EtOH with 10 mM NH_4OH while modified samples were resuspended in 75 µL of EtOH. The lipid extracts were directly infused into the ionspray source at a rate of 1.5 µL per minute using a Harvard 11 Plus syringe pump (Harvard Apparatus, Holliston, MA, USA). An ESI voltage of 5000 V and DP of 40 V were used for positive ion mode scans and a voltage of -4000 V and DP of -40 V for negative ion scans. A scan rate of 250 Da/s, unit resolution for Q1 and Q3 and an ion source gas value of 8 were used for all scans. Final mass spectra were obtained by averaging 30 scans. The unmodified scans included a positive NL for 185.1 Da from 600 to 1000 Th (CE of 23eV) and a negative NL for 87.0 Da from 600 to 1000 Th (CE of -28eV). The modified scans included a positive PIS for m/z 148.1 from 600 to 1000 Th (CE of 60eV) and a positive PIS for m/z 261.1 from 600 to 1000 Th (CE of 40eV). The chemical triplicate derivatized aliquots were individually analyzed. Unmodified aliquots were also analyzed in triplicate.

Data analysis. Analyst 1.5.1 was used for the acquisition of the mass spectra and data was exported to MultiQuant 2.1.1 (AB Sciex, Framingham, MA, USA) where peak area measurements were performed on the extracted ion chromatographs (XICs) of each species. The

different PIS and NL scans served to determine the glycerophospholipid polar head group identity, and ^{13}C-TrEnDi modified scans provided head group identity confirmation. The limit of detection (LoD) area threshold and limit of quantitation (LoQ) area threshold were calculated following the Clinical and Laboratory Standards Institute (CLSI) guideline EP17, Protocols for Determination of Limits of Detection and Limits of Quantitation as summarized by Armbruster and Pry[25] by measuring 90 limit of blank (LoB) measurements and 90 low concentration standard deviations for each unmodified and modified scan used. Non-standardized peak area averages were used to determine if the lipid was below the limit of detection (BLoD) area threshold [noise], above the LoD area threshold or above the LoQ area threshold. All unmodified and modified areas were standardized by dividing by the area of the lipid standard which allowed relative quantitation. To calculate the fold sensitivity increase after methylation the standardized area averages of ^{13}C-TrEnDi-modified lipids were divided by their respective unmodified standardized area average equivalent. Only standardized areas with standard deviation values less than 30% and with non-standardized values above the LoQ area threshold were used to calculate the fold increase. For qualitative sensitivity improvement (species area values changing after ^{13}C-TrEnDi modification from: being above the LoD to above the LoQ, being BLoD to above the LoD, or being BLoD to above the LoQ) a standard deviation cutoff of 40% or less was used, otherwise the qualitative improvement was discarded. All standardized area value enhancements after derivatization were assessed for statistical significance via Student's *t*-test at a 95% confidence level. Methylation efficiency (% yield) was calculated by analyzing any remaining unmodified species (or, in the case of PE, unmodified and partially modified species) in the modified aliquots using optimal conditions for unmodified species and their respective unmodified scans. Comparing the standardized areas of unmodified lipids in modified aliquots

with unmodified standardized areas in unmodified aliquots allowed for the calculation of the percent standardized area values of unmodified lipids post-methylation. To calculate SM areas the M+1 area of the corresponding PC (if present) was subtracted. SM area values had to be 10% higher than the predicted M+1 PC peak (if present) in order to be considered a SM species. All lipids in all lipid classes had to have area values 10% higher than the predicted M+2 areas (if present) in order to be considered a different lipid species.

4.4 Results and Discussion

We have recently reported the use of TrEnDi to create methylated derivatives of peptides[21] and several classes of lipids[20]. TrEnDi has been demonstrated to rapidly and fully convert substrates/analytes into species that ionize with greater efficiency and fragment in a predictable and more sensitive manner. A key feature of this chemistry is the introduction of a fixed, permanent positive charge via the formation of quaternary ammonium groups. In the case of lipids, the use of HBF_4 as a strong acid that forms a non-coordinating, non-nucleophilic conjugate base allows for the concomitant methylation of phosphate moieties, thereby permanently neutralizing their negative charge and affording a lipid with a single permanent, fixed positive charge. Lipid derivatization via TrEnDi obviates the need for analyte protonation, eliminating ion suppression and rendering TrEnDi inherently quantitative. TrEnDi-derivatized glycerophospholipids do not form adducts (e.g. with sodium); the MS signal is consolidated into a single peak even in salty solvents, enhancing sensitivity. Furthermore, MS/MS of TrEnDi-derivatized glycerophospholipids yields one or two fragmentation channels with high intensity, thus increasing sensitivity and simplifying data analysis. The TrEnDi chemistry is rapid and

straightforward and uses a minimal amount of diazomethane; when carefully conducted behind a blast shield in a fumehood, the technique poses minimal risk to the user.

Our initial publication on TrEnDi with lipids demonstrated significant sensitivity enhancements to PE analysis; however, the applicability of TrEnDi to biological samples was hampered by the fact that TrEnDi-modified PC derivatives (PC^{Tr}) yield the same head group as TrEnDi-modified PE derivatives (PE^{Tr}). This issue was overcome through the synthesis of ^{13}C-labelled diazomethane[22] for use in TrEnDi derivatization (Scheme 4.4.1). Derivatization with this reagent results in a PIS of m/z 202.1, exclusive to PE species, and a PIS of m/z 199.1 for PC and SM species (Figure 4.4.1).

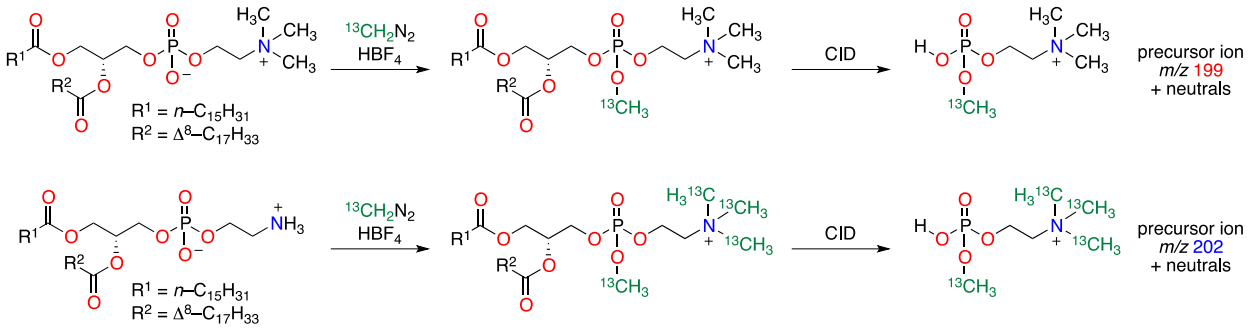

Scheme 4.4.1: TrEnDi derivatization of PC(16:0/18:1(9Z)) and PE(16:0/18:1(9Z)) with $^{13}CH_2N_2$.

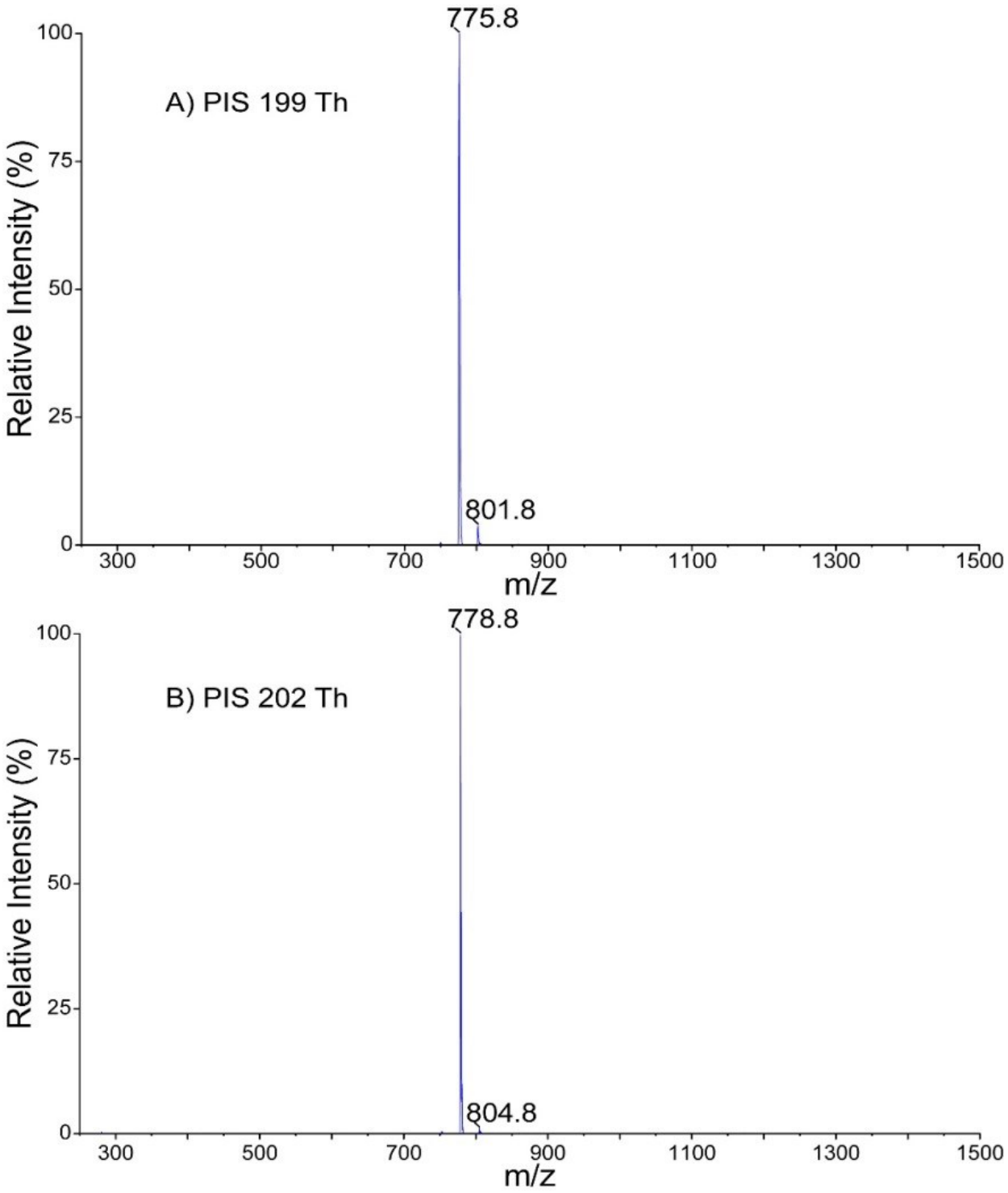

Figure 4.4.1: ^{13}C-TrEnDi modification differentiates modified PE species from modified PC species by providing a PC^{Tr}-specific +PIS of m/z 199.1 (A) and a PE^{Tr}-specific +PIS of m/z 202 (B). PC (16:0/18:1) and PE (16:0/18:1), which would have been isobaric (m/z 774.8, +PIS m/z 198.1) using unlabeled TrEnDi, yield m/z of 775.9 (A) and 778.9 (B), respectively, after ^{13}C-TrEnDi modification.

^{13}C-TrEnDi on PE analysis in HeLa cells lipid extracts

As predicted, the sensitivity of PE analyses increased following ^{13}C-TrEnDi modification and every PE increased in mass by 60 Da, as the three protons on the 1° amine group and the proton on the phosphate moiety were each substituted with a ^{13}C-methyl group. The unmodified PE spectra were acquired via a NL scan of 141.1 Da, while the modified PE spectra were acquired via a PIS of m/z 202.1 (Figure 4.4.2). The three most intense unmodified PE peaks of 718.8, 744.8 and 768.6 Th in the unmodified spectrum (Figure 4.4.2A) correspond to the three tallest modified PE peaks of 778.9, 804.9, and 828.9 Th in the modified spectrum (Figure 4.4.2B). All modified PE peaks have a significantly stronger signal in comparison to their unmodified PE counterparts.

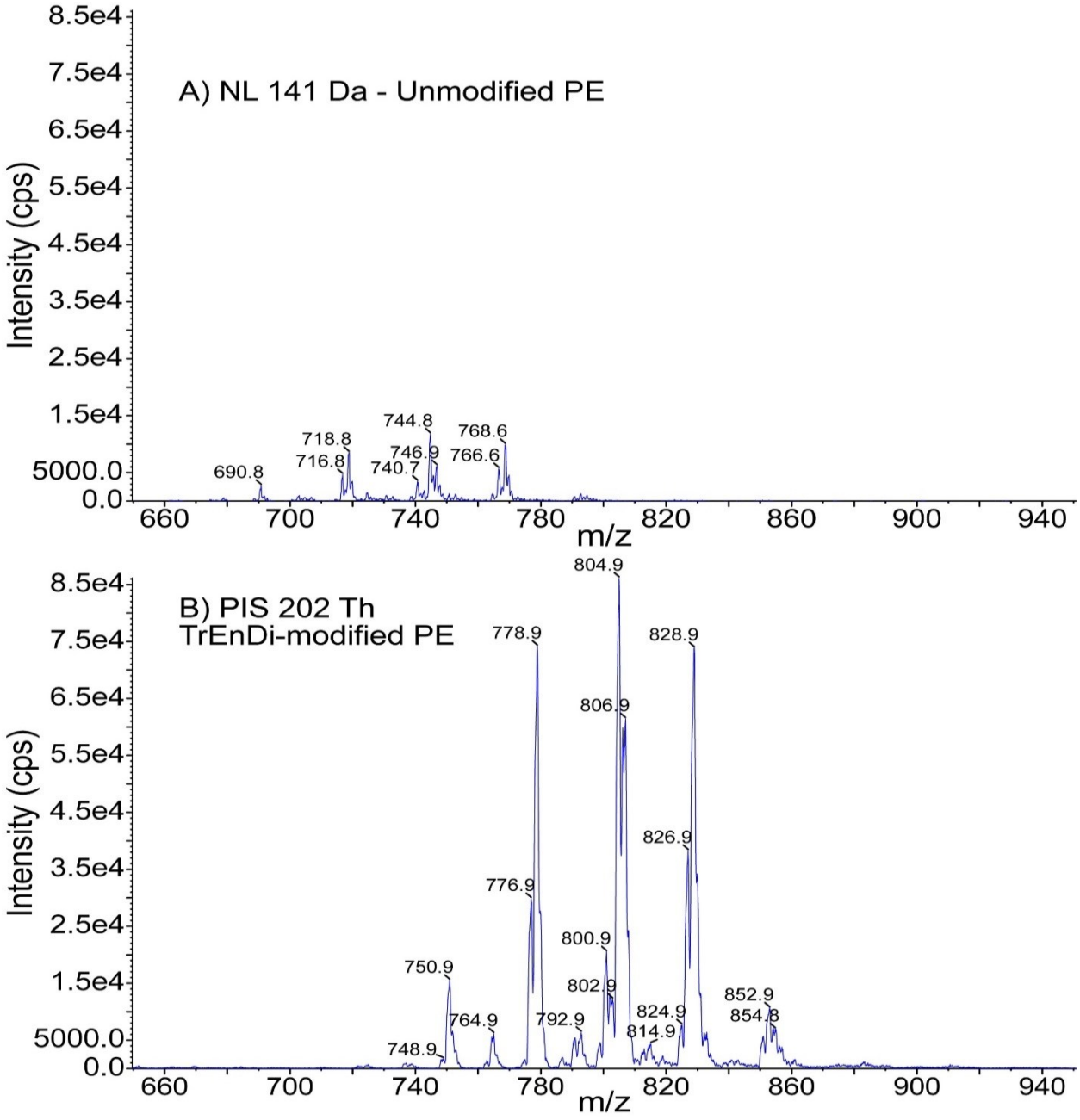

Figure 4.4.2: Mass spectrum of unmodified PE from HeLa cell lipid extract acquired via +NL scan of 141.1 Da (A). Mass spectrum of ^{13}C-TrEnDi-modified PE from HeLa cells lipid extract acquired via +PIS of m/z 202 (B). The y-axis was set to the same scale for both spectra and only peaks above a 2% maximum intensity threshold are labelled. Both spectra were acquired via reversed phase LC-MS/MS and represent a 40 minute average of all spectra obtained during the time that lipid species eluted. The LC-MS parameters were optimized to provide the best signal possible for unmodified species to provide a fair assessment when comparing them against their modified counterparts.

Every PE peak identified in the unmodified scan had a modified equivalent with a higher intensity and area; a total of 55 unmodified PE species and 63 modified PE species were identified. The comparison of the 20 highest standardized peak area averages between unmodified and modified PE triplicate runs are presented on Figure 4.4.3A. The TrEnDi-modified PE elution areas are higher following modification and show low standard deviations for both the unmodified and modified species. The remaining 43 PE standardized peak area averages are presented in Figures 4.6.1 and 4.6.2. It is noteworthy that after TrEnDi modification we observed a significant sensitivity increase between peaks with area values that differed across 4 orders of magnitude, from the most abundant species (Figure 4.4.3) to the least-abundant species (Figure 4.6.2). All PE species experienced a statistically significant standardized area increase after TrEnDi modification.

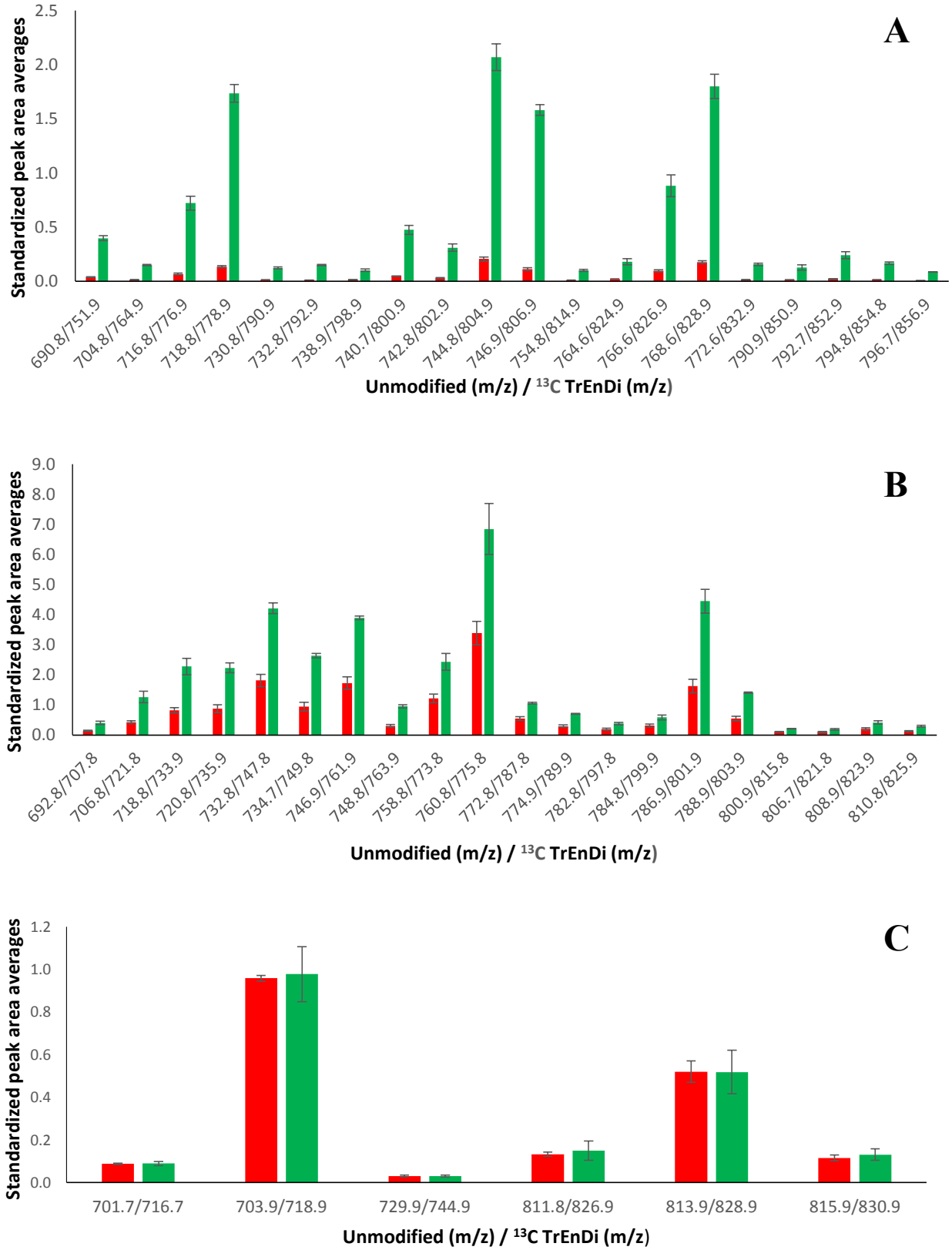

Figure 4.4.3: Comparison of standardized peak area averages between unmodified triplicates (red bars) and ^{13}C-TrEnDi chemical triplicates (green bars) for (A) PE, (B) PC and (C) SM extracted from HeLa

cells. The twenty highest standardized peak area averages for PE species are presented (A) out of 63 PE species identified revealing a statistically significant intensity increase following modification. The twenty highest standardized peak area averages for PC species are presented (B) out of 63 PC species identified. A less prominent yet statistically significant increase was observed for the standardized area of PC species. All PE and PC species experienced statistically significant enhancements to their standardized peak area average values. The standardized area values of SM species (C) did not change following TrEnDi modification.

An average standardized area fold increase of 10.72 ± 2.01 after ^{13}C-TrEnDi modification (Table 4.4.1) was calculated by averaging all 30 quantifiable PE species whose individual fold increase values are presented in Table 4.6.3 (the determination of all statistical parameters used in all experiments is thoroughly discussed in the supplementary information). The small relative standard deviation values of PE standardized areas (Figure 4.4.3, 4.6.1, 4.6.2) calculated from ^{13}C-TrEnDi chemical triplicates demonstrate a constant and reliable sensitivity increase. This is further corroborated by the small relative standard deviation average calculated from all 30 PE species quantified (Table 4.4.1).

The 10.72-fold increase is slightly higher than the previous 7.96-fold increase reported for a PE standard,[20] which highlights the detrimental effects of proton competition in a complex biological standard (even after chromatographic separation) in comparison to the much simpler standard mixture used in TrEnDi II.[20] There were 24 PE species whose area values increased from being above the LoD threshold to being above the LoQ threshold after modification with ^{13}C-labeled diazomethane. This highlights the power of our technique to properly and accurately quantify lower abundant PE species that otherwise could only be detected. Four unmodified species with area values BLoD increased above the LoD threshold after TrEnDi modification and an additional four unmodified PE species with area values BLoD increased above the LoQ threshold (Table 4.6.4). The area values of these four species lie slightly above their LoQ

threshold and when divided by 10.72 their calculated unmodified area values fall below their respective LoD threshold (Table 4.6.2). ^{13}C-TrEnDi was able to identify and quantify 8 low-abundance PE species that would otherwise be unidentifiable because they were below the noise level when using conventional PE analysis methods. The capability to identify and quantify low abundance lipids that may possess significant biological roles or be a strategic biomarker or molecular signaling molecule demonstrates the importance and potential of ^{13}C-TrEnDi analysis.

Table 4.4.1: Summary of ^{13}C-TrEnDi enhancements on identification and quantitation of PE, PC and SM in HeLa cells.

	PE	**PC**	**SM**
Quantitative enhancements			
Average Fold increase	**10.72**	**2.36**	**1.05**
Relative standard deviation (%)	18.76	21.04	6.41
Percentage of remaining unmethylated or partially methylated species (%)	0[#]	0.37	0[#]
Number of species used to calculate the average	n=30	n=51	n=6
Qualitative enhancements			
Number of species increasing from LoD to LoQ*	**24**	**6**	0
Number of species increasing from BLoD to LoD*	**4**	0	0
Number of species increasing from BLoD to LoQ*	**4**	0	0

[#]All of the unmethylated or partially methylated area values were below the limit of detection (BLoD).

*LoQ= Limit of Quantitation, LoD = Limit of Detection, BLoD= Below the Limit of Detection.

^{13}C-TrEnDi on PC and SM in HeLa cells

PC and SM species experienced a 15 Da mass increase following TrEnDi modification via ^{13}C-methylation of the phosphate group; unmodified PC and SM spectra were acquired via PIS of m/z 184.1 while the modified PC and SM spectra were acquired via PIS of m/z 199.1.

PC species obtained a modest sensitivity increase following ^{13}C-TrEnDi modification. A total of 63 unmodified PC species were identified prior to TrEnDi derivatization. All 63 were also observed after modification and the 20 most intense signals are presented in Figure 4.4.3B. The remaining 43 PC standardized peak area averages are presented in Figures 4.6.3 and 4.6.4. As with PE, PC species, despite having peak areas varying across four orders of magnitude, all displayed a sensitivity increase after TrEnDi (Figures 4.4.3 and 4.6.4). All 63 PC species present a statistically significant standardized area increase post-modification with exception of two PC species with m/z of 876.8/891.9 and 920.8/935.9 (unmodified m/z, modified m/z) presented in Fig 4.6.4. The peaks presented in Figure 4.6.4 are close to the LoD threshold and hence contain higher standard deviation values than the other 42 PC species identified. The overall small relative standard deviation values of PC standardized areas (Figure 4.4.3, 4.6.3, 4.6.4) calculated from ^{13}C-TrEnDi chemical triplicates demonstrate a constant and reliable sensitivity enhancement.

An average standardized area fold increase of 2.36 ± 0.50 after ^{13}C-TrEnDi modification (Table 4.4.1) was calculated by averaging all 51 quantifiable PC species whose individual fold increase values are presented in Table 4.6.5. The 21.04% relative standard deviation average calculated from all 51 PC species quantified demonstrates a constant and reliable sensitivity increase across all PC species (Table 4.4.1). There were 6 PC species whose area values increased from above the LoD threshold to above the LoQ threshold after modification. A global

sensitivity increase was achieved after ^{13}C-TrEnDi modification, and several PC species that could only be identified before modification became quantifiable.

^{13}C-TrEnDi modification did not lead to a sensitivity boost or hindrance for SM species. A total of 6 SM species were identified in the unmodified and modified spectra and are presented in Figure 4.4.3C. After performing average standardized area fold increase calculations for the six SM species a value of 1.05 ± 0.07 was obtained (Table 4.4.1). The individual fold increase values are presented in Table 4.6.7. Analysis of the PC (5:0/5:0) external standard on its own revealed a SM contaminant with a m/z of 675.8. The lipid standard solution was always added after TrEnDi modification, and the fold increase for the modified 690.8 m/z peak demonstrates a 0.53-fold increase, revealing the amount of indigenous 675.8 m/z SM in HeLa cells happened to be approximately the same amount as the standard's SM contaminant.

The ^{13}C-TrEnDi average standardized area fold increase values of 2.36 for PC species (n=51) and 1.05 for SM species (n=6) are significantly lower than that which was reported in our previous work[20]. In our previous publication, the same optimized concentration of ammonium acetate as the protonating agent was used as in the experiments presented here, yet the phospholipid standard mixture had no chromatographic separation since it was analyzed via direct infusion. Without chromatographic separation, the unmodified PC and SM species experienced a division between protonated and sodiated states (even with the optimal concentration addition of protonation agent). This effectively divided and reduced the unmodified PC and SM signal because their respective MS/MS studies only analyze the protonated component. This led to a more significant fold increase reported in our previous work as the modified species do not experience different ionization states, nor require a protonating agent. In the experiments reported herein, the chromatographic separation helped reduce sodium

adducts and produced proportionally stronger signals for the unmodified species, explaining the smaller fold increase observed in the PC and SM populations in HeLa cells.

^{13}C-TrEnDi methylation efficiency

In order to ensure quantitative performance of ^{13}C-TrEnDi, the percent yield (methylation efficiency) of the chemical derivatization for PE, PC and SM species present in the HeLa cell lipid extract was assessed by scanning for unmodified species in the modified aliquots using optimal unmodified conditions (including a protonation source). Since PC and SM exhibit a single ^{13}C-methyl addition, analyzing their unmodified counterparts in the derivatized lipid solution directly provides the percent yield of the chemical derivatization. The percent standardized area of unmodified lipids after methylation for PC species is presented in Table 4.6.5, for SM species in Table 4.6.7 and for PE species in Table 4.6.3.

In order to quantify the percentage of unmodified lipids after ^{13}C-TrEnDi modification, unmodified species with area values higher than the LoQ threshold were used. An average of 0.37% standardized area was observed for unmodified PC post-modification, thus demonstrating a virtually quantitative yield of 99.63%. For SM and PE species a 100% yield was obtained since there were no unmodified remaining species with areas higher than the LoQ threshold. Even when using unmodified area values above the LoD (and LoQ) threshold, an average of 0.30% unmodified PC standardized area remained; while using all unmodified area values (BLoD, LoD and LoQ) revealed 1.08% unmodified PC standardized area remained, a 0.42% unmodified SM standardized area remained and 0.55% unmodified PE standardized area remained.

In order to properly assess the percent yield for PE species, PIS and NL scans corresponding to full methylation and lack of 1, 2, 3 or 4 ^{13}C-methylation events were performed

on three of the highest intensity PE species found in the HeLa cell extract (fully modified m/z values of 804.9, 806.9 and 828.9). The methylation efficiency results showed no remaining unmodified areas above the LoD threshold for all the PIS and NL scans (Table 4.6.8). This confirmed a 100% yield of fully modified PE post ^{13}C-TrEnDi modification.

The content of ^{12}C and ^{13}C after synthesis of ^{13}C-diazomethane from ^{13}C-methanol[22] was evaluated with MS quantitation experiments. The synthesis yielded 99.07% ^{13}C-diazomethane and 0.93% ^{12}C-diazomethane (Table 4.6.1).

^{13}C-TrEnDi on PS in HeLa cells

All PS species exhibited a mass shift of 75 Da following ^{13}C-TrEnDi modification, corresponding to the exchange of five protons for five ^{13}C-methyl groups in the carboxylic acid, amine (x3) and phosphate groups of the PS head group. ^{13}C-TrEnDi modification provided an outstanding sensitivity increase to PS species. There were no unmodified species above the LoD identified by the +NL scan of 185.1 Da or the –NL scan of 87.0 Da (Figure 4.4.4A and 4.4.4B). By contrast, the modified scans of +PIS of m/z 261.1 (Figure 4.4.4D) was able to identify three PS species above the LoQ and one above the LoD, while the +PIS of m/z 148.1 (Figure 4.4.4C) was able to identify three PS species above the LoQ and seven above the LoD. Both modified scans identified the same PS species and highlight the importance of our technique in identifying and quantifying phospholipid species that otherwise would go unidentified.

Unlike the PE, PC and SM experiments that were performed via LC-MS, the PS studies were performed via direct infusion after realization that modified PS species were not compatible with the solvents used in our HPLC separation. In contrast, 100% EtOH direct infusion experiments provided no hindrance to the modified PS spectrum, demonstrating its efficacy for

direct spray studies. A TrEnDi modified PS (5:0/5:0) standard was successfully analyzed in EtOH via direct spray but also demonstrated lack of compatibility with our LC-MS separation solvents, indicating this was not a sample-specific occurrence.

In order to determine that the peaks observed in the PIS of m/z 261.1 and 148.1 were modified PS species, the unmodified aliquot was concentrated by a factor of 4 and analyzed via a +NL scan of 185.1 Da. This revealed three peaks above the LoD with m/z values of 762.7, 788.8 and 790.7 (Figure 4.4.5C). These three peaks correspond with the three tallest peaks identified by both modified scans, demonstrating that the three peaks are indeed modified PS species whose areas increased above the LoQ threshold from noise after modification. Table 4.4.2 summarizes the results obtained by the triplicate modified and four-fold concentrated unmodified runs. Even after the four-fold concentration of the unmodified sample, the intensity values are significantly lower and there are fewer PS species identified in comparison to the modified scans. Having two different PISs (m/z 261.1 and 148.1) for TrEnDi-modified PS species enabled us to identify a non-PS contaminant at m/z 810 via its exclusivity to the PIS of m/z 148.1. This approach also provided confident identification of the other peaks as modified PS species, since only modified PS head groups would be able to dissociate via both fragmentation pathways. The m/z 810 contaminant peak has an even m/z value while all ^{13}C-TrEnDi modified PS species have odd masses and is absent on the PIS of m/z 261.1, indicating that it is not a PS.

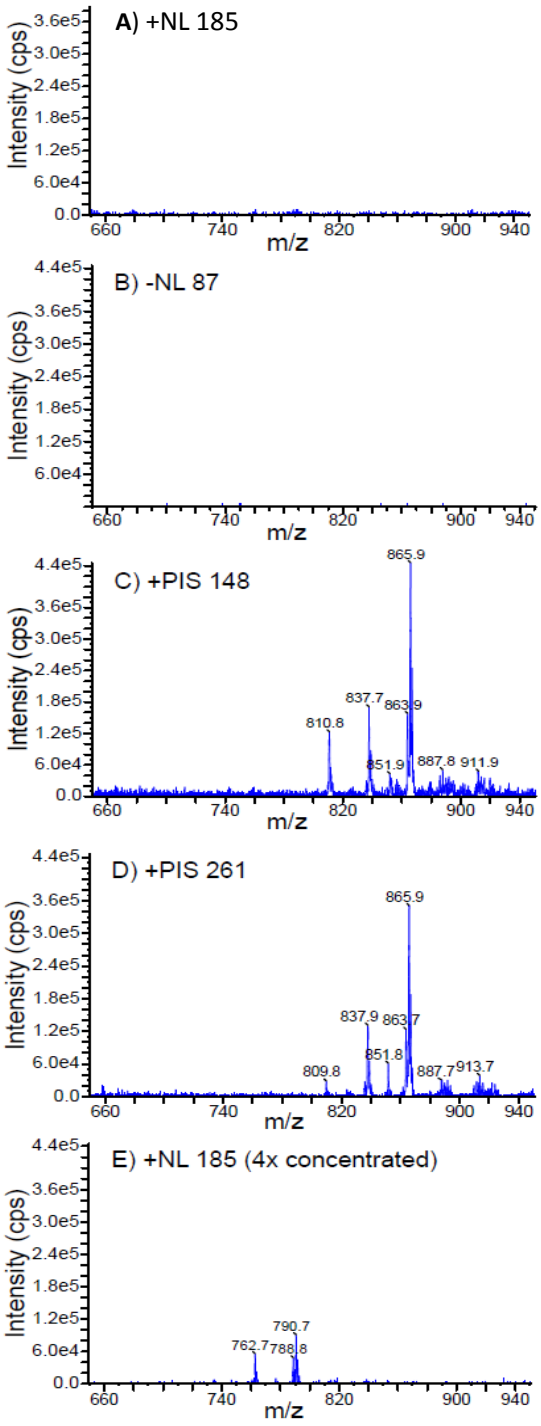

Figure 4.4.4: The unmodified HeLa cell PS lipidome was dissolved in EtOH with 10 mM ammonium acetate or 10 mM ammonium hydroxide and analyzed via their respective +NL of 185.1 Da (A) or –NL of 87.0 Da scans (B). No PS species were identified with either scan. The ^{13}C-TrEnDi-modified HeLa cell PS lipidome was analyzed via +PIS of m/z 148.1 in EtOH (C) and +PIS of m/z 261.1 in EtOH (D). Both modified scans had an outstanding sensitivity increase allowing the identification of several modified PS

species. The unmodified HeLa cell extract was concentrated 4 times and analyzed via +NL 185.1 Da in a solution of 10 mM ammonium acetate in EtOH (E). The three highest unmodified species in pane E correspond with the three highest species in pane C and D (after considering the 75 Da increase post-modification) corroborating their identity as unmodified and modified PS species. The y-axis was set to the same value for all spectra.

Table 4.4.2: ^{13}C-TrEnDi enhancements on the PS lipidome of HeLa cells.

+NL 185.1 Da Unmodified lipids (4x concentrated)				**+PIS m/z 261.1 TrEnDi lipids**				**+PIS m/z 148.1 TrEnDi lipids**			
m/z	Analytical sensitivity	Average area	Relative standard deviation (%)	m/z	Analytical sensitivity	Average area	Relative standard deviation (%)	m/z	Analytical sensitivity	Average area	Relative standard deviation (%)
734.7	BLoD	$7.50x10^3$	88.19	809.8	BLoD	$2.00x10^4$	25.00	810.8	**LoQ**	$1.03x10^6$	11.71
748.9	BLoD	$9.17x10^3$	41.66	823.8	BLoD	$2.42x10^4$	46.65	823.7	BLoD	$5.25x10^4$	38.98
760.7	BLoD	$1.00x10^4$	50.00	835.9	BLoD	$1.08x10^5$	26.21	835.9	**LoD**	$2.08x10^5$	31.40
762.7	**LoD**	$1.74x10^5$	54.04	837.9	**LoQ**	**$7.58x10^5$** #	10.00	837.7	**LoQ**	**$1.13x10^6$** #	16.37
776.8	BLoD	$2.08x10^4$	36.66	851.8	**LoD**	$1.88x10^5$	32.03	851.9	**LoD**	$2.43x10^5$	7.71
788.8	**LoD**	$1.57x10^5$	53.79	863.7	**LoQ**	**$7.66x10^5$** #	10.94	863.9	**LoQ**	**$1.12x10^6$** #	10.36
790.7	**LoD**	$4.13x10^5$	37.10	865.9	**LoQ**	**$2.05x10^6$** #	8.24	865.9	**LoQ**	**$3.11x10^6$** #	16.20
812.4	BLoD	$3.33x10^3$	86.60	887.7	BLoD	$8.00x10^4$	62.50	887.8	**LoD**	$1.83x10^5$	17.54
814.5	BLoD	$6.67x10^3$	114.6	889.8	BLoD	$1.05x10^5$	16.67	889.9	**LoD**	$1.92x10^5$	13.19
816.6	BLoD	$1.33x10^4$	28.53	891.9	BLoD	$9.75x10^4$	10.26	891.9	**LoD**	$2.18x10^5$	9.41
836.8	BLoD	$6.67x10^3$	43.31	911.6	BLoD	$1.19x10^5$	26.73	911.9	**LoD**	$2.91x10^5$	12.04
838.8	BLoD	$9.17x10^3$	56.77	913.7	BLoD	$1.16x10^5$	32.47	913.9	**LoD**	$2.31x10^5$	15.18

*LoQ= Limit of Quantitation, LoD = Limit of Detection, BLoD= Below the Limit of Detection.

#Standardized area values above the LoQ for both +PIS m/z 261.1 and +PIS m/z 148.1 scans used to calculate how more sensitive the +PIS of m/z 148.1 is.

The unmodified PS lipidome was further investigated to verify the identity of every peak present in the modified scans. An unmodified sample aliquot was concentrated 2x and analyzed via LC-MS/MS using a +NL of 185.1 Da and lower resolution settings for Q1 to achieve higher sensitivity. The zoomed-in spectra presented in Supplemental Figure 4.6.5 was produced by exclusively selecting the chromatographic time frame when PS species elute, eliminating other interfering signals, reducing the background noise and allowing for confident PS identification via the spectrum produced, regardless of many peaks being minute. All of the peaks in the modified spectra produced via PIS of m/z 261.1 have a matching unmodified equivalent in the spectra portrayed in Figure 4.6.5 and vice versa (considering the modification of a 75 Da shift). This guaranteed all peaks in the modified spectra (with exception of m/z 810) to be modified PS species. Even m/z 809.8 was verified as a modified PS (independent of the 810 m/z contaminant) since its unmodified counterpart of m/z 734.7 appears on the unmodified spectrum. A small peak of m/z 748.9 in the unmodified spectrum has a small and thin modified equivalent of m/z 823.8 in both modified spectra. Even though the intensity of unmodified and modified peaks are slightly higher than the noise, their corresponding unmodified and modified areas are BLoD making them undistinguishable from noise when evaluated by area threshold parameters.

The modified PIS of m/z 148.1 is 1.49 ± 0.02 times more sensitive than the PIS of m/z 261 but has a higher noise background as a result of using a higher CE, and showed a non-PS contaminant in the spectrum (Figure 4.4.4A). The PIS of m/z 261 has a lower background noise and is exclusive for modified PS peaks making it the better scan for identification and quantitation (Figure 4.4.4B). Having two different scans easily verifies the polar head group identity of PS species. Even though the background noise in both scans for the TrEnDi-modified PS species is higher than that for unmodified PS species (leading to a mildly higher LoD and

LoQ threshold as presented in Table 4.6.2) the sensitivity boost obtained post ^{13}C-TrEnDi modification is greater than an order of magnitude and provides the ability to identify and quantify PS species that otherwise would be invisible via conventional methods.

4.5 Conclusion

The creation of permanently charged analytes, with no protonation requirement and therefore elimination of ion suppression make ^{13}C-TrEnDi an inherently quantitative technique vastly superior than conventional analysis methods. Permanently charged analytes will provide the same signal regardless of the complexity or simplicity of the sample being analyzed. ^{13}C-TrEnDi modification boasts percent yield values higher than 99.63% for complete methylation in all four phospholipid classes; the synthesis of ^{13}C-diazomethane from ^{13}C-methanol affords material with a 99.07% ^{13}C content, corroborating the quantitative nature of the technique. Even after thorough optimization of unmodified phospholipid studies to achieve maximum sensitivity via conventional MS/MS methods, ^{13}C-TrEnDi conclusively demonstrated vastly superior phospholipid sensitivity. An outstanding sensitivity enhancement for PE and PS species enabled the identification and quantitation of several species that lied below the limit of quantitation and detection prior to modification. A modest increase for PC species enabled the possibility of quantitation of several PC species. Modification of the sample does not hinder the identification or quantitation of SM species, enabling their study in modified samples just as well as their unmodified equivalents. The ^{13}C-TrEnDi modification process on biological lipid extracts proved to be a beneficial, easy, fast, and cost-effective method compatible with LC-MS and direct infusion experiments, with the exception of PS studies, which remain exclusive to direct infusion studies. ^{13}C-TrEnDi modification provides a more sensitive and robust methodology for the general study of the PE, PS, and PC lipidomes. It also provides the ability to identify and

quantify low abundance phospholipids with the potential to be key components in cellular signaling pathways or biomarkers of a particular diseased state, which otherwise would go undetected via conventional methods.

4.6 Supplementary information

The synthesis of ^{13}C-diazomethane from ^{13}C-methanol according to Shields and Manthorpe[22] was reported to contain 1% ^{12}C-diazomethane after ^{1}H NMR analysis. The content of ^{12}C-diazomethane in modified PC^{Tr} (5:0/5:0) and PE^{Tr} (8:0/8:0) lipid standards was analyzed via MS and MS/MS; results are presented in Table 4.6.1. The ^{13}C-TrEnDi-modified PC standard contained 0.93% ± 0.12% ^{12}C-modified PC, while the ^{13}C-TrEnDi modified PE standard contained 3.66% ± 0.43% ^{12}C-modified PE. The PE standard contains 3.94 times more ^{12}C than the PC standard because 4 methyl groups are added to PE in comparison to one methyl added to PC. ^{13}C-diazomethane synthesis yields 99.07% ^{13}C-diazomethane and 0.93% ^{12}C-diazomethane.

Table 4.6.1: Total ^{12}C content present in ^{13}C-diazomethane.

Lipid species	^{13}C			^{12}C			Percentage of ^{12}C content in diazomethane*	Relative standard deviation of ^{12}C content in diazomethane (%)
	m/z	area	Relative standard deviation (%)	m/z	area	Relative standard deviation (%)		
PC(5:0/5:0)	441.3	3.08×10^8	4.79	440.3	3.16×10^6	17.91	**0.93**	12.88
PE(8:0/8:0)	528.3	5.96×10^7	18.50	527.3	3.08×10^8	30.06	**3.66**	11.81

Determination of statistical parameters

In order to determine the analytical enhancements of ^{13}C-TrEnDi modification on the HeLa cell phospholipidome, aliquots of the same extract were modified and analyzed as chemical triplicates while keeping unmodified aliquots as controls. The HPLC separation containing 10 mM ammonium acetate was optimized to provide the best results for unmodified PC, SM, PE and PS species via MS/MS scans, with the parameters specified in the materials and methods section of this chapter. ^{13}C-TrEnDi modified samples were run under the same chromatographic conditions to guarantee identical experimental parameters between unmodified and modified samples, despite a protonation source being redundant post-modification.

Relative quantitation was performed to effectively and quantitatively compare the sensitivity increase after modification via the use of an external standard. The LoD and LoQ area threshold for every unmodified and modified scan are presented in Supplemental Table 4.6.2. The thresholds provided a clear cut-off between low signal species and noise, the ability to properly assess if unmodified species experienced qualitative enhancements (such as surpassing the LoD or LoQ threshold post-modification) and allowed comparisons between species with area values above their respective LoQ threshold. In general, the unmodified scans' thresholds values are slightly lower than their modified counterparts (Table 4.6.2), but sensitivity enhancement provided by TrEnDi modification readily overcomes the problem of having slightly higher noise thresholds. The sensitivity enhancement provided post-modification for all phospholipid classes tested overcame the problem of having mildly higher thresholds.

Table 4.6.2: Calculated LoD and LoQ area thresholds for PC, SM, PE and PS modified and unmodified scans.

		Scan type	LoD area threshold	LoQ area threshold
PC and SM	^{13}C-TrEnDi	PIS 199.1	$5.11x10^5$	$1.70x10^6$
	Unmodified	PIS 184.1	$5.02x10^5$	$1.67x10^6$
PE	^{13}C-TrEnDi	PIS 202.1	$4.32x10^5$	$1.44x10^6$
	Unmodified	NL 141.1	$4.05x10^5$	$1.35x10^6$
PS	^{13}C-TrEnDi	PIS 148.1	$1.83x10^5$	$6.11x10^5$
		PIS 261.1	$1.76x10^5$	$5.87x10^5$
	Unmodified	NL 185.1	$1.43x10^5$	$4.77x10^5$

Each specific scan threshold was calculated by measuring 90 LoB measurements along with 90 low concentration standard deviations as described by Armbruster and Pry[25].

Tables 4.6.3 and 4.6.4 present all the unmodified and modified PE peaks along with their standardized areas, relative standard deviations and area fold increases / qualitative enhancements. All unmodified and modified PC peaks are presented in Tables 4.6.5 and 4.6.6. All unmodified and modified SM peaks are presented in Table 4.6.7. All of the modified and unmodified PS peaks are presented in Table 4.4.2. All fold increase after derivatization values were calculated by dividing the average standardized area of the modified lipids by the standardized peak area of their respective unmodified counterparts. The analytical sensitivity is classified as below the limit of detection (BLoD), above the limit of detection (LoD) or above the limit of quantitation (LoQ) according to the value of the non-standardized peak area.

The standard deviation thresholds allowed the quantitative exclusion of one PE and six PC peaks (bottom of Table 4.6.3 and 4.6.5) out of the 143 phospholipid species identified. These

7 peaks were unfit for quantitation despite demonstrating a significant sensitivity fold increase post-modification, due to their sporadic area changes between triplicates.

Table 4.6.3: ^{13}C-TrEnDi quantitative enhancements on the PE lipidome of HeLa cells.

Unmodified lipids				**Remaining unmodified/under-modified lipids after TrEnDi**			**TrEnDi-Modified lipids**				**Fold increase after modification**
m/z	Analytical sensitivity	standardized area	Relative standard deviation (%)	Analytical sensitivity	standardized area	% standardized area of unmodified/ under-modified lipids after TrEnDi	m/z	Analytical sensitivity	standardized area	Relative standard deviation (%)	
676.8	LoQ	$2.15x10^{-3}$	26.80	BLoD	0.00	**0.00**	736.9	LoQ	$2.27x10^{-2}$	11.41	**10.54**
688.7	LoQ	$6.00x10^{-3}$	2.83	BLoD	$5.19x10^{-5}$	**0.86**	748.9	LoQ	$4.57x10^{-2}$	15.67	**7.62**
690.8	LoQ	$3.68x10^{-2}$	9.24	BLoD	$1.66x10^{-4}$	**0.45**	750.9	LoQ	$3.97x10^{-1}$	5.93	**10.79**
704.8	LoQ	$1.10x10^{-2}$	15.60	BLoD	$2.89x10^{-5}$	**0.26**	764.9	LoQ	$1.48x10^{-1}$	3.94	**13.47**
714.8	LoQ	$4.16x10^{-3}$	4.13	BLoD	0.00	**0.00**	774.9	LoQ	$3.36x10^{-2}$	10.32	**8.08**
716.8	LoQ	$6.67x10^{-2}$	11.05	BLoD	$1.86x10^{-4}$	**0.28**	776.9	LoQ	$7.21x10^{-1}$	8.93	**10.81**
718.8	LoQ	$1.33x10^{-1}$	7.35	BLoD	$3.00x10^{-4}$	**0.23**	778.9	LoQ	1.74	4.67	**13.09**
730.8	LoQ	$1.35x10^{-2}$	6.26	BLoD	$2.75x10^{-4}$	**2.03**	790.9	LoQ	$1.24x10^{-1}$	8.11	**9.12**
732.8	LoQ	$1.06x10^{-2}$	8.88	BLoD	0.00	**0.00**	792.9	LoQ	$1.49x10^{-1}$	3.49	**14.09**
738.9	LoQ	$1.24x10^{-2}$	9.94	BLoD	0.00	**0.00**	798.9	LoQ	$1.02x10^{-1}$	11.09	**8.20**
740.7	LoQ	$4.70x10^{-2}$	1.31	BLoD	$8.60x10^{-5}$	**0.18**	800.9	LoQ	$4.75x10^{-1}$	8.87	**10.11**
742.8	LoQ	$2.87x10^{-2}$	10.90	BLoD	$1.54x10^{-4}$	**0.54**	802.9	LoQ	$3.09x10^{-1}$	11.15	**10.79**
744.8	LoQ	$2.04x10^{-1}$	8.98	BLoD	$2.57x10^{-4}$	**0.13**	804.9	LoQ	2.07	5.92	**10.13**
746.9	LoQ	$1.12x10^{-1}$	11.62	BLoD	$3.40x10^{-4}$	**0.30**	806.9	LoQ	1.58	3.11	**14.08**

754.8	LoQ	$9.37x10^{-3}$	4.47	BLoD	$8.60x10^{-5}$	**0.92**	814.9	LoQ	$9.93x10^{-2}$	8.88	**10.60**
756.9	LoQ	$3.08x10^{-3}$	22.04	BLoD	$2.32x10^{-5}$	**0.76**	816.9	LoQ	$2.83x10^{-2}$	3.94	**9.21**
758.8	LoQ	$3.82x10^{-3}$	16.43	BLoD	$5.73x10^{-5}$	**1.50**	818.9	LoQ	$4.96x10^{-2}$	3.51	**12.98**
762.7	LoQ	$2.65x10^{-3}$	14.63	BLoD	0.00	**0.00**	822.8	LoQ	$2.15x10^{-2}$	7.73	**8.11**
764.6	LoQ	$2.19x10^{-2}$	7.24	BLoD	0.00	**0.00**	824.9	LoQ	$1.79x10^{-1}$	15.17	**8.18**
766.6	LoQ	$9.72x10^{-2}$	9.27	BLoD	0.00	**0.00**	826.9	LoQ	$8.82x10^{-1}$	11.45	**9.07**
768.6	LoQ	$1.76x10^{-1}$	7.14	BLoD	$1.60x10^{-4}$	**0.09**	828.9	LoQ	1.80	6.27	**10.23**
772.6	LoQ	$1.14x10^{-2}$	9.58	BLoD	$4.87x10^{-5}$	**0.43**	832.9	LoQ	$1.55x10^{-1}$	7.39	**13.55**
780.6	LoQ	$4.18x10^{-3}$	9.58	BLoD	$2.32x10^{-5}$	**0.56**	840.8	LoQ	$3.51x10^{-2}$	1.36	**8.40**
790.9	LoQ	$1.42x10^{-2}$	10.59	BLoD	$5.09x10^{-5}$	**0.36**	850.9	LoQ	$1.25x10^{-1}$	19.58	**8.81**
792.7	LoQ	$2.09x10^{-2}$	10.18	BLoD	$5.73x10^{-5}$	**0.27**	852.9	LoQ	$2.42x10^{-1}$	13.34	**11.58**
794.8	LoQ	$1.52x10^{-2}$	3.59	BLoD	$5.41x10^{-5}$	**0.36**	854.8	LoQ	$1.67x10^{-1}$	7.45	**10.99**
796.7	LoQ	$6.76x10^{-3}$	17.38	BLoD	$4.65x10^{-5}$	**0.69**	856.9	LoQ	$8.48x10^{-2}$	2.97	**12.55**
798.7	LoQ	$2.01x10^{-3}$	21.00	BLoD	$2.54x10^{-5}$	**1.27**	858.9	LoQ	$2.74x10^{-2}$	2.99	**13.65**
800.8	LoQ	$2.89x10^{-3}$	28.40	BLoD	$2.87x10^{-5}$	**0.99**	860.9	LoQ	$3.54x10^{-2}$	13.51	**12.07**
822.9	LoQ	$2.29x10^{-3}$	9.41	BLoD	$2.54x10^{-5}$	**1.11**	882.9	LoQ	$2.47x10^{-2}$	3.32	**10.78**
Species with a standard deviation higher than 30% and therefore unfit for quantitation											
782.7	LoQ	$3.25x10^{-3}$	36.20	BLoD	$8.06x10^{-5}$	2.48	842.9	LoQ	$3.79x10^{-2}$	6.94	11.66

Table 4.6.4: ^{13}C-TrEnDi qualitative enhancement on the PE lipidome of HeLa cells.

Unmodified lipids					TrEnDi-Modified lipids				
m/z	Average Area	Analytical sensitivity	standardized area	% standard deviation	m/z	Average Area	Analytical sensitivity	standardized area	% standard deviation
Increase from BLoD to LoD									
660.9	$7.79x10^{4}$	BLoD	$1.08x10^{-4}$	53.73	720.9	$1.15x10^{6}$	LoD	$2.41x10^{-3}$	27.71
710.9	$1.27x10^{5}$	BLoD	$1.76x10^{-4}$	34.38	770.9	$6.91x10^{5}$	LoD	$1.46x10^{-3}$	33.45
860.9	$7.79x10^{4}$	BLoD	$1.11x10^{-4}$	77.46	920.9	$1.25x10^{6}$	LoD	$2.63x10^{-3}$	34.34
886.9	$4.87x10^{4}$	BLoD	$7.34x10^{-5}$	132.99	946.9	$1.18x10^{6}$	LoD	$2.50x10^{-3}$	27.51
Increase from BLoD to LoQ									
840.9	$1.75x10^{5}$	BLoD	$2.46x10^{-4}$	12.27	900.9	$2.50x10^{6}$	LoQ	$5.29x10^{-3}$	17.72
844.8	$1.12x10^{5}$	BLoD	$1.58x10^{-4}$	18.77	904.8	$2.46x10^{6}$	LoQ	$5.24x10^{-3}$	32.92
846.9	$1.85x10^{5}$	BLoD	$2.52x10^{-4}$	27.91	906.9	$2.69x10^{6}$	LoQ	$5.64x10^{-3}$	18.75
854.7	$1.75x10^{5}$	BLoD	$2.51x10^{-4}$	40.78	914.7	$3.22x10^{6}$	LoQ	$6.79x10^{-3}$	19.41
Increase from LoD to LoQ									
662.8	$6.91x10^{5}$	LoD	$9.73x10^{-4}$	32.56	722.8	$4.15x10^{6}$	LoQ	$8.70x10^{-3}$	27.01
664.7	$8.18x10^{5}$	LoD	$1.16x10^{-3}$	19.65	724.9	$7.56x10^{6}$	LoQ	$1.59x10^{-2}$	22.13
678.9	$9.64x10^{5}$	LoD	$1.36x10^{-3}$	16.69	738.8	$9.96x10^{6}$	LoQ	$2.10x10^{-2}$	13.81
712.7	$5.06x10^{5}$	LoD	$7.11x10^{-4}$	25.53	772.8	$2.45x10^{6}$	LoQ	$5.20x10^{-3}$	21.66
736.9	$1.06x10^{6}$	LoD	$1.45x10^{-3}$	27.72	796.9	$5.45x10^{6}$	LoQ	$1.15x10^{-2}$	1.46
760.9	$1.33x10^{6}$	LoD	$1.83x10^{-3}$	19.66	820.9	$1.35x10^{7}$	LoQ	$2.85x10^{-2}$	10.02
784.8	$8.67x10^{5}$	LoD	$1.22x10^{-3}$	10.55	844.8	$9.26x10^{6}$	LoQ	$1.95x10^{-2}$	6.54
786.9	$5.45x10^{5}$	LoD	$7.46x10^{-4}$	28.18	846.9	$6.27x10^{6}$	LoQ	$1.32x10^{-2}$	16.79
788.7	$5.36x10^{5}$	LoD	$7.62x10^{-4}$	29.57	848.7	$5.69x10^{6}$	LoQ	$1.19x10^{-2}$	19.81
802.7	$8.67x10^{5}$	LoD	$1.20x10^{-3}$	15.73	862.7	$8.03x10^{6}$	LoQ	$1.69x10^{-2}$	24.74
804.9	$5.74x10^{5}$	LoD	$7.99x10^{-4}$	38.01	864.9	$4.25x10^{6}$	LoQ	$8.96x10^{-3}$	16.62
806.8	$4.48x10^{5}$	LoD	$6.41x10^{-4}$	34.75	866.8	$3.92x10^{6}$	LoQ	$8.24x10^{-3}$	27.12
810.7	$4.19x10^{5}$	LoD	$5.87x10^{-4}$	10.49	870.7	$3.38x10^{6}$	LoQ	$7.11x10^{-3}$	16.94
812.6	$4.67x10^{5}$	LoD	$6.38x10^{-4}$	24.52	872.7	$3.89x10^{6}$	LoQ	$8.21x10^{-3}$	23.25
814.9	$4.28x10^{5}$	LoD	$5.97x10^{-4}$	14.56	874.9	$5.54x10^{6}$	LoQ	$1.17x10^{-2}$	33.27
816.8	$4.07x10^{5}$	LoD	$5.77x10^{-4}$	24.50	876.7	$4.82x10^{6}$	LoQ	$1.02x10^{-2}$	34.08
818.8	$5.16x10^{5}$	LoD	$7.13x10^{-4}$	24.71	878.9	$5.32x10^{6}$	LoQ	$1.12x10^{-2}$	9.32
820.9	$4.97x10^{5}$	LoD	$6.99x10^{-4}$	20.53	880.8	$6.44x10^{6}$	LoQ	$1.36x10^{-2}$	5.79
824.7	$8.86x10^{5}$	LoD	$1.26x10^{-3}$	29.89	884.8	$8.15x10^{6}$	LoQ	$1.72x10^{-2}$	2.13
826.9	$6.23x10^{5}$	LoD	$8.74x10^{-4}$	17.41	886.9	$4.86x10^{6}$	LoQ	$1.03x10^{-2}$	7.25
828.9	$6.13x10^{5}$	LoD	$8.53x10^{-4}$	4.93	888.9	$5.56x10^{6}$	LoQ	$1.17x10^{-2}$	12.27
848.9	$4.48x10^{5}$	LoD	$6.38x10^{-4}$	48.53	908.9	$3.40x10^{6}$	LoQ	$7.16x10^{-3}$	0.95
850.7	$7.20x10^{5}$	LoD	$1.00x10^{-3}$	5.84	910.8	$6.49x10^{6}$	LoQ	$1.37x10^{-2}$	5.01
852.9	$5.55x10^{5}$	LoD	$7.93x10^{-4}$	35.48	912.9	$5.08x10^{6}$	LoQ	$1.08x10^{-2}$	12.75

Table 4.6.5: ^{13}C-TrEnDi quantitative enhancement on the PC lipidome of HeLa cells.

Unmodified lipids				**Remaining unmodified/under-modified lipids after TrEnDi**			**TrEnDi-Modified lipids**				**Fold increase after TrEnDi$^{\#}$**
m/z	Analytical sensitivity	standardized area	Relative standard deviation (%)	Analytical sensitivity	standardized area	% standardized area of unmodified /under-modified lipids after TrEnDi	m/z	Analytical sensitivity	standardized area	Relative standard deviation (%)	
664.7	LoQ	3.03×10^{-3}	16.34	BLoD	5.18×10^{-5}	**1.71**	679.7	LoQ	8.10×10^{-3}	29.91	**2.67**
678.8	LoQ	2.16×10^{-2}	6.10	BLoD	9.25×10^{-4}	**4.28**	693.7	LoQ	4.22×10^{-2}	20.86	**1.96**
692.8	LoQ	1.47×10^{-1}	15.77	BLoD	3.36×10^{-4}	**0.23**	707.8	LoQ	4.07×10^{-1}	14.14	**2.77**
706.8	LoQ	4.29×10^{-1}	11.81	BLoD	1.26×10^{-3}	**0.29**	721.8	LoQ	1.26	15.16	**2.95**
718.8	LoQ	8.29×10^{-1}	10.86	LoD	2.13×10^{-3}	**0.26**	733.9	LoQ	2.28	12.07	**2.75**
720.8	LoQ	8.85×10^{-1}	14.82	LoD	2.21×10^{-3}	**0.25**	735.9	LoQ	2.24	7.27	**2.53**
732.8	LoQ	1.82	11.13	LoQ	6.16×10^{-3}	**0.34$^{\Omega}$**	747.8	LoQ	4.22	4.12	**2.32**
734.7	LoQ	9.47×10^{-1}	15.15	LoD	3.84×10^{-3}	**0.41**	749.8	LoQ	2.64	2.92	**2.79**
746.9	LoQ	1.73	11.52	LoD	3.65×10^{-3}	**0.21**	761.9	LoQ	3.90	1.52	**2.25**
748.8	LoQ	3.04×10^{-1}	15.28	BLoD	7.28×10^{-4}	**0.24**	763.9	LoQ	9.58×10^{-1}	5.28	**3.15**
752.8	LoQ	4.13×10^{-3}	14.66	BLoD	1.00×10^{-4}	**2.44**	767.9	LoQ	1.21×10^{-2}	28.58	**2.93**
756.8	LoQ	7.35×10^{-2}	13.80	BLoD	1.95×10^{-4}	**0.27**	771.7	LoQ	1.36×10^{-1}	5.97	**1.85**
758.8	LoQ	1.22	11.45	LoD	3.82×10^{-3}	**0.31**	773.8	LoQ	2.44	11.31	**2.00**
760.8	LoQ	3.39	11.48	LoQ	1.36×10^{-2}	**0.40$^{\Omega}$**	775.8	LoQ	6.85	12.39	**2.02**
772.8	LoQ	5.58×10^{-1}	11.43	BLoD	9.53×10^{-4}	**0.17**	787.8	LoQ	1.06	2.33	**1.90**
774.9	LoQ	3.00×10^{-1}	11.96	BLoD	5.25×10^{-4}	**0.18**	789.9	LoQ	7.10×10^{-1}	1.39	**2.37**
778.9	LoQ	1.54×10^{-2}	23.41	BLoD	2.03×10^{-4}	**1.32**	793.8	LoQ	2.40×10^{-2}	11.53	**1.56**
780.9	LoQ	7.31×10^{-2}	17.18	BLoD	1.96×10^{-4}	**0.27**	795.8	LoQ	1.09×10^{-1}	12.67	**1.49**

782.8	LoQ	$2.02x10^{-1}$	18.06	BLoD	$5.18x10^{-4}$	**0.26**	797.8	LoQ	$3.84x10^{-1}$	10.63	**1.90**
784.8	LoQ	$3.18x10^{-}_{1}$	15.24	BLoD	$6.21x10^{-4}$	**0.20**	799.9	LoQ	$5.89x10^{-1}$	14.71	**1.85**
786.9	LoQ	1.64	13.85	LoD	$4.37x10^{-3}$	**0.27**	801.9	LoQ	4.46	8.93	**2.72**
788.9	LoQ	$5.56x10^{-1}$	14.15	LoD	$1.66x10^{-3}$	**0.30**	803.9	LoQ	1.42	1.48	**2.55**
798.8	LoQ	$4.82x10^{-2}$	12.02	BLoD	$8.59x10^{-5}$	**0.18**	813.9	LoQ	$9.63x10^{-2}$	2.83	**2.00**
800.9	LoQ	$1.08x10^{-1}$	13.26	BLoD	$1.28x10^{-4}$	**0.12**	815.8	LoQ	$2.17x10^{-1}$	2.26	**2.00**
802.8	LoQ	$6.50x10^{-2}$	16.13	BLoD	$2.47x10^{-4}$	**0.38**	817.9	LoQ	$1.78x10^{-1}$	9.04	**2.75**
804.7	LoQ	$3.04x10^{-2}$	19.42	BLoD	$1.03x10^{-4}$	**0.34**	819.7	LoQ	$5.08x10^{-2}$	3.30	**1.67**
806.7	LoQ	$1.04x10^{-1}$	17.16	BLoD	$1.61x10^{-4}$	**0.15**	821.8	LoQ	$1.92x10^{-1}$	14.22	**1.85**
808.9	LoQ	$2.07x10^{-1}$	17.07	BLoD	$4.00x10^{-4}$	**0.19**	823.9	LoQ	$4.21x10^{-1}$	13.54	**2.04**
810.8	LoQ	$1.28x10^{-1}$	17.40	BLoD	$2.55x10^{-4}$	**0.20**	825.9	LoQ	$2.97x10^{-1}$	9.03	**2.32**
832.8	LoQ	$6.18x10^{-2}$	15.67	BLoD	$1.24x10^{-4}$	**0.20**	847.8	LoQ	$1.38x10^{-1}$	9.06	**2.23**
834.7	LoQ	$6.82x10^{-2}$	15.84	BLoD	$2.33x10^{-4}$	**0.34**	849.9	LoQ	$1.33x10^{-1}$	13.47	**1.95**
836.9	LoQ	$4.56x10^{-2}$	14.81	BLoD	$2.04x10^{-4}$	**0.45**	851.9	LoQ	$1.18x10^{-1}$	1.96	**2.59**
838.9	LoQ	$1.94x10^{-2}$	12.04	BLoD	$1.29x10^{-4}$	**0.66**	853.9	LoQ	$3.77x10^{-2}$	6.82	**1.94**
840.9	LoQ	$1.63x10^{-2}$	15.96	BLoD	$2.54x10^{-5}$	**0.16**	855.8	LoQ	$4.05x10^{-2}$	3.51	**2.48**
842.9	LoQ	$2.12x10^{-2}$	9.19	BLoD	$1.11x10^{-4}$	**0.52**	857.9	LoQ	$4.67x10^{-2}$	8.98	**2.20**
844.9	LoQ	$9.95x10^{-3}$	12.95	BLoD	$5.40x10^{-5}$	**0.54**	859.9	LoQ	$3.08x10^{-2}$	7.74	**3.10**
846.8	LoQ	$9.54x10^{-3}$	11.43	BLoD	$3.49x10^{-4}$	**3.66**	861.9	LoQ	$2.22x10^{-2}$	19.17	**2.33**
852.9	LoQ	$1.00x10^{-2}$	8.01	BLoD	$1.31x10^{-4}$	**1.31**	867.9	LoQ	$1.74x10^{-2}$	12.97	**1.74**
854.7	LoQ	$1.40x10^{-2}$	16.33	BLoD	$5.18x10^{-5}$	**0.37**	869.9	LoQ	$2.66x10^{-2}$	3.56	**1.90**
856.9	LoQ	$1.51x10^{-2}$	15.43	BLoD	$7.41x10^{-5}$	**0.49**	871.9	LoQ	$3.92x10^{-2}$	6.31	**2.59**
860.9	LoQ	$5.93x10^{-3}$	8.47	BLoD	$9.83x10^{-5}$	**1.66**	875.9	LoQ	$2.21x10^{-2}$	17.03	**3.72**
862.9	LoQ	$6.83x10^{-3}$	27.58	BLoD	$7.73x10^{-5}$	**1.13**	877.9	LoQ	$2.07x10^{-2}$	26.87	**3.03**

864.9	LoQ	$6.79x10^{-3}$	25.80	BLoD	$5.59x10^{-4}$	**8.24**	879.9	LoQ	$1.53x10^{-2}$	17.50	**2.25**
866.8	LoQ	$3.72x10^{-3}$	22.94	BLoD	$1.50x10^{-4}$	**4.05**	881.7	LoQ	$1.00x10^{-2}$	19.23	**2.70**
868.9	LoQ	$5.88x10^{-3}$	14.49	BLoD	$5.18x10^{-5}$	**0.88**	883.9	LoQ	$1.20x10^{-2}$	18.69	**2.04**
870.9	LoQ	$5.55x10^{-3}$	5.00	BLoD	$1.06x10^{-4}$	**1.91**	885.9	LoQ	$1.49x10^{-2}$	20.15	**2.68**
872.9	LoQ	$3.39x10^{-3}$	22.15	BLoD	$2.32x10^{-5}$	**0.68**	887.9	LoQ	$1.09x10^{-2}$	22.90	**3.22**
878.8	LoQ	$4.31x10^{-3}$	2.49	BLoD	$1.18x10^{-4}$	**2.74**	893.7	LoQ	$1.08x10^{-2}$	25.37	**2.51**
880.7	LoQ	$4.72x10^{-3}$	15.95	BLoD	$1.62x10^{-4}$	**3.44**	895.8	LoQ	$9.56x10^{-3}$	24.26	**2.03**
882.9	LoQ	$3.20x10^{-3}$	28.78	BLoD	$2.54x10^{-5}$	**0.79**	897.9	LoQ	$1.07x10^{-2}$	29.41	**3.35**
892.9	LoQ	$2.92x10^{-3}$	25.38	BLoD	$1.31x10^{-4}$	**4.49**	907.8	LoQ	$5.89x10^{-3}$	26.12	**2.01**
Species with a standard deviation higher than 30% and therefore unfit for quantitation											
848.9	LoQ	$1.15x10^{-2}$	8.41	BLoD	$1.00x10^{-4}$	0.87	863.9	LoQ	$2.78x10^{-2}$	32.45	2.42
874.9	LoD	$1.95x10^{-3}$	38.45	BLoD	$2.32x10^{-5}$	1.19	889.9	LoQ	$9.71x10^{-3}$	40.40	4.98
876.8	LoQ	$2.63x10^{-3}$	32.06	BLoD	$1.06x10^{-4}$	4.03	891.9	LoQ	$1.24x10^{-2}$	73.14	4.73
894.6	LoD	$1.43x10^{-3}$	25.05	BLoD	$2.32x10^{-5}$	1.62	909.7	LoQ	$7.22x10^{-3}$	43.72	5.05
896.9	LoD	$1.74x10^{-3}$	16.84	BLoD	$2.54x10^{-5}$	1.46	911.7	LoQ	$8.96x10^{-3}$	48.44	5.14
920.8	LoQ	$4.41x10^{-3}$	25.87	BLoD	$1.21x10^{-4}$	2.75	935.9	LoQ	$8.27x10^{-3}$	32.20	1.87

$^{\Omega}$Values used to calculate the percentage of unmodified lipids after ^{13}C-TrEnDi since their non-standardized areas have values greater than their respective LoQ threshold.

Table 4.6.6: ^{13}C-TrEnDi qualitative enhancement on the PC lipidome of HeLa cells.

Unmodified lipids					**TrEnDi-Modified lipids**				
m/z	Average Area	Analytical sensitivity	standardized area	% standard deviation	m/z	Average Area	Analytical sensitivity	standardized area	% standard deviation
Increase from LoD to LoQ									
884.8	$1.62x10^{6}$	LoD	$2.30x10^{-3}$	31.52	899.9	$3.14x10^{6}$	LoQ	$6.58x10^{-3}$	34.55
886.8	$1.21x10^{6}$	LoD	$1.71x10^{-3}$	29.94	901.9	$2.74x10^{6}$	LoQ	$5.82x10^{-3}$	35.22
888.9	$6.43x10^{5}$	LoD	$9.01x10^{-4}$	15.98	903.8	$2.85x10^{6}$	LoQ	$6.01x10^{-3}$	36.75
890.9	$1.13x10^{6}$	LoD	$1.61x10^{-3}$	39.53	905.9	$3.28x10^{6}$	LoQ	$6.90x10^{-3}$	28.92
898.9	$1.48x10^{6}$	LoD	$2.08x10^{-3}$	14.20	913.9	$3.17x10^{6}$	LoQ	$6.67x10^{-3}$	33.96
902.9	$1.52x10^{6}$	LoD	$2.14x10^{-3}$	20.09	917.9	$4.13x10^{6}$	LoQ	$8.69x10^{-3}$	13.36

Table 4.6.7: ^{13}C-TrEnDi effects on the SM lipidome of HeLa cells.

Unmodified lipids				**Remaining unmodified/under-modified lipids after TrEnDi**			**TrEnDi-Modified lipids**				**Fold increase after TrEnDi #**
m/z	Analytical sensitivity	standardized area	Relative standard deviation (%)	Analytical sensitivity	standardized area	% standardized area of unmodified/ under-modified lipids after TrEnDi	m/z	Analytical sensitivity	standardized area	Relative standard deviation (%)	
701.7	LoQ	$8.82x10^{-2}$	3.00	BLoD	$5.09x10^{-5}$	0.06	716.7	LoQ	$8.89x10^{-2}$	11.39	**1.01**
703.9	LoQ	$9.58x10^{-1}$	1.37	BLoD	$9.30x10^{-4}$	0.10	718.9	LoQ	$9.77x10^{-1}$	13.22	**1.02**
729.9	LoQ	$3.06x10^{-2}$	10.62	BLoD	$1.40x10^{-4}$	0.46	744.9	LoQ	$3.03x10^{-2}$	17.28	**0.99**
811.8	LoQ	$1.33x10^{-1}$	7.29	BLoD	$3.99x10^{-4}$	0.30	826.9	LoQ	$1.48x10^{-1}$	29.94	**1.12**
813.9	LoQ	$5.20x10^{-}_{1}$	9.78	BLoD	$4.28x10^{-4}$	0.08	828.9	LoQ	$5.18x10^{-1}$	19.61	**1.00**
815.9	LoQ	$1.15x10^{-1}$	11.73	BLoD	$3.66x10^{-4}$	0.32	830.9	LoQ	$1.31x10^{-1}$	19.94	**1.14**
Contaminant peak from the PC(5:0/5:0) standard											
675.8	LoQ	$5.35x10^{-2}$	2.69	LoQ	$2.75x10^{-2}$	51.51	690.8	LoQ	$2.83x10^{-2}$	19.36	0.53

Comparison of the remaining PE and PC standardized peak area averages between unmodified and ^{13}C-TrEnDi chemical triplicates

Figure 4.4.3 presents a comparison between the ^{13}C-TrEnDi –modified and their respective unmodified standardized peak area averages of the 20 PE and 20 PC species with highest values. The remaining 43 PE modified and unmodified standardized peak area comparisons are presented in Figure 4.6.1 and 4.6.2, the latter containing the species with lowest standardized peak area averages. The remaining 43 PC modified and unmodified standardized peak area comparisons are presented in Figure 4.6.3 and 4.6.4. Figure 4.6.4 contains 21 PC species with the lowest standardized peak area values out of which two PC species did not demonstrate a statistically significant change.

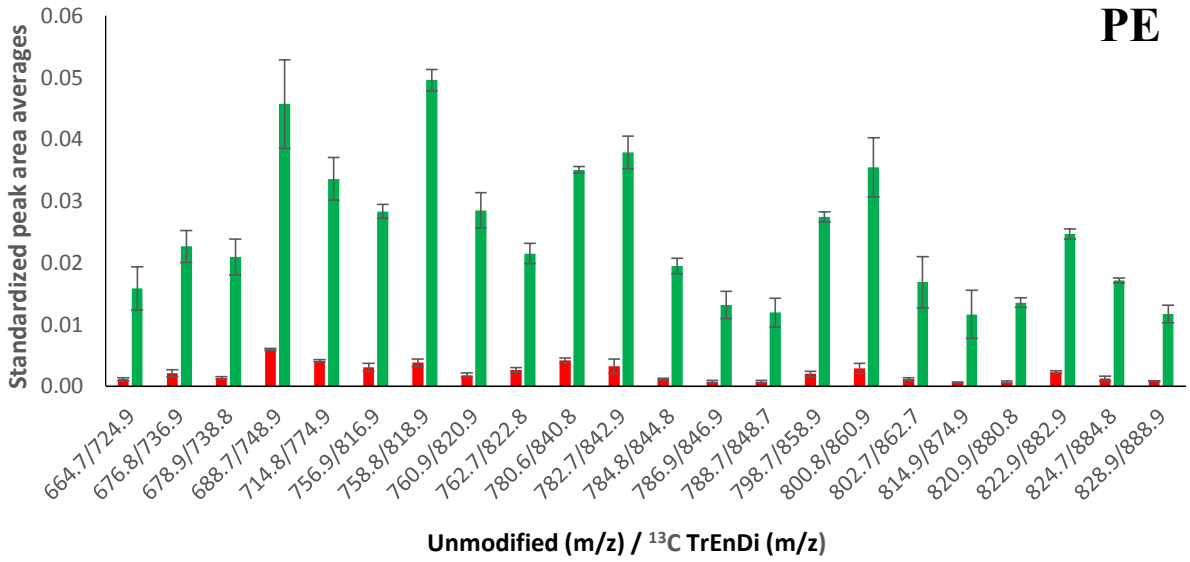

Figure 4.6.1: Comparison of standardized peak area averages between unmodified triplicates (red bars) and ^{13}C-TrEnDi chemical triplicates (green bars) for PE extracted from HeLa cells. The peaks represent 22 peaks with medium standardized peak area values out of 63 PE species found. All PE species experienced statistically significant enhancements to their standardized peak area average values.

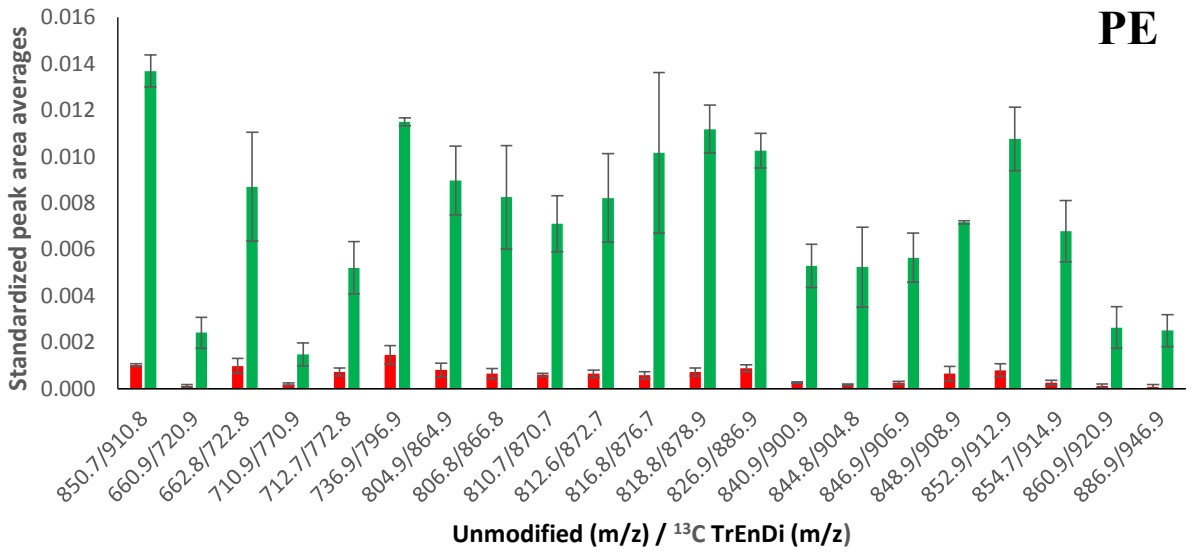

Figure 4.6.2: Comparison of standardized peak area averages between unmodified triplicates (red bars) and ^{13}C-TrEnDi chemical triplicates (green bars) for PE extracted from HeLa cells. These peaks represent 21 peaks with lowest standardized peak area values out of 63 PE species found. All PE species experienced statistically significant enhancements to their standardized peak area average values.

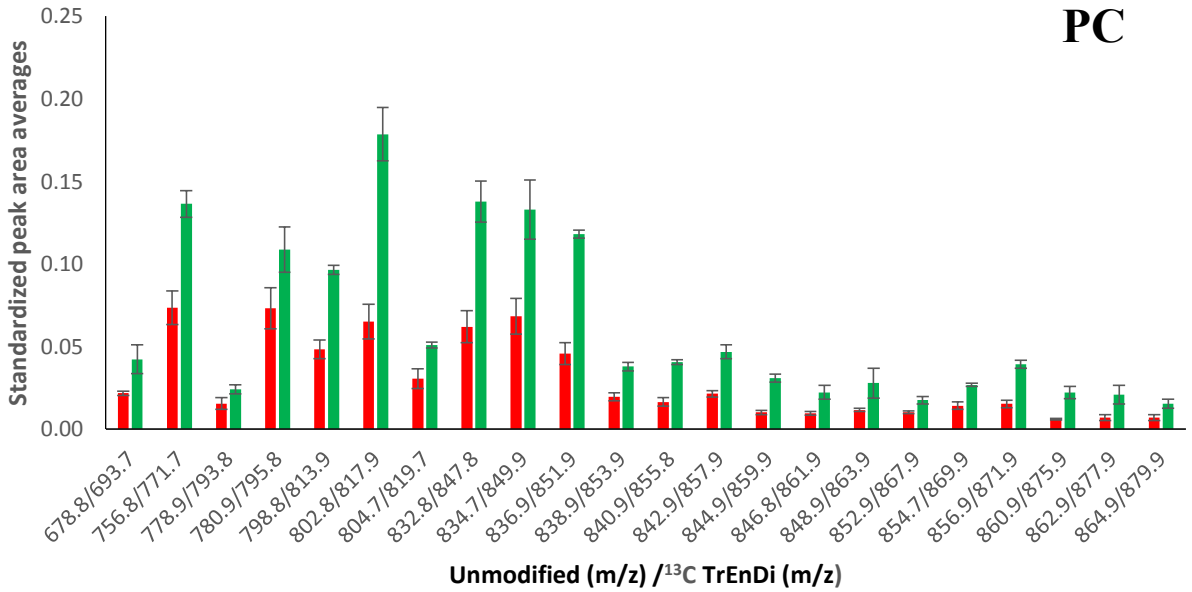

Figure 4.6.3: Comparison of standardized peak area averages between unmodified triplicates (red bars) and ^{13}C-TrEnDi chemical triplicates (green bars) for PC extracted from HeLa cells. These peaks represent 22 peaks with medium standardized peak area values out of 63 PC species found. All PC species experienced statistically significant enhancements to their standardized peak area average values.

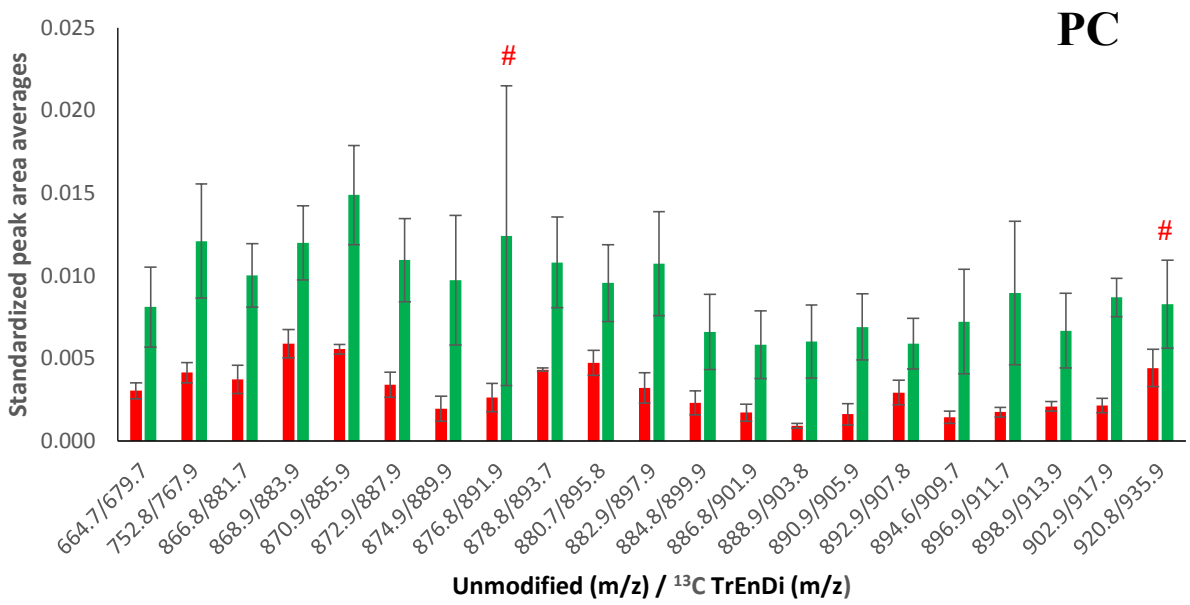

Figure 4.6.4: Comparison of standardized peak area averages between unmodified triplicates (red bars) and ^{13}C TrEnDi chemical triplicates (green bars) for PC extracted from HeLa cells. These peaks represent 21 peaks with lowest standardized peak area values out of 63 PC species found. All PC species experienced statistically significant enhancements to their standardized peak area average values with exception of two PC species marked by the red # symbols.

^{13}C-TrEnDi methylation efficiency of PE species

Derivatization of PE species results in the addition of four ^{13}C-methyl groups, thus the analysis of unmodified PE species in a derivatized aliquot is not useful in assessing the methylation efficiency of the reaction. In order to properly assess PE methylation efficiency, scans analyzing the lack of one or more methylation events were performed and the results presented in Table 4.6.8. No partially methylated species were discovered above the LoD, indicating the reaction goes to completion. The results are further discussed in the ^{13}C-TrEnDi methylation efficiency section of the 4.4 results and discussion section.

Table 4.6.8: PE methylation efficiency test results on three PE species present in the HeLa cell extract.

Scan type	m/z	Average area	Analytical sensitivity	Relative standard deviation (%)	Percent area of species not fully modified
Fully unmodified m/z= 798.9, fully methylated m/z= 828.9					
+PIS 202.1	828.9	$1.20x10^8$	**LoQ**	15.58	
+PIS 187.1	813.9	$5.9x10^4$	**BLoD**	55.47	0.53
+PIS 172.1	798.9	$3.13x10^3$	**BLoD**	173.21	0.03
+PIS 157.1	783.9	$9.40x10^3$	**BLoD**	99.95	0.08
+NL 186.1	813.9	$3.76x10^4$	**BLoD**	43.30	0.34
+NL 171.1	798.9	$3.44x10^4$	**BLoD**	78.73	0.31
+NL 156.1	783.9	$6.57x10^4$	**BLoD**	42.85	0.59
+NL 141.1	768.9	$1.25x10^4$	**BLoD**	114.57	0.11
Fully unmodified m/z= 746.9, fully methylated m/z= 806.9					
+PIS 202.1	806.9	$9.32x10^7$	**LoQ**	15.53	
+PIS 187.1	791.9	$8.77x10^4$	**BLoD**	30.93	1.01
+PIS 172.1	776.9	$3.13x10^3$	**BLoD**	173.21	0.04
+PIS 157.1	761.9	$9.39x10^3$	**BLoD**	99.98	0.11
+NL 186.1	791.9	$3.13x10^4$	**BLoD**	69.28	0.36
+NL 171.1	776.9	$3.76x10^4$	**BLoD**	43.30	0.43
+NL 156.1	761.9	$1.88x10^4$	**BLoD**	132.29	0.22
+NL 141.1	746.9	0.00	**BLoD**	0.00	0.00
Fully unmodified m/z= 744.9, fully methylated m/z= 804.9					
+PIS 202.1	804.9	$1.13x10^8$	**LoQ**	15.32	
+PIS 187.1	789.9	$1.06x10^5$	**BLoD**	43.53	1.01

+PIS 172.1	774.9	$9.39x10^3$	**BLoD**	99.99	0.09
+PIS 157.1	759.9	$6.27x10^3$	**BLoD**	86.60	0.06
+NL 186.1	789.9	$7.20x10^4$	**BLoD**	30.16	0.68
+NL 171.1	774.9	$5.01x10^4$	**BLoD**	114.55	0.47
+NL 156.1	759.9	$8.15x10^4$	**BLoD**	35.15	0.77
+NL 141.1	744.9	$9.39x10^3$	**BLoD**	99.98	0.09

LC-MS study of PS species in concentrated HeLa cell extract

As described in the ^{13}C-TrEnDi on PS in HeLa cells sub-section of the results and discussion section of this chapter, Figure 4.6.5 presents the spectrum obtained after analysis of unmodified PS species via a PIS of m/z 185 using a concentrated sample with lower resolution on Q1 to maximize signal of the low sensitivity unmodified PS species. The identified unmodified PS species allowed for the verification of their modified m/z counterparts as PS species, despite of their weak signal, as the temporal separation of the complex sample allowed to remove a significant portion of the background noise.

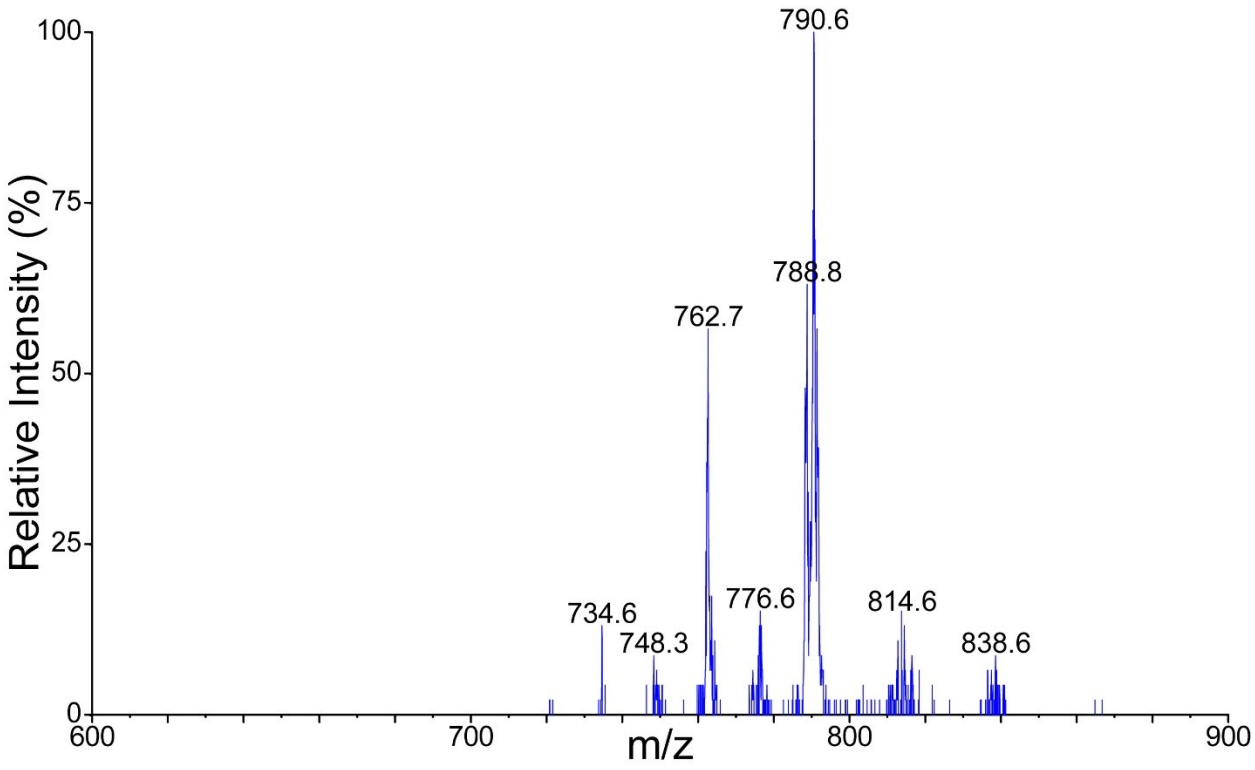

Figure 4.6.5: Mass spectrum of unmodified PS extracted from HeLa cells separated by reversed phase HPLC-ESI-MS/MS with an eluent containing 10 mM ammonium acetate and analyzed via +NL of 185.1 Da. The spectra presented is a two minute window average (24.2 to 26.2 min) corresponding to the time frame where all PS species present in the sample elute. The concentration of sample injected was twice the amount of sample injected via direct infusion. The quadrupole resolution for Q1 was set to low (in comparison to unit for direct spray studies) in order to achieve higher sensitivity for the PS species. The y-axis was set to the highest peak found in the unmodified spectra unlike the direct spray studies where all y-axis were set to 4.4 x 10^5 corresponding to the highest peak intensity found within all scans. The intensity threshold was deliberately lowered to 1 x 10^3 to showcase all the PS species with small intensities.

4.7 References

(1) Fahy, E.; Subramaniam, S.; Murphy, R. C.; Nishijima, M.; Raetz, C. R. H.; Shimizu, T.; Spener, F.; van Meer, G.; Wakelam, M. J. O.; Dennis, E. A. *J. Lipid Res.* **2009**, *50* (Suppl), 9–14.

(2) Fhaner, C. J.; Liu, S.; Ji, H.; Simpson, R. J.; Reid, G. E. *Anal. Chem.* **2012**, *84* (21), 8917–8926.

(3) Wang, M.; Hayakawa, J.; Yang, K.; Han, X. *Anal. Chem.* **2014**, *86* (4), 2146–2155.

(4) Bou Khalil, M.; Hou, W.; Zhou, H.; Elisma, F.; Swayne, L. A.; Blanchard, A. P.; Yao, Z.; Bennet, S. A. .; Figeys, D. *Mass Spectrom. Rev.* **2010**, *29*, 877–929.

(5) Ohkawa, R.; Kishimoto, T.; Kurano, M.; Dohi, T.; Miyauchi, K.; Daida, H.; Nagasaki, M.; Uno, K.; Hayashi, N.; Sakai, N.; Matsuyama, N.; Nojiri, T.; Nakamura, K.; Okubo, S.; Yokota, H.; Ikeda, H.; Yatomi, Y. *Clin. Biochem.* **2012**, *45* (16-17), 1463–1470.

(6) van Meer, G.; Voelker, D. R.; Feigenson G. W. *Nat.Rev. Mol. Cell Biol.* **2008**, 9 (2), 112-124.

(7) Whiley, L.; Sen, A.; Heaton, J.; Proitsi, P.; García-Gómez, D.; Leung, R.; Smith, N.; Thambisetty, M.; Kloszewska, I.; Mecocci, P.; Soininen, H.; Tsolaki, M.; Vellas, B.; Lovestone, S.; Legido-Quigley, C. *Neurobiol. Aging* **2014**, *35* (2), 271–278.

(8) Guan, Z. Z.; Wang, Y. N.; Xiao, K. Q.; Hu, P. S.; Liu, J. L. *Neurochem. Int.* **1999**, *34* (1), 41–47.

(9) Phoenix, D. A.; Harris, F.; Mura, M.; Dennison, S. R. *Prog. Lipid Res.* **2015**, *59*, 26–37.

(10) Van Tits, L. J.; van Heerde, W. L.; Landburg, P. P.; Boderie, M. J.; Muskiet, F. a J.; Jacobs, N.; Duits, A. J.; Schnog, J. B. *Biochem. Biophys. Res. Commun.* **2009**, *390* (1), 161–164.

(11) Schutters, K.; Reutelingsperger, C. *Apoptosis* **2010**, *15* (9), 1072–1082.

(12) Brügger, B. *Annu. Rev. Biochem.* **2014**, *83*, 79–98.

(13) Distler, U.; Hülsewig, M.; Souady, J.; Dreisewerd, K.; Haier, J.; Senninger, N.; Friedrich, A. W.; Karch, H.; Hillenkamp, F.; Berkenkamp, S.; Peter-Katalinić, J.; Müthing, J. *Anal. Chem.* **2008**, *80* (6), 1835–1846.

(14) Graff, G.; Anderson, L. A.; Jaques, L. W.; Scannell, R. T. *Chem. Phys. Lipids* **1990**, *53* (1), 27–36.

(15) Mueller, H. W. *J. Chromatogr. B Biomed. Appl.* **1996**, *679* (1-2), 208–209.

(16) Schlenk, H.; Gellerman, J. L. *Anal. Chem.* **1960**, *32* (11), 1412–1414.

(17) Smith, G. A.; Montecucco, C.; Bennett, J. P. *Lipids* **1978**, *13* (1), 92–94.

(18) Lee, J. W.; Nishiumi, S.; Yoshida, M.; Fukusaki, E.; Bamba, T. *J. Chromatogr. A* **2013**, *1279*, 98–107.

(19) Kielkowska, A.; Niewczas, I.; Anderson, K. E.; Durrant, T. N.; Clark, J.; Stephens, L. R.; Hawkins, P. T. *Adv. Biol. Regul.* **2014**, *54* (1), 131–141.

(20) Wasslen, K. V; Canez, C. R.; Lee, H. *Anal. Chem.* **2014**, *86*, 9523–9532.

(21) Wasslen, K. V.; Tan, L. H.; Manthorpe, J. M.; Smith, J. C. *Anal. Chem.* **2014**, *86* (7), 3291–3299.

(22) Shields, S. W. J.; Manthorpe, J. M. *J. Label. Compd. Radiopharm.* **2014**, *57* (12), 674–679.

(23) *Aldrich Technical Bulletin AL-180 [Online]*; Sigma-Aldrich: St. Louis, MO, **2007**.

(24) Bonin, F.; Ryan, S. D.; Migahed, L.; Mo, F.; Lallier, J.; Franks, D. J.; Arai, H.; Bennett, S. A. *J. Biol. Chem.* **2004**, *279* (50), 52425–52436.

(25) Armbruster, D. A; Pry, T. *Clin. Biochem. Rev.* **2008**, *29* (Suppl 1), 49–52.

Chapter 5: Conclusion

TrEnDi is an inherently quantitative technique superior to conventional analysis methods. It creates permanently charged species and hence eliminates proton competition and signal splitting due to different ionization states. TrEnDi is compatible with simple and complex lipid mixtures, where isotopically labelled diazomethane provides the ability to create exclusive tandem MS scans for PE, PS, and PC/SM species. The sensitivity enhancement provided by TrEnDi for PE and PS species is drastic and allows the identification and quantitation of previously unidentified species. TrEnDi-modified PC species receive a modest boost in sensitivity enabling the quantitation of several PC species that could only be identified prior to modification. SM species do not receive an improvement nor hindrance to their sensitivities post modification, enabling their study in either modified or unmodified samples. The methylation efficiency of samples is ideal for a quantitative technique as it yields more than 99.07 percent yield post-derivatization. PC, PE and PS are compatible with LC-MS and direct infusion analysis while PS is exclusive to direct infusion since modified PS species were not compatible with the chromatographic solvents used. TrEnDi and ^{13}C-TrEnDi proved to be vastly superior techniques to analyze PC, PE and PS lipids in comparison to conventional techniques commonly used. Overall, TrEnDi and ^{13}C-TrEnDi are cost-effective, fast and efficient methods to enhance sensitivity of MS and tandem MS phospholipidomic studies.

Unfortunately TrEnDi-modified analytes lose the ability for further characterization of their radyl structural moieties. As discussed in Chapter 1, the fatty acid characterization of phospholipids can be achieved by CID of their deprotonated versions via negative ESI, or by CID of lithiated or sodiated adducts via charge induced dissociation. The modified lipids cannot

be analyzed in negative ion mode because they possess a permanent fixed charge and no longer have the capability to adduct an alkali metal ion since their phosphate group is methylated. The sensitivity enhancement comes at the cost of further radyl group characterization. High resolution mass spectrometry on modified phospholipids (as well as unmodified) can provide the total number of carbons and number of unsaturation events in the radyl groups of a phospholipid, but cannot characterize the individual *sn*-1 or *sn*-2 number of carbons or unsaturation composition. Radyl group characterization in unmodified phospholipids requires a much higher amount of analyte than the amount required for detection using positive or negative ionization via MS or MS/MS studies. The fragmentation products that provide radyl structural information are less abundant than fragmentation products that provide headgroup information. The radyl structural information of low abundance unmodified lipids cannot be obtained because the signal of CID generated fragments containing radyl structural information occurs below the limit of detection. TrEnDi allows identifying and quantifying many lipid species that would otherwise go unidentified, but lacks the ability to provide further *sn*-1 and *sn*-2 radyl structural information. Further work needs to be conducted in order to develop a methodology capable of combining the phospholipid sensitivity enhancements provided by TrEnDi-modification along with the possibility for *sn*-1 and *sn*-2 radyl structural characterization.